Electronic Supplementary Information (ESI)

for

Synthesis of isomeric maltose-based Glc/Man glycoclusters as inhibitors of bacterial adhesion: The effect of carbohydrate presentation

Sven Ole Jaeschke, Ingo vom Sondern and Thisbe K. Lindhorst

Christiana Albertina University of Kiel, Otto Diels Institute of Organic Chemistry,
Otto-Hahn-Platz 3-4, D-24118, Kiel, Germany.
tklind@oc.uni-kiel.de

Table of contents

1 General methods for synthesis

General information

Moisture-sensitive reactions were carried out in flame-dried glassware and under a positive pressure of nitrogen. Analytical thin layer chromatography (TLC) was performed on silica gel plates (GF 254, Merck). Visualization was achieved by UV light and/or with 10 % sulfuric acid in ethanol, vanillin (3.0 g vanillin and 0.5 mL H_2SO_4 in 100 mL EtOH) or ninhydrin, followed by heat treatment at approx. 200 °C. The products were purified by flash chromatography on silica gel columns (Merck, 230–400 mesh, particle size 0.040–0.063 mm) or by automated flash chromatography using a puriFlash 450 device from the Interchim® company. MeOH was dried over magnesium under a nitrogen atmosphere. Optical rotations were measured with a PerkinElmer 241 polarimeter with a sodium D-line (589 nm) and a cuvette of 10 cm path length, in the solvents indicated. Proton (^{1}H) nuclear magnetic resonance spectra and carbon (^{13}C) nuclear magnetic resonance spectra were recorded on a Bruker DRX-500 and AV-600 spectrometer at 300 K. Chemical shifts are referenced to the internal standard tetramethylsilane (TMS) or to the residual proton of the NMR solvent. Multiplets (multiplicity s=singlet, d=doublet, t=triplet, q=quartet, m=multiplet, br=broad) are listed according to chemical shift, coupling constants are given in Hertz (Hz). Full assignment of the signals was achieved by using 2D NMR techniques (^{1}H-^{1}H COSY, ^{1}H-^{13}C HMBC and ^{1}H-^{13}C HSQC). The first glucose unit at the reducing end of the maltose scaffold is numbered from 1 to 6, the following glucose unit from 1’ to 6’. Ligated carbohydrate units are indicated as “Man” or “Glc” and numbered with primed or unprimed numbers depending on the regiochemistry of their conjugation. Infrared (IR) spectra were measured with a PerkinElmer FT-IR Paragon 1000 (ATR) spectrometer and are reported in cm^{-1}. ESI mass spectra were recorded on a LCQ Classic from Thermo Finnigan.

General procedure A: Staudinger ligation. The carboxylic acid was dissolved in dry THF (*c* = 0.03 M) and *N*-hydroxy succinimide (NHS) and EDC·HCl were added. After stirring for 2 h at room temperature, the reaction mixture was cooled to 0 °C and the azido-functionalized maltoside was added. Trimethylphosphine (1M in THF) was added dropwise, the reaction mixture was allowed to warm to RT and was stirred until completion of the reaction. The reaction was quenched with water and the aqueous layer extracted with ethyl acetate. The combined organic layers were dried over $MgSO_4$, it was filtered and the filtrate concentrated under reduced pressure to yield the crude Staudinger ligation product, which was purified by flash column chromatography on silica gel.

General procedure B: Zemplén transesterification. The respective maltose-based glycocluster was dissolved in dry MeOH (*c* = 0.03 M) and a catalytic amount of a sodium methoxide solution (5.4 M in MeOH) was added. The mixture was stirred at RT until completion of the reaction and then neutralized with Amberlite IR120, diluted with MeOH, filtered and concentrated under reduced pressure. The residue was taken up in H_2O and washed with diethyl ether (3 x). The aqueous layer was concentrated under reduced pressure to yield the transesterification product, which was purified by size exclusion chromatography on Sephadex GP-10 (deionized water as eluent). The resulting product was lyophilized.

General procedure C: Amide coupling. The phthalimido-protected maltoside was dissolved in a round bottom flask in acetonitrile/tetrahydrofuran (4:1, *c* = 0.07 M) and ethylenediamine was added. The mixture was heated to 55 °C and stirred until completion of the reaction. The volatiles were removed under reduced pressure and the residual was taken up in ethyl acetate and washed with H_2O. The organic layer was dried over $MgSO_4$, it was filtered, and the filtrate concentrated under reduced pressure to yield the respective amine which was used in the next step without purification. For amide coupling, the carboxylic acid was dissolved in dry DMSO (*c* = 0.07 M) and NHS and EDC·HCl were added. After stirring for 2 h at RT, DIPEA and the amino-functionalized maltoside (dissolved in dry DMSO) were subsequently added. The mixture was stirred at RT until completion of the reaction. Then it was diluted with ethyl acetate and washed with 1 M HCl and H_2O. The organic layer was dried over $MgSO_4$, it was filtered, and the filtrate concentrated under reduced pressure to yield the crude product, which was purified by flash column chromatography on silica gel.

2 Synthesis of the maltose-based glycoclusters

2-Propargyl 2,3-di-*O*-benzoyl-6-*O*-tosyl-4-*O*-(2',3',4'-tri-*O*-benzoyl-6'-*O*-tosyl-*α*-D-glucopyranosyl)-*β*-D-glucopyranoside (7)

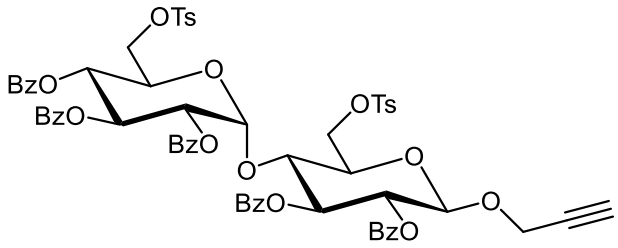

Maltoside **6**[1] (9.20 g, 25.0 mmol) was dissolved in dry pyridine (80.0 mL) and it was cooled to 0 °C. Then tosyl chloride (15.2 g, 79.9 mmol) was added portionwise. The reaction mixture was stirred for 2 h. Then at 0 °C benzoyl chloride (23.2 mL, 200 mmol) was added dropwise. The mixture was allowed to warm to RT and stirring was

continued for 16 h. MeOH was added and the reaction mixture was stirred for 15 min before the volatiles were removed under reduced pressure. The crude product was taken up in ethyl acetate and it was washed with 1 N HCl, sodium bicarbonate and brine. The organic layer was dried over magnesium sulfate, filtered and concentrated to dryness. Purification by flash column chromatography on silica (cyclohexane/ ethyl acetate, 3:1) gave **7** (19.1 g, 67 %) as a colorless solid; R_f 0.30 (cyclohexane/ethyl acetate, 3:2); $[\alpha]^{20}_D$ = +6.67 (*c* 0.01, CH_2Cl_2); IR (ATR): ν_{max}/cm^{-1} = 2925, 1731, 1600, 1451, 1362, 1265, 1176, 1091, 1068, 1026, 995, 936, 514; ^{1}H NMR (500 MHz, $CDCl_3$, 300 K): δ = 7.92-7.65 (m, 14H, Ts*ortho*, Bz*ortho*), 7.55-7.17 (19H, Ts*meta*, Bz*meta,* Bz*para*), 5.93 (dd, $^3J_{2',3'}$ = 10.3 Hz, $^3J_{3',4'}$ = 9.7 Hz, 1H, H-3'), 5.62-5.57 (m, 2H, H-1', H-3), 5.47 (t, $^3J_{3',4'}$ = 9.9 Hz, $^3J_{4',5'}$ = 9.9 Hz, 1H, H-4'), 5.13 (dd, $^3J_{2,3}$ = 9.3 Hz, $^3J_{1,2}$ = 7.5 Hz, 1H, H-2), 5.05 (dd, $^3J_{2',3'}$ = 10.4 Hz, $^3J_{1',2'}$ = 3.9 Hz, 1H, H-2'), 4.90 (d, $^3J_{1,2}$ = 7.5 Hz, 1H, H-1), 4.53 (dd, $^2J_{6a,6b}$ = 11.3 Hz, $^3J_{5,6b}$ = 3.9 Hz, 1H, H-6b), 4.49 (dd, $^2J_{6a,6b}$ = 11.4 Hz, $^3J_{5,6a}$ = 2.4 Hz, 1H, H-6a), 4.43 (ddd, $^2J_{6a',6b'}$ =11.4 Hz, $^3J_{5',6b'}$ = 1.9 Hz, 1H, H-6b'), 4.36 (ddd, $^3J_{4',5'}$ = 10.0 Hz, $^3J_{5',6a'}$ = 3.7 Hz, $^3J_{5',6b'}$ = 1.7 Hz, 1H, H-5'), 4.26-4.13 (m, 4H, OC*H*$_2$, H-4, H-6a'), 3.86 (dd, $^3J_{4,5}$ = 9.6 Hz, $^3J_{5,6a}$ = 3.7 Hz, $^3J_{5,6b}$ = 2.4 Hz, 1H, H-5), 2.45 (s, 1H, Ts-C*H*$_3$), 2.38 (t, $^4J_{OCH',C\equiv CH}$ = 2.4 Hz, $^4J_{OCH,C\equiv CH}$ = 2.4 Hz, 1H, C≡C*H*), 2.30 (s, 1H, Ts-C*H*$_3$), ppm; ^{13}C NMR (125 MHz, $CDCl_3$, 300 K): δ = 165.59, 165.19, 165.08, 164.99, 164.74 (5 C(O)Ph), 145.33, 144.87 (2 Ts-CH), 133.40, 133.30, 133.19, 133.11, 133.07 (5 Bz-CH*para*), 132.54, 132.36 (2 Ts-CH), 129.98, 129.87, 129.78, 129.75, 129.73 (10 Bz-CH*ortho(a,b)*), 129.61, 129.58 (4 Ts-CH), 129.08, 128.89, 128.69, 128.66, 128.49 (5 Bz-C$_q$), 128.38, 128.27, 128.23, 128.21, 128.17, 128.13, 128.07 (14C, Ts-CH, Bz-CH*meta(a,b)*), 97.60 (C-1), 96.02 (C-1'), 77.99 (OCH$_2$C≡CH), 75.61 (OCH$_2$C≡CH), 74.64 (C-3), 72.48 (C-5), 71.81 (C-4), 71.51 (C-2), 70.64 (C-2'), 69.84 (C-3'), 68.73 (C-5'), 68.14 (C-4'), 68.13 (C-6'), 67.43 (C-6), 55.57 (OCH$_2$C≡CH), 21.70, 21.59 (2 Ts-CH$_3$) ppm; ESI-HRMS: *m/z* = 1231.2668.1 $[M+Na]^+$ (calcd *m/z* = 1231.2698 for $[M+Na]^+$).

2-Propargyl 6-azido-2,3-di-*O*-benzoyl-6-deoxy-4-O-(6'-azido-2',3',4'-tri-*O*-benzoyl-6'-deoxy-*α*-D-glucopyranosyl)-*β*-D-glucopyranoside (8)

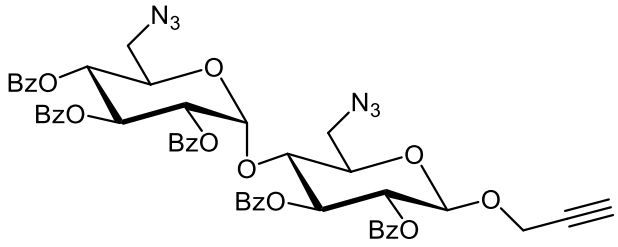

Maltoside **7** (19.0 g, 16.6 mmol) was dissolved in DMF (500 mL) and sodium azide (25.8 g, 397 mmol) was added. The mixture was heated to 80 °C for 16 h. After cooling down to RT, the solvent was removed under reduced pressure. The crude product was diluted with CH_2Cl_2 and washed with brine. The organic layer was dried over magnesium sulfate, filtered and concentrated. Purification by flash column

chromatography (cyclohexane/ ethyl acetate, 4:1 → 3:1) gave **8** (13.3 g, 84 %) as a colorless solid; R_f 0.44 (cyclohexane/ethyl acetate, 3:1); $[\alpha]^{20}_D$ = +35.4 (*c* 0.01, CH_2Cl_2); IR (ATR): ν_{max}/cm^{-1} = 2102, 1725, 1601, 1492, 1451, 1263, 1178, 1090, 1067, 1025, 849, 705, 685; ^{1}H NMR: (600 MHz, $CDCl_3$, 300 K): δ = 7.96-7.89 (m, 2H, Bz_{ortho}), 7.86-7.80 (m, 2H, Bz_{ortho}), 7.76-7.70 (m, 4H, Bz_{ortho}), 7.69-7.63 (m, 2H, Bz_{ortho}), 7.57-7.23 (m, 15H, $Bz_{meta,}$ Bz_{para}), 5.97 (dd, $^3J_{2',3'}$ = 10.0 Hz, $^3J_{3',4'}$ = 10.0 Hz, 1H, H-3'), 5.76-5.69 (m, 2H, H-1', H-3), 5.46 (t, $^3J_{3',4'}$ = 9.8 Hz, $^3J_{4',5'}$ = 9.8 Hz, 1H, H-4'), 5.35 (dd, $^3J_{2,3}$ = 9.5 Hz, $^3J_{1,2}$ = 7.8 Hz, 1H, H-2), 5.19 (dd, $^3J_{2',3'}$ = 10.5 Hz, $^3J_{1',2'}$ = 4.0 Hz, 1H, H-2'), 5.09 (d, $^3J_{1,2}$ = 7.7 Hz, 1H, H-1), 4.18 (ddd, $^3J_{4',5'}$ = 8.8 Hz, $^3J_{5',6a'}$ = 5.5 Hz, $^3J_{5',6b'}$ = 2.6 Hz, 1H, H-5'), 3.98 (ddd, $^3J_{4,5}$ = 9.2 Hz, $^3J_{5,6a}$ = 5.2 Hz, $^3J_{5,6b}$ = 2.4 Hz, 1H, H-5), 4.49-4.34 (m, 3H, OCH_2, H-4), 3.81 (dd, $^2J_{6a,6b}$ = 13.2 Hz, $^3J_{5,6b}$ = 2.3 Hz, 1H, H-6b), 3.72 (dd, $^2J_{6a,6b}$ = 13.2 Hz, $^3J_{5,6a}$ = 5.3 Hz, 1H, H-6a), 3.56 (dd, $^2J_{6a',6b'}$ = 13.4 Hz, $^3J_{5',6b'}$ = 2.6 Hz, 1H, H-6b'), 3.48 (dd, $^2J_{6a',6b'}$ = 13.4 Hz, $^3J_{5',6a'}$ = 5.6 Hz, 1H, H-6a'), 2.42 (t, $^4J_{OCH',C\equiv CH}$ = 2.3 Hz, $^4J_{OCH,C\equiv CH}$ = 2.3 Hz, 1H, C≡C*H*) ppm; ^{13}C NMR (125 MHz, $CDCl_3$, 300 K): δ = 165.80, 165.43, 165.37, 165.34, 165.19 (5 C(O)Ph), 133.80, 133.43, 133.43, 133.33, 133.20 (5 Bz-CH_{para}), 130.07, 130.05, 129.97, 129.87, 129.71 (10 Bz-C$H_{ortho(a,b)}$), 129.28, 128.93, 128.82, 128.69, 128.59 (5 Bz-C_q), 128.65, 128.41, 128.37, 128.31, 128.25 (10 Bz-C$H_{meta(a,b)}$), 97.96 (C-1), 96.18 (C-1'), 78.17 ($OCH_2C\equiv CH$), 75.83 ($OCH_2C\equiv CH$), 74.93 (C-3), 74.60 (C-5), 73.10 (C-4), 71.97 (C-2), 70.82 (C-2'), 70.44 (C-5'), 69.90 (C-4'), 69.71 (C-3'), 55.91 ($OCH_2C\equiv CH$), 51.58 (C-6), 51.34 (C-6') ppm; ESI-HRMS: *m/z* = 951.2830 $[M+H]^+$ (calcd *m/z* = 951.2831 for $[M+H]^+$).

Maltosan (10)[2]

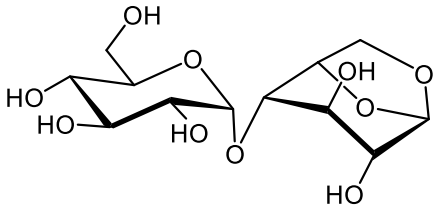

D-Maltose (10.0 g, 27.8 mmol) was dissolved in water (400 mL) and, at 0 °C 2-chloro dimethyl imidazolinium chloride (DMC, 14.1 g, 83.3 mmol) and triethylamine (34.7 mL, 250 mmol) were added. While stirring for 2 h the reaction mixture was allowed to warm to RT until complete conversion of the starting material. The mixture was washed with CH_2Cl_2 and the aqueous layer was concentrated and co-evaporated with toluene under reduced pressure. The residue was dissolved in pyridine (100 mL) and acetic anhydride (35.0 mL, 371 mmol) was added. The mixture was stirred for 2.5 h. Afterwards the volatiles were removed under reduced pressure, the residue was dissolved in ethyl acetate (200 mL) and washed with 1 N HCl and water. The aqueous layer was extracted with ethyl acetate and the combined organic layers were washed with brine, dried over magnesium sulfate, it was filtered and concentrated to dryness. The residue was dissolved in dry MeOH (50 mL) and sodium methoxide (5.4 M solution,

2.00 mL, 10.8 mmol) was added dropwise. The mixture was stirred for 1 h and then neutralized by adding Amberlite IR120. The resin was filtered off, washed with MeOH and the solvent was removed under reduced pressure to afford **10** (8.51 g, 94 %) as a colorless solid. Analytical and spectroscopic data were in full agreement with reported literature;[2] R_f 0.30 (acetonitrile/water, 4:1); $[\alpha]^{20}_D$ = +47.1 (*c* 0.02, H_2O); IR (ATR): ν_{max}/cm^{-1} = 3359, 2909, 1148, 1075, 1032; ^{1}H NMR (500 MHz, D_2O, 300 K): δ = 5.50 (s, 1H, H-1), 5.16 (d, $^3J_{1,2}$ = 3.9 Hz, 1H, H-1'), 4.86-4.79 (m, 1H, H-5), 4.16 (dd, $^3J_{1,2}$ = 7.8 Hz, $^3J_{2,3}$ = 0.9 Hz, 1H, H-6a), 3.94-3.73 (m, 7H, H-3, H-4, H-6b, H-3', H-5', H-6a', H-6b'), 3.63-3.55 (m, 2H, H-2, H-2'), 3.45 (t, $^3J_{4,5}$ = 8.86 Hz, $^3J_{3,4}$ = 8.86 Hz, 1H, H-4') ppm; ^{13}C NMR (125 MHz, D_2O, 300 K): δ = 101.1 (C-1), 97.7 (C-1'), 75.6 (C-4), 75.3 (C-5), 72.9 (C-3'), 72.4 (C-5'), 71.4 (C-2'), 69.6 (3C, C-2, C-3, C-4'), 65.2 (C-6), 60.6 (C-6') ppm; ESI-HRMS: *m/z* = 347.0961 $[M+Na]^+$ (calcd *m/z* = 347.0954 for $[M+Na]^+$).

2,3-Di-*O*-benzoyl-1,6-anhydro-4-*O*-(2',3',4'-tri-*O*-benzoyl-6'-*tert*-butyldimethylsilyl-*α*-D-glucopyranosyl)-*β*-D-glucopyranose (11)

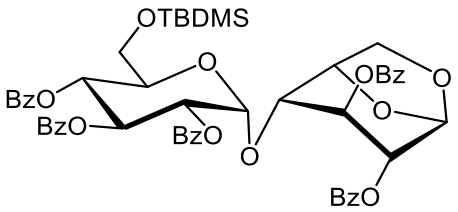

Maltosan (**10**, 4.00 g, 12.3 mmol) was dissolved in dry pyridine (24 mL) and *tert*-butyldimethylsilyl chloride (2.78 g, 18.5 mmol) and 4-(dimethylamino)-pyridine (300 mg, 2.46 mmol) were added. After stirring at RT for 4 h, a further portion of *tert*-butyldimethylsilyl chloride (927 mg, 6.15 mmol) was added and stirring was continued for 1 h. Then, at 0 °C, benzoyl chloride (8.57 mL, 73.8 mmol) was added and the mixture was stirred for 1 h at RT. After completion, MeOH (15.0 mL) was added to the suspension and it was stirred for 15 min. The volatiles were removed under reduced pressure and the crude product was dissolved in ethyl acetate and washed with 1 N HCl. The aqueous layer was extracted with ethyl acetate and the combined organic phases were washed with brine, dried over magnesium sulfate, filtered and the solvent was removed under reduced pressure. The crude product was purified by column chromatography (cyclohexane → cyclohexane/ethyl acetate, 4:1) to give **11** (9.08 g, 77 %) as a colorless foam; R_f 0.41 (cyclohexane/ethyl acetate, 3:1); $[\alpha]^{20}_D$ = +41.0 (*c* 0.02, CH_2Cl_2); IR (ATR): ν_{max}/cm^{-1} = 2927, 1722, 1451, 1249, 1092, 1025, 836, 706; ^{1}H NMR (500 MHz, $CDCl_3$, 300 K): δ = 8.35-8.28 (m, 2H, 2 BZ_{ortho}), 8.01-7.96 (m, 2H, 2 Bz_{ortho}), 7.96-7.85 (m, 6H, 6 Bz_{ortho}), 7.63-7.54 (m, 4H, 4 Bz_{meta}), 7.54-7.40 (m, 4H, 4 Bz_{meta}), 7.36-7.28 (m, 5H, 5 Bz_{para}), 7.11-7.03 (m, 2H, 2 Bz_{meta}), 6.36 (t, $^3J_{2,3}$ = 10.0 Hz, $^3J_{3,4}$ = 10.0 Hz, 1H, H-3'), 5.72 (s, 1H, H-1), 5.67 (d, $^3J_{1,2}$ = 3.8 Hz, 1H, H-1'), 5.58 (t, $^3J_{3,4}$ = 10.0 Hz, $^3J_{4,5}$ = 10.0 Hz, 1H, H-4'), 5.39 (dd, $^3J_{2,3}$ = 10.3 Hz, $^3J_{1,2}$ = 3.8 Hz, 1H H-2'), 5.17-5.12 (m, 1H, H-3), 5.06 (d, $^3J_{5,6b}$ = 5.4 Hz, 1H, H-5), 5.04 (s, 1H, H-2), 4.61

(ddd, $^3J_{4,5}$ = 10.2 Hz, $^3J_{5,6a}$ = 4.8 Hz, $^3J_{5,6b}$ = 3.6 Hz, 1H, H-5'), 4.15 (d, $^3J_{6a,6b}$ = 7.2 Hz, 1H, H-6a), 3.89 (dd, $^3J_{6a,6b}$ = 7.6 Hz, $^3J_{5,6b}$ = 5.8 Hz, 1H, H-6b), 3.85-3.81 (m, 2H, H-6a', H-6b'), 3.76 (s, 1H, H-4), 0.84 (s, 9H, Si-*t*-Bu), -0.01 (s, 3H, Si-CH_3), -0.02 (s, 3H, Si-CH_3) ppm; ^{13}C NMR (125 MHz, $CDCl_3$, 300 K): δ = 166.1, 165.8, 165.6, 165.5, 164.8 (5 C(O)Ph), 133.7, 133.7, 133.4, 133.3, 133.2 (5 Bz-CH$_{para}$), 130.5, 130.1, 130.0, 129.9, 129.9 (10 Bz-CH$_{ortho(a,b)}$), 129.5, 129.4, 129.3, 129.2, 128.9 (5 Bz-C$_q$), 129.1, 128.7, 128.5, 128.4, 128.3 (10 Bz-CH$_{ortho(a,b)}$), 99.2 (C-1), 98.8 (C-1'), 77.2 (C-3), 75.0 (C-5), 71.9 (2C, C-2, C-5'), 71.7 (C-2'), 70.8 (C-3'), 69.5 (C-4'), 69.0 (C-2), 65.3 (C-6), 62.8 (C-6'), 26.0 (3 Si-*t*-Bu-CH$_3$), 18.5 (C$_q$), -5.4 (2 Si-CH$_3$) ppm; ESI-HRMS: *m/z* = 982.0732 $[M+Na]^+$ (calcd *m/z* = 982.0748 for $[M+Na]^+$).

2,3-Di-*O*-benzoyl-1,6-anhydro-4-*O*-(2',3',4'-tri-*O*-benzoyl-*α*-D-glucopyranosyl)-*β*-D-glucopyranose (12)

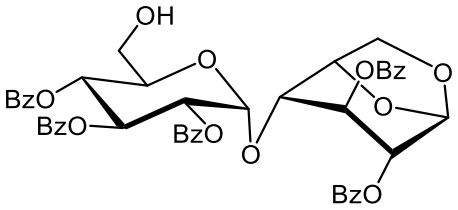

The maltose derivative **11** (2.79 g, 2.91 mmol) was dissolved in dry THF (20 mL) and at 0 °C acetic acid (886 µL, 15.5 mmol) and tetra-*n*-butylammonium fluoride (1 M solution in tetrahydrofuran) (7.73 mL, 7.73 mmol) were added. While stirring the mixture was allowed to warm to RT and stirring was continued for 16 h. Then the mixture was diluted with ethyl acetate and washed with water, satd. sodium bicarbonate solution and brine. The aqueous layer was extracted with CH_2Cl_2 and ethyl acetate and the combined organic layers were dried over magnesium sulfate, filtered and the solvent was removed under reduced pressure. The crude product was purified by flash chromatography (cyclohexane/ethyl acetate, 3:2→1:1) to afford **12** (2.25 g, 92 %) as a colorless foam; R_f 0.11 (cyclohexane/ethyl acetate, 3:1); $[\alpha]^{20}_D$ = +41.8 (*c* 0.01, CH_2Cl_2); IR (ATR): ν_{max}/cm^{-1} = 2925, 1723, 1451, 1256, 1092, 1025, 706; ^{1}H NMR (500 MHz, $CDCl_3$, 300 K): δ = 8.36-8.28 (m, 2H, 2 Bz$_{ortho}$), 8.02-7.84 (m, 8H, 8 Bz$_{ortho}$), 7.68-7.29 (m, 13H, 4 Bz$_{meta,\ para}$), 7.28-7.22 (m, 2H, 2 Bz$_{meta,\ para}$), 6.45 (t, $^3J_{2,3}$ = 10.0 Hz, $^3J_{3,4}$ = 10.0 Hz, 1H, H-3'), 5.73 (s, 1H, H-1), 5.71 (d, $^3J_{1,2}$ = 3.8 Hz, 1H, H-1'), 5.57 (t, $^3J_{3,4}$ = 10.0 Hz, $^3J_{4,5}$ = 10.0 Hz, 1H, H-4'), 5.44 (dd, $^3J_{2,3}$ = 10.3 Hz, $^3J_{1,2}$ = 3.8 Hz, 1H, H-2'), 5.28-5.19 (m, 1H, H-3), 5.03 (s, 1H, H-2), 5.01 (d, $^3J_{5,6b}$ = 5.4 Hz, 1H, H-5), 4.56 (ddd, $^3J_{4,5}$ = 10.3 Hz, $^3J_{5,6a}$ = 3.9 Hz, $^3J_{5,6b}$ = 2.2 Hz, 1H, H-5'), 4.19 (d, $^2J_{6a,6b}$ = 7.7 Hz, 1H, H-6a), 3.92 (dd, $^2J_{6a,6b}$ = 7.6 Hz, $^3J_{5,6b}$ = 5.9 Hz, 1H, H-6b), 3.83 (dd, $^2J_{6'A,6'B}$ = 13.0 Hz, $^3J_{5,6'A}$ = 2.1 Hz, 1H, H-6a'), 3.79 (s, 1H, H-4), 3.75 (dd, $^2J_{6'A,6'B}$ = 13.0 Hz, $^3J_{5,6'B}$ = 4.0 Hz, 1H, H-6b') ppm; ^{13}C NMR (125 MHz, $CDCl_3$, 300 K): δ = 166.6, 166.1, 165.8, 165.6, 164.8 (5 C(O)Ph), 133.8, 133.7, 133.7, 133.4, 133.3 (5 Bz-CH$_{para}$), 130.4, 130.2, 130.0, 129.9, 129.9 (10 Bz-CH$_{ortho(a,b)}$), 129.4, 129.4, 129.2,

128.9, 128.6 (5 Bz-<u>C</u>$_q$), 128.7, 128.6, 128.5, 128.4, 128.4 (10 Bz-<u>C</u>H$_{meta(a,b)}$), 99.2 (C-1), 98.4 (C-1'), 77.2 (C-3), 74.8 (C-5), 71.7 (C-2'), 71.4 (C-2), 71.1 (C-5'), 70.2 (C-3'), 69.6 (C-4'), 69.1 (C-2), 65.1 (C-6), 61.2 (C-6') ppm; ESI-HRMS: *m/z* = 867.2258 $[M+Na]^+$ (calcd *m/z* = 867.2265 for $[M+Na]^+$).

2,3-Di-*O*-benzoyl-1,6-anhydro-4-*O*-(6'-azido-2',3',4'-tri-*O*-benzoyl-6'-deoxy-*α*-D-glucopyranosyl)-*β*-D-glucopyranose (13)

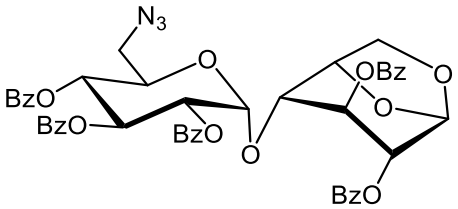

The maltose derivative **12** (2.00 g, 2.37 mmol) and triphenylphosphine (931 mg, 3.55 mmol) were dissolved in dry THF (10.0 mL) and the mixture was cooled to -15 °C. Then diisopropyl azodicarboxylate (1.16 mL, 5.92 mmol) was added dropwise and the mixture was stirred at -15 °C for 15 min. Afterwards the mixture was allowed to warm to RT and diphenylphosphoryl azide (765 µL, 3.55 mmol) was added dropwise while stirring was continued. After stirring for 16 h the solvent was removed under reduced pressure. The crude product was purified by column chromatography (cyclohexane/ethyl acetate, 4:1→3:1) to yield **13** (1.49 g, 72 %) as a colorless amorphous solid; R_f 0.77 (cyclohexane/ethyl acetate, 3:2); $[\alpha]^{20}_D$ = +50.1 (*c* 0.01, CH_2Cl_2); IR (ATR): ν_{max}/cm^{-1} = 2097, 1715, 1450, 1255, 1093, 1024, 878, 706; ^{1}H NMR (500 MHz, $CDCl_3$, 300 K): δ = 8.36-8.26 (m, 2H, 2 Bz$_{ortho}$), 8.01-7.82 (m, 8H, 8 Bz$_{ortho}$), 7.66-7.29 (m, 13H, 4 Bz$_{meta,\ para}$), 7.21-7.05 (m, 2H, 2 Bz$_{meta,\ para}$), 6.38 (t, $^3J_{2',3'}$ = 10.0 Hz, $^3J_{3',4'}$ = 10.0 Hz, 1H, H-3'), 5.75 (s, 1H, H-1), 5.70 (d, $^3J_{1',2'}$ = 3.7 Hz, 1H, H-1'), 5.60 (t, $^3J_{3',4'}$ = 9.9 Hz, $^3J_{4',5'}$ = 9.9 Hz, 1H, H-4'), 5.43 (dd, $^3J_{2',3'}$ = 10.4 Hz, $^3J_{1',2'}$ = 3.7 Hz, 1H H-2'), 5.23-5.17 (m, 1H, H-3), 5.05 (s, 1H, H-2), 5.02 (d, $^3J_{5,6b}$ = 5.2 Hz, 1H, H-5), 4.73-4.68 (m, 1H, H-5'), 4.20 (d, $^2J_{6a,6b}$ = 7.2 Hz, 1H, H-6a), 3.92 (dd, $^2J_{6a,6b}$ = 7.7 Hz, $^3J_{5,6b}$ = 5.9 Hz, 1H, H-6b), 3.80 (s, 1H, H-4), 3.55-3.45 (m, 2H, H-6a', H-6b') ppm; ^{13}C NMR (125 MHz, $CDCl_3$, 300 K): δ = 166.3, 166.01, 165.8, 165.8, 165.05 (5 <u>C</u>(O)Ph), 134.0, 134.0, 133.9, 133.7, 133.6 (5 Bz-<u>C</u>H$_{para}$), 130.7, 130.4, 130.3, 130.2, 130.1 (10 Bz-<u>C</u>H$_{ortho(a,b)}$), 129.7, 129.6, 129.4, 129.0, 128.9 (5 Bz-<u>C</u>$_q$), 129.3, 129.0, 128.8, 128.8, 128.6 (10 Bz-<u>C</u>H$_{meta(a,b)}$), 99.5 (C-1), 98.8 (C-1'), 77.8 (C-3), 75.2 (C-5), 71.9 (C-2'), 71.8 (C-2), 70.4 (C-5'), 70.3 (C-3'), 69.4 (C-4'), 65.5 (C-6), 51.7 (C-6') ppm; ESI-HRMS: *m/z* = 892.2370 $[M+Na]^+$ (calcd *m/z* = 892.2330 for $[M+Na]^+$).

***O*-[6-*O*-acetyl-2,3-di-*O*-benzoyl-4-*O*-(6'-azido-2',3',4'-tri-*O*-benzoyl-6'-deoxy-*α*-D-glucopyranosyl)-*α*-D-glucopyranosyl]-2,2,2-trichloroacetimidate (14)**

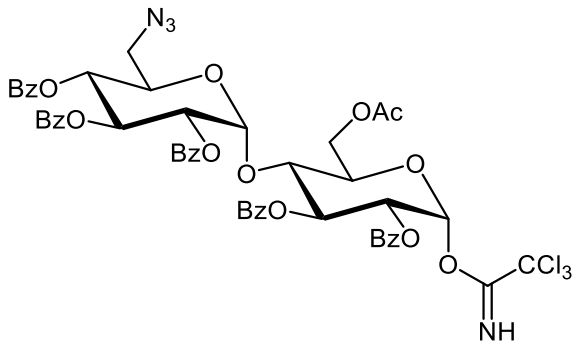

The maltose derivative **13** (1.50 g, 1.72 mmol) was dissolved in a mixture of acetic anhydride and acetic acid (24.0 mL, 7:3) and sulfuric acid (300 µL) was added. The mixture was stirred at RT for 1 h and then diluted with ethyl acetate. Afterwards the mixture was added into an ice-cold sodium bicarbonate solution and it was stirred for 2 h at 0 °C. The aqueous layer was extracted with ethyl acetate and the combined organic layers were washed with brine. The solvent was removed under reduced pressure. The crude product was dissolved in DMF (12 mL) and the mixture was heated to 55 °C. Then N_2H_4·AcOH (266 mg) was added and stirring was continued for 2 h. The mixture was diluted with ethyl acetate and washed with brine and then concentrated to dryness. The crude product was dissolved in dry CH_2Cl_2 (3.5 mL) and, at 0 °C, DBU (33 µL) and Cl_3CCN (1.67 mL) were added. It was stirred for 20 min at 0 °C and then the mixture was allowed to warm to RT while stirring was continued for 2 h. Afterwards the solvent was removed and the crude product was purified by column chromatography (cyclohexane/ethyl acetate, 3:1→7:3) to afford **14** (1.25 g, 68 % over three steps) as a colorless foam; R_f 0.77 (cyclohexane/ethyl acetate, 3:2); $[\alpha]^{20}_D$ = +67.2 (*c* 0.01, CH_2Cl_2); IR (ATR): ν_{max}/cm^{-1} = 2104, 1726, 1677, 1451, 1258, 1091, 1025, 794, 704; ^{1}H NMR (600 MHz, $CDCl_3$, 300 K): δ = 8.58 (s, 1H, NH), 7.97-7.64 (m, 10H, 10 Bz$_{ortho}$), 7.55-7.26 (m, 15H, 10 Bz$_{meta,}$ 5 Bz$_{para}$), 6.69 (d, $^3J_{1,2}$ = 3.5 Hz, 1H, H-1), 6.12 (dd, $^3J_{2,3}$ = 9.9 Hz, $^3J_{3,4}$ = 8.6 Hz, 1H, H-3), 6.02 (dd, $^3J_{2',3'}$ = 10.0 Hz, $^3J_{3',4'}$ = 10.0 Hz, 1H, H-3'), 5.76 (d, $^3J_{1,2}$ = 3.9 Hz, 1H, H-1'), 5.49 (t, $^3J_{3',4'}$ = 9.8 Hz, $^3J_{4',5'}$ = 9.8 Hz, 1H, H-4'), 5.37 (dd, $^3J_{2,3}$ = 10.0 Hz, $^3J_{1,2}$ = 3.5 Hz, 1H H-2), 5.28 (dd, $^3J_{2,3}$ = 10.5 Hz, $^3J_{1,2}$ = 3.9 Hz, 1H, H-2'), 4.65 (d, $^2J_{6a,6b}$ = 10.4 Hz, 1H, H-6a), 4.49 (m, 3H, H-4, H-5, H-6b), 4.24 (ddd, $^3J_{4',5'}$ = 9.9 Hz, $^3J_{5',6a'}$ = 5.1 Hz, $^3J_{5',6b'}$ = 2.9 Hz, 1H, H-5'), 3.45 (m, 2H, H-6a', H-6b'), 2.19 (s, 3H, OAc) ppm; ^{13}C NMR (125 MHz, $CDCl_3$, 300 K): δ = 170.9, 165.8, 165.6, 165.6, 165.4 (5 C(O)Ph), 133.8, 133.6, 133.4, 133.3, 133.2 (4 Bz-CH$_{para}$), 130.1, 130.1, 130.1, 130.0, 130.0 (10 Bz-CH$_{ortho(a,b)}$), 129.2, 129.0 (2 Bz-C$_q$), 128.7, 128.5, 128.5, 128.3, 128.3 (10 Bz-CH$_{meta(a,b)}$), 96.6 (C-1), 93.1 (C-1'), 77.2 (CCl_3), 73.1 (C-4), 71.9 (C-3), 71.1 (C-5), 71.1 (C-2), 70.8 (C-2'), 70.7 (C-5'), 69.9 (C-4'), 69.8 (C-3'), 62.7 (C-6), 51.2 (C-6'), 21.0 (C(O)CH$_3$) ppm; ESI-HRMS: *m/z* = 1095.1641 $[M+Na]^+$ (calcd *m/z* = 1095.1637 for $[M+Na]^+$).

2-Propargyl 6-*O*-acetyl-2,3-di-*O*-benzoyl-4-*O*-(6'-azido-2',3',4'-tri-*O*-benzoyl-6'-deoxy-*α*-D-glucopyranosyl)-*β*-D-glucopyranoside (15)

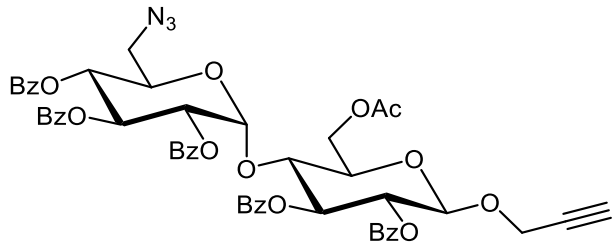

The maltose derivate **14** (500 mg, 465 µmol) and propargyl alcohol (29.6 mL, 512 µmol) were dissolved in dry CH_2Cl_2 (1.00 mL) and 3 Å molecular sieves (500 mg) were added. The mixture was stirred for 15 min at RT before the mixture was cooled to 0 °C and $BF_3{\cdot}Et_2O$ (58.4 µL, 465 µmol) was added. The reaction was allowed to warm to RT while stirring was continued for 16 h. Afterwards the mixture was diluted with CH_2Cl_2 and filtrated over celite. The solvent was removed under reduced pressure and the crude product was purified by column chromatography (cyclohexane/ethyl acetate, 3:1→7:3) to obtain **15** (417 mg, 91 %) as a colorless solid; R_f 0.33 (cyclohexane/ethyl acetate, 3:2); $[\alpha]^{20}_D$ = +19.4 (*c* 0.01, CH_2Cl_2); IR (ATR): ν_{max}/cm^{-1} = 2105, 1725, 1451, 1251, 1091, 1025, 706; ^{1}H NMR (500 MHz, $CDCl_3$, 300 K): δ = 7.97-7.61 (m, 10H, 10 Bz*ortho*), 7.56-7.16 (m, 15H, 10 Bz*meta,* 5 Bz*para*), 6.00 (dd, $^3J_{2',3'}$ = 10.4 Hz, $^3J_{3',4'}$ = 9.7 Hz, 1H, H-3'), 5.72 (t, $^3J_{2,3}$ = 9.3 Hz, $^3J_{3,4}$ = 9.3 Hz, 1H, H-3), 5.70 (d, $^3J_{1,2}$ = 3.8 Hz, 1H, H-1'), 5.49 (t, $^3J_{3',4'}$ = 9.8 Hz, $^3J_{4',5'}$ = 9.8 Hz, 1H, H-4'), 5.31 (dd, $^3J_{2,3}$ = 9.3 Hz, $^3J_{1,2}$ = 7.6 Hz, 1H, H-2), 5.22 (dd, $^3J_{2,3}$ = 10.5 Hz, $^3J_{1,2}$ = 3.9 Hz, 1H H-2'), 5.05 (d, $^3J_{1,2}$ = 7.5 Hz, 1H, H-1), 4.71 (dd, $^2J_{6a,6b}$ = 12.1 Hz, $^3J_{5,6b}$ = 2.7 Hz, 1H, H-6b), 4.45-4,39 (m, 2H, H-4, H-6a), 4.39-4.33 (m, 2H, OCH_2), 4.25 (ddd, $^3J_{4',5'}$ = 10.6 Hz, $^3J_{5',6a'}$ = 5.2 Hz, $^3J_{5',6b'}$ = 2.5 Hz, 1H, H-5'), 4.00 (ddd, $^3J_{4,5}$ = 9.4 Hz, $^3J_{5,6a}$ = 4.3 Hz, $^3J_{5,6b}$ = 2.8 Hz, 1H, H-5), 3.50 (dd, $^2J_{6a',6b'}$= 13.4 Hz, $^3J_{5',6b'}$ = 2.9 Hz, 1H, H-6b'), 3.45 (dd, $^2J_{6a',6b'}$= 13.4 Hz, $^3J_{5',6a'}$ = 5.4 Hz, 1H, H-6a'), 2.40 (t, $^4J_{OCH',C\equiv CH}$ = 2.4 Hz, $^4J_{OCH,C\equiv CH}$ = 2.4 Hz, 1H, C≡C*H*), 2.21 (s, 3H, OAc) ppm; ^{13}C NMR (125 MHz, $CDCl_3$, 300 K): δ = 170.9, 165.8, 165.6, 165.4, 165.1 (5 C(O)Ph), 133.8, 133.4, 133.4, 133.3, 133.2 (5 Bz-CH_{para}), 130.1, 130.1, 130.0, 129.9, 129.7 (10 Bz-C$H_{ortho(a,b)}$), 128.7, 128.4, 128.4, 128.3, 128.2 (10 Bz-C$H_{meta(a,b)}$), 129.3, 129.0, 128.9, 128.7, 128.6 (5 Bz-C_q), 98.0 (C-1'), 96.6 (C-1), 78.1 (OCH$_2$≡CH), 75.0 (C-3), 73.4 (C-4), 72.8 (C-5), 72.0 (C-2), 70.8 (C-2'), 70.5 (C-5'), 69.7 (C-4'), 69.6 (C-3'), 63.0 (C-6), 55.8 (OCH$_2$≡CH) 51.2 (C-6'), 21.0 (C(O)CH_3) ppm; ESI-HRMS: *m/z* = 990.2295 $[M+Na]^+$ (calcd *m/z* = 990.2698 for $[M+Na]^+$).

2-Propargyl 2,3-di-*O*-benzoyl-4-*O*-(6'-azido-2',3',4'-tri-*O*-benzoyl-6'-deoxy-*α*-D-glucopyranosyl)-*β*-D-glucopyranoside (16)

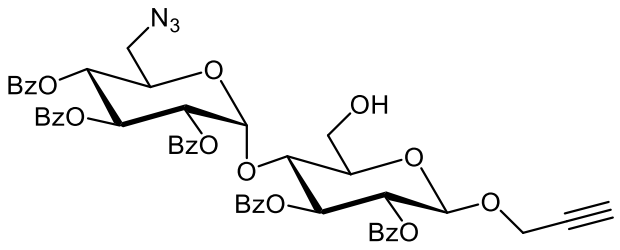

Maltoside **15** (142 mg, 147 µmol) was dissolved in a mixture of CH_2Cl_2 and MeOH (3 mL, 1:1). Then acetyl chloride (94.2 µL, 1.32 mmol) was added dropwise, at 0 °C, and the mixture was stirred for 16 h at RT. Afterwards, the reaction mixture was neutralized by adding triethylamine and the volatiles were removed under reduced pressure. The solid residue was suspended in ethyl acetate and the insoluble solid was filtered off. The filtrate was concentrated and purified by column chromatography (cyclohexane/ethyl acetate, 3:1→7:3) to afford **16** (103 mg, 76 %) as a colorless solid; R_f 0.31 (cyclohexane/ethyl acetate, 3:2); $[\alpha]^{20}_D$ = +18.6 (*c* 0.01, CH_2Cl_2); IR (ATR): ν_{max}/cm^{-1} = 2923, 2105, 1725, 1451, 1263, 1091, 1025, 706, 685; ^{1}H NMR (600 MHz, $CDCl_3$, 300 K): δ = 7.97-7.63 (m, 10H, 10 Bz*ortho*), 7.56-7.18 (m, 15H, 10 BZ*meta,* 5 Bz*para*), 6.01 (t, $^3J_{2',3'}$ = 10.1 Hz, $^3J_{3',4'}$ = 10.1 Hz, 1H, H-3'), 5.76 (t, $^3J_{2,3}$ = 9.5 Hz, $^3J_{3,4}$ = 9.5 Hz, 1H, H-3), 5.73 (d, $^3J_{1,2}$ = 4.0 Hz, 1H, H-1'), 5.49 (t, $^3J_{3',4'}$ = 9.8 Hz, $^3J_{4',5'}$ = 9.8 Hz, 1H, H-4'), 5.32 (dd, $^3J_{2,3}$ = 9.7 Hz, $^3J_{1,2}$ = 7.8 Hz, 1H H-2), 5.20 (dd, $^3J_{2,3}$ = 10.5 Hz, $^3J_{1,2}$ = 4.0 Hz, 1H, H-2'), 5.05 (d, $^3J_{1,2}$ = 7.8 Hz, 1H, H-1), 4.51 (t, $^3J_{3,4}$ = 9.3 Hz, $^3J_{4,5}$ = 9.3 Hz, 1H, H-4), 4.43 (dd, $^2J_{OCH,OCH'}$ = 16.0 Hz, $^4J_{OCH,C\equiv CH}$ = 2.4 Hz, 1H, O*CH*$_2$), 4.35 (dd, $^2J_{OCH,OCH'}$ = 16.0 Hz, $^4J_{OCH,C\equiv CH}$ = 2.4 Hz, 1H, O*CH*$_2$), 4.30 (ddd, $^3J_{4',5'}$ = 10.0 Hz, $^3J_{5',6a'}$ = 5.3 Hz, $^3J_{5',6b'}$ = 2.7 Hz, 1H, H-5'), 4.14 (dd, $^2J_{6a,6b}$= 12.3 Hz, $^3J_{5,6b}$ = 2.0 Hz, 1H, H-6b), 4.08 (dd, $^2J_{6a,6b}$ = 12.3 Hz, $^3J_{5,6a}$ = 3.4 Hz, 1H, H-6a), 3.85-3.79 (m, 1H, H-5), 3.59 (dd, $^2J_{6'A,6'B}$ = 13.4 Hz, $^3J_{5',6'B}$ = 2.7 Hz, 1H, H-6b'), 3.48 (dd, $^2J_{6'A,6'B}$ = 13.4 Hz, $^3J_{5',6'A}$ = 5.4 Hz, 1H, H-6a'), 2.40 (t, $^4J_{OCH',C\equiv CH}$ = 2.4 Hz, $^4J_{OCH,C\equiv CH}$ = 2.4 Hz, 1H, C≡C*H*) ppm; ^{13}C NMR (125 MHz, $CDCl_3$, 300 K): δ = 165.8, 165.6, 165.4, 165.4, 165.3 (5 C(O)Ph), 133.7, 133.4, 133.4, 133.3, 133.2 (5 Bz-CH*para*), 130.1, 130.0, 130.0, 129.9, 129.7 (10 Bz-CH*ortho(a,b)*), 129.3, 129.0, 128.9, 128.8, 128.7 (5 Bz-C$_q$), 128.6, 128.4, 128.4, 128.3, 128.2 (10 Bz-CH*meta(a,b)*), 98.7 (C-1'), 96.1 (C-1), 78.5 (OCH$_2$≡CH), 75.7 (C-5), 75.2 (C-3), 72.1 (C-2), 71.3 (C-4), 70.9 (C-2'), 70.2 (C-5'), 70.0 (C-4'), 70.0 (C-3'), 61.6 (C-6), 56.4 (OCH$_2$≡CH), 51.3 (C-6') ppm; ESI-HRMS: *m/z* = 948.2590 $[M+Na]^+$ (calcd *m/z* = 948.2592 for $[M+Na]^+$).

2-Propargyl 6-deoxy-2,3-di-*O*-benzoyl-6-tetrachlorophthalimido-4-*O*-(6'-azido-2',3',4'-tri-*O*-benzoyl-6'-deoxy-α-D-glucopyranosyl)-β-D-glucopyranoside (17)

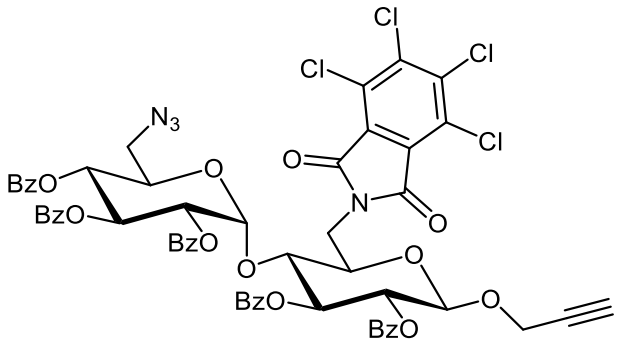

Maltoside **16** (600 mg, 648 µmol) and triphenylphosphine (679 mg, 2.59 mmol) were dissolved in dry THF (30 mL) and 3,4,5,6-tetrachlorophthalimide (554 mg, 1.94 mmol) was added. The solution was cooled to 0 °C and diisopropyl azodicarboxylate (558 µL, 2.59 mmol) was added dropwise. Stirring was continued for 16 h until complete conversion of the starting material. The volatiles were removed under reduced pressure and the crude product was purified by column chromatography on silica gel (cyclohexane/ethyl acetate, 4:1) to give **17** (626 mg, 81 %) as a colorless solid; R_f 0.49 (cyclohexane/ethyl acetate, 3:2); $[\alpha]^{20}_D$ = +28.0 (*c* 0.01, CH_2Cl_2); IR (ATR): ν_{max}/cm^{-1} = 2103, 1721, 1602, 1451, 1370, 1315, 1248, 1177, 1090, 1068, 1025, 739, 705; ^{1}H NMR (500 MHz, $CDCl_3$, 300 K): δ = 8.02-7.95 (m, 2H, 2 Bz*ortho*), 7.86-7.82 (m, 2H, 2 Bz*ortho*), 7.74-7.69 (m, 2H, 2 Bz*ortho*), 7.66-7.62 (m, 2H, 2 Bz*ortho*), 7.61-7.58 (m, 2H, 2 Bz*ortho*), 7.55-7.23 (m, 15H, 10 Bz*meta,* 5 Bz*para*), 6.08 (dd, $^3J_{2',3'}$ = 10.3 Hz, $^3J_{3',4'}$ = 9.5 Hz, 1H, H-3'), 5.74-5.68 (m, 2H, H-3, H-1'), 5.49 (t, $^3J_{3',4'}$ = 9.7 Hz, $^3J_{4',5'}$ = 9.7 Hz, 1H, H-4'), 5.34-5.28 (m, 2H, H-2, H-2'), 4.97 (d, $^3J_{1,2}$ = 7.3 Hz, 1H, H-1), 4.56 (ddd, $^3J_{4',5'}$ = 9.7 Hz, $^3J_{5',6a'}$ = 6.2 Hz, $^3J_{5',6b'}$ = 2.7 Hz, 1H, H-5'), 4.36 (dd, $^2J_{6a,6b}$ = 13.6 Hz, $^3J_{5,6b}$ = 2.8 Hz, 1H, H-6b), 4.33-4.19 (m, 5H, H-4, H-5, H-6a, OCH_2), 3.56 (dd, $^2J_{6a',6b'}$ = 13.3 Hz, $^3J_{5',6b'}$ = 2.7 Hz, 1H, H-6b'), 3.51 (dd, $^2J_{6a',6b'}$= 13.4 Hz, $^3J_{5',6a'}$ = 6.1 Hz, 1H, H-6a'), 2.27 (t, $^4J_{OCH',C\equiv CH}$ = 2.4 Hz, $^4J_{OCH,C\equiv CH}$ = 2.4 Hz, 1H, C≡C*H*) ppm; ^{13}C NMR (125 MHz, $CDCl_3$, 300 K): δ = 165.61, 165.59, 165.44, 165.27, 165.06 (5 C(O)Ph), 163.50 (2 C(O)TCP), 140.46 (2 TCP-CCl), 138.02 (2 TCP-C_q) 133.78, 133.32, 133.28, 133.22, 133.22 (5 Bz-CH_{para}), 130.17, 130.06, 130.00, 129.80, 129.69 (10 Bz-C$H_{ortho(a,b)}$), 129.25, 129.18, 129.00, 128.77, 128.71 (5 Bz-C_q), 128.62, 128.37, 128.34, 128.32, 128.15 (10 Bz-C$H_{meta(a,b)}$), 127.68 (2 TCP-CCl), 97.52 (C-1), 97.47 (C-1'), 77.58 (C-4), 75.65 ($OCH_2\equiv CH$), 74.89 (C-3), 72.18 (C-2), 71.77 (C-5), 70.90 (C-2'), 70.63 (C-5'), 70.02 (C-4'), 69.82 (C-3'), 55.49 ($OCH_2\equiv CH$), 51.57 (C-6'), 40.67 (C-6) ppm; ESI-HRMS: *m/z* = 1213.1243 $[M+Na]^+$ (calcd *m/z* = 1213.1242 for $[M+Na]^+$).

2-Propargyl 2,3-di-*O*-benzoyl-6-deoxy-6-[3-(2,3,4,6-tetra-*O*-acetyl-α-D-mannopyranosyloxy)acetamido]-4-*O*-(6'-azido-2',3',4'-tri-*O*-benzoyl-6'-deoxy-*α*-D-glucopyranosyl)-*β*-D-glucopyranoside (19)

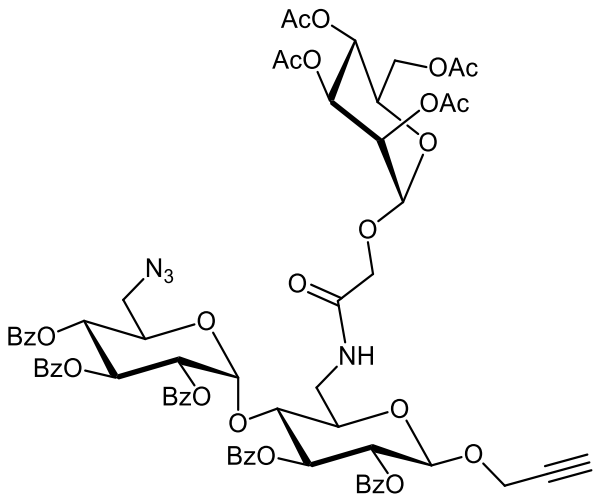

The maltoside scaffold **17** (500 mg, 419 µmol) and the carboxymethylmannoside **4** (341 mg, 838 µmol) were reacted according to the general procedure C using ethylenediamine (56.0 µL, 838 µmol), NHS (120 mg, 1.48 mmol), EDC·HCl (200 mg, 1.48 mmol), DIPEA (356 µL, 2.10 mmol). Flash chromatography with cyclohexane/ethyl acetate (1:1) yielded the protected glycocluster **19** (330 mg, 60 %) as an amorphous solid; R_f 0.40 (cyclohexane/ethyl acetate, 2:3); $[\alpha]^{20}_D$ = +35.4 (*c* 0.01, CH_2Cl_2); IR (ATR): ν_{max}/cm^{-1} = 3330, 2105, 1732, 1676, 1537, 1451, 1369, 1246, 1090, 1067, 1025, 707 cm^{-1}; ^{1}H NMR (500 MHz, $CDCl_3$, 300 K): δ = 7.98-7.94 (m, 2H, Bz*ortho*), 7.86-7.81 (m, 2H, Bz*ortho*), 7.71-7.66 (m, 2H, Bz*ortho*), 7.63-7.59 (m, 2H, Bz*ortho*), 7.55-7.49 (m, 3H, Bz*ortho*, Bz*para*), 7.47-7.28 (m, 8H, Bz*meta,* Bz*para*), 7.24-7.15 (m, 6H, Bz*meta*), 7.03 (dd, $^3J_{NH,6a}$ = 7.7 Hz, $^3J_{NH,6b}$ = 3.7 Hz, 1H, N*H*), 6.01 (dd, $^3J_{2',3'}$ = 10.4 Hz, $^3J_{3',4'}$ = 9.6 Hz, 1H, H-3'), 5.75-5.68 (m, 2H, H-1', H-3), 5.51 (t, $^3J_{3',4'}$ = 9.8 Hz, $^3J_{4',5'}$ = 9.8 Hz, 1H, H-4'), 5.40-5.27 (m, 5H, H-2$_{Man}$, H-2, H-2', H-4$_{Man}$, H-3$_{Man}$), 5.08 (d, $^3J_{1,2}$ = 7.7 Hz, 1H, H-1), 4.95 (d, $^3J_{1,2}$ = 1.2 Hz, 1H, H-1$_{Man}$), 4.47-4.40 (m, 2H, H-5', OCH_2), 4.40-4.23 (m, 4H, OCH_2, H-6b, H-6a$_{Man}$, Man-OCH_2), 4.23-4.11 (m, 3H, H-4, H-6b$_{Man}$, Man-OCH_2), 4.04-4.00 (m, 1H, H-5$_{Man}$), 3.99-3.94 (m, 1H, H-5), 3.66 (dd, $^2J_{6a',6b'}$ = 13.4 Hz, $^3J_{5',6b'}$ = 2.5 Hz, 1H, H-6b'), 3.54 (dd, $^2J_{6a',6b'}$ = 13.5 Hz, $^3J_{5',6a'}$ = 5.7 Hz, 1H, H-6a'), 3.48 (ddd, $^2J_{6a,6b}$ = 13.8 Hz, $^3J_{NH,6a}$ = 7.5 Hz, $^3J_{5,6a}$ = 4.1 Hz, 1H, H-6a), 2.44 (t, $^4J_{OCH',C\equiv CH}$ = 2.4 Hz, $^4J_{OCH,C\equiv CH}$ = 2.4 Hz, 1H, C≡C*H*), 2.20, 2.11, 2.06, 2.02, (each s, each 3H, 4 OAc) ppm; ^{13}C NMR (125 MHz, $CDCl_3$, 300 K): δ = 170.60, 170.11, 169.85, 169.69 (4 C(O)CH_3), 168.10 (NHC(O)), 165.51,165.33, 165.30, 165.17, 164.92 (5 C(O)Ph), 133.54, 133.13, 133.07, 133.01, 133.01 (5 Bz-CH_{para}), 130.01, 129.94, 129.82, 129.62, 129.51 (10 Bz-C$H_{ortho(a,b)}$), 129.21, 128.83, 128.60, 128.59, 128.24 (5 Bz-C_q), 128.46, 128.14, 128.11, 128.11, 127.93 (10 Bz-C$H_{meta(a,b)}$), 98.10 (C-1), 97.55 (C-1'), 97.44 (C-1$_{Man}$), 78.68 (OCH$_2$C≡CH), 76.04 (C-4), 75.32 (OCH$_2$C≡CH), 74.78 (C-3), 73.38 (C-5), 71.98 (C-2'), 70.55 (C-2), 70.41 (C-5'), 69.75 (C-3'), 69.63 (C-4'), 69.38 (C-5$_{Man}$), 69.22 (C-2$_{Man}$), 68.75 (C-3$_{Man}$), 66.73 (Man-OCH$_2$), 65.74 (C-4$_{Man}$), 62.32 (C-6$_{Man}$), 56.22

(O<u>C</u>H$_2$C≡CH), 51.13 (C-6'), 40.20 (C-6), 20.84, 20.73, 20.66, 20.65 (4 C(O)<u>C</u>H$_3$) ppm; ESI-HRMS: *m/z* = 1335.3747 $[M+Na]^+$ (calcd *m/z* = 1335.3751 for $[M+Na]^+$).

2-Propargyl 2,3-di-*O*-benzoyl-6-deoxy-6-[3-(2,3,4,6-tetra-*O*-acetyl-β-D-glucopyranosyloxy)acetamido]-4-*O*-(6'-azido-2',3',4'-tri-*O*-benzoyl-6'-deoxy-*α*-D-glucopyranosyl)-*β*-D-glucopyranoside (20)

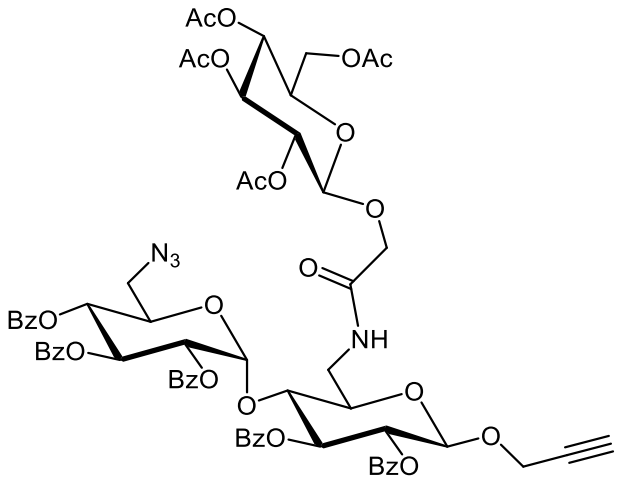

The maltoside scaffold **17** (250 mg, 210 µmol) and the carboxymethylglucoside **5** (171 mg, 420 µmol) were reacted according to the general procedure C using ethylenediamine (30.8 µL, 420 µmol), NHS (60.3 mg, 524 µmol), EDC·HCl (100 mg, 524 µmol) and DIPEA (179 µL, 1.05 mmol). Flash chromatography with cyclohexane/ethyl acetate (1:1) yielded the protected glycocluster **19** (176 mg, 64 %) as an amorphous solid; R_f 0.31 (cyclohexane/ethyl acetate, 2:3); $[\alpha]^{20}_D$ = +12.1 (*c* 0.01, CH_2Cl_2); IR (ATR): ν_{max}/cm^{-1} = 2103, 1732, 1683, 1602, 1532, 1451, 1368, 1247, 1218, 1177, 1091, 1067, 1026, 706; ^{1}H NMR (500 MHz, $CDCl_3$, 300 K): δ = 7.99-7.96 (m, 2H, Bz*ortho*), 7.86-7.81 (m, 2H, Bz*ortho*), 7.73-7.69 (m, 2H, Bz*ortho*), 7.68-7.64 (m, 2H, Bz*ortho*), 7.58-7.54 (m, 2H, Bz*ortho*), 7.53-7.28 (m, 9H, Bz*meta,* Bz*para*), 7.25-7.15 (m, 6H, Bz*meta*), 7.03 (t, $^3J_{NH,6a}$ = 5.6 Hz, $^3J_{NH,6b}$ = 5.6 Hz, 1H, N*H*), 6.01 (dd, $^3J_{2',3'}$ = 10.1 Hz, $^3J_{3',4'}$ = 9.7 Hz, 1H, H-3'), 5.72 (t, $^3J_{2,3}$ = 9.3 Hz, $^3J_{3,4}$ = 9.3 Hz, 1H, H-3), 5.68 (d, $^3J_{1',2'}$ = 4.0 Hz, 1H, H-1'), 5.50 (t, $^3J_{3',4'}$ = 9.8 Hz, $^3J_{4',5'}$ = 9.8 Hz, 1H, H-4'), 5.43 (dd, $^3J_{2,3}$ = 9.6 Hz, $^3J_{1,2}$ = 7.8 Hz, 1H, H-2), 5.28 (t, $^3J_{2,3}$ = 9.6 Hz, $^3J_{3,4}$ = 9.6 Hz, 1H, H-3$_{Glc}$), 5.22 (dd, $^3J_{2',3'}$ = 10.5 Hz, $^3J_{1',2'}$ = 4.0 Hz, 1H, H-2'), 5.13-5.04 (m, 3H, H-1, H-2$_{Glc}$, H-4$_{Glc}$,), 4.58 (d, $^3J_{1,2}$ = 7.9 Hz, 1H, H-1$_{Glc}$), 4.51 (dd, $^2J_{OCH,OCH'}$ = 16.1 Hz, $^4J_{OCH,C≡CH}$ = 2.4 Hz 1H, OC*H*$_2$), 4.44-4.37 (m, 3H, H-5', OC*H*$_2$, Glc-OC*H*$_2$), 4.34 (dd, $^2J_{6a,6B}$ = 12.4 Hz, $^3J_{5,6a}$ = 5.0 Hz, 1H, H-6a$_{Glc}$), 4.19 (t, $^3J_{3,4}$ = 9.2 Hz, $^3J_{4,5}$ = 9.2 Hz, 1H, H-4), 4.16-4.04 (m, 3H, H-6b, H-6b$_{Glc}$, Glc-OC*H*$_2$), 3.98-3.91 (m, 1H, H-5), 3.79-3.74 (m, 1H, H-5$_{Glc}$), 3.68 (dt, $^2J_{6a,6b}$ = 13.6 Hz, $^3J_{NH,6a}$ = 5.9 Hz, $^3J_{5,6a}$ = 5.9 Hz, 1H, H-6a), 3.59 (dd, $^2J_{6a',6b'}$ = 13.6 Hz, $^3J_{5',6b'}$ = 2.5 Hz, 1H, H-6b'), 3.47 (dd, $^2J_{6a',6b'}$ = 13.4 Hz, $^3J_{5',6a'}$ = 5.5 Hz, 1H, H-6a'), 2.50 (t, $^4J_{OCH',C≡CH}$ = 2.4 Hz, $^4J_{OCH,C≡CH}$ = 2.4 Hz, 1H, C≡C*H*), 2.17, 2.12, 2.04, 2.03, (each s, each 3H, 4 OAc) ppm; ^{13}C NMR (125 MHz, $CDCl_3$, 300 K): δ = 170.57,

170.14, 169.61, 169.42 (4 C(O)CH_3), 168.56 (NHC(O)), 165.51, 165.41, 165.32, 165.32, 164.94 (5 C(O)Ph), 133.51, 133.16, 133.12, 133.02, 133.01 (5 Bz-CH_{para}), 130.04, 129.94, 129.81, 129.58, 129.53 (10 Bz-C$H_{ortho(a,b)}$), 129.21, 128.89, 128.73, 128.62, 128.39 (5 Bz-C_q), 128.45, 128.16, 128.15, 128.13, 128.00 (10 Bz-C$H_{meta(a,b)}$), 100.47 (C-1_{Glc}), 98.13 (C-1), 96.85 (C-1'), 78.42 (OCH_2C≡CH), 75.80 (OCH_2C≡CH), 75.12 (C-3), 76.64 (C-4), 73.13 (C-5), 72.23 (C-5_{Glc}), 72.15 (C-3_{Glc}), 71.77 (C-2), 71.19 (C-2_{Glc}), 70.83 (C-2'), 70.19 (C-5'), 69.64 (C-3'), 69.55 (C-4'), 68.48 (Glc-OCH_2), 68.25 (C-4_{Glc}), 61.71 (C-6_{Glc}), 56.17 (OCH_2C≡CH), 51.17 (C-6'), 40.04(C-6), 20.75, 20.75, 20.62, 20.57 (4 C(O)CH_3) ppm; ESI-HRMS: *m/z* = 1335.3745 $[M+Na]^+$ (calcd *m/z* = 1335.3751 for $[M+Na]^+$).

2-Propargyl 6-acetamido-2,3-di-*O*-benzoyl-6-deoxy-4-*O*-(6'-azido-2',3',4'-tri-*O*-benzoyl-6'-deoxy-*α*-D-glucopyranosyl)-*β*-D-glucopyranoside (23)

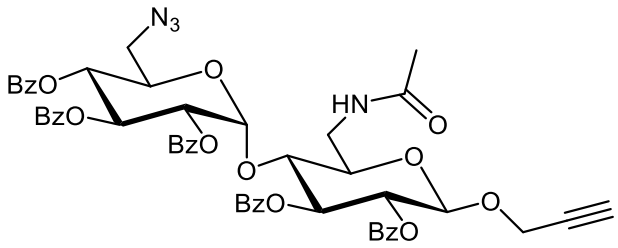

Maltoside **17** (200 mg, 168 µmol) was dissolved in a mixture of acetonitrile/tetrahydrofuran (4:1, 2.5 mL) and ethylenediamine (22.0 µL, 336 µmol) was added. It was stirred for 3 h at 55 °C. Then the solvent was removed under reduced pressure and it was co-evaporated with toluene (3 x). The crude product was dissolved in dry pyridine (3.00 mL) and acetic anhydride (1.5 mL) was added. It was stirred at RT for 16 h. Afterwards it was diluted with ethyl acetate and washed with 1 M HCl, sodium bicarbonate and brine. The organic layer was dried over magnesium sulfate, it was filtered and concentrated to dryness. The crude product was purified by column chromatography on silica gel (cyclohexane/ethyl acetate, 1:1) to give **23** (114 mg, 70 %) as a colorless solid; R_f 0.44 (cyclohexane/ethyl acetate, 1:1); $[\alpha]^{20}_D$ = +59.6 (*c* 0.01, CH_2Cl_2); IR (ATR): ν_{max}/cm^{-1} = 3324, 2929, 2850, 1733, 1625, 1573, 1451, 1369, 1244, 1088, 1069, 1026, 707; ^{1}H NMR (600 MHz, $CDCl_3$, 300 K): δ = 8.01-7.94 (m, 2H, Bz_{ortho}), 7.87-7.82 (m, 2H, Bz_{ortho}), 7.73-7.64 (m, 4H, Bz_{ortho}), 7.61-7.55 (m, 2H, Bz_{ortho}), 7.54-7.19 (m, 15H, $Bz_{meta,}$ Bz_{para}), 6.05-5.98 (m, 2H, N*H*Ac, H-3'), 5.71 (t, $^3J_{2,3}$ = 9.2 Hz, $^3J_{3,4}$ = 9.2 Hz, 1H, H-3), 5.682 (d, $^3J_{1',2'}$ = 4.0 Hz, 1H, H-1'), 5.53 (t, $^3J_{3',4'}$ = 9.8 Hz, $^3J_{4',5'}$ = 9.8 Hz, 1H, H-4'), 5.29 (dd, $^3J_{2,3}$ = 9.6 Hz, $^3J_{1,2}$ = 7.8 Hz, 1H, H-2), 5.24 (dd, $^3J_{2',3'}$ = 10.5 Hz, $^3J_{1',2'}$ = 4.0 Hz, 1H, H-2'), 5.02 (d, $^3J_{1,2}$ = 7.7 Hz, 1H, H-1), 4.47-4.39 (m, 2H, H-5', OCH_2), 4.35 (dd, $^2J_{OCH',OCH}$ = 16.0 Hz, $^4J_{OCH,C≡CH}$ = 2.4 Hz, 1H, OCH_2), 4.19 (t, $^3J_{3,4}$ = 9.1 Hz, $^3J_{4,5}$ = 9.1 Hz, 1H, H-4), 4.04 (ddd, $^2J_{6a,6b}$ = 13.9 Hz, $^3J_{5,6a}$ = 5.3 Hz, $^3J_{NH,6a}$ = 3.4 Hz,1H, H-6a), 3.93 (ddd, $^3J_{4,5}$ = 9.3 Hz, $^3J_{5,6a}$ = 5.9 Hz, $^3J_{5,6b}$ = 3.3 Hz, 1H, H-5), 3.69-3.61 (m, 2H, H-6b, H-6a'), 3.49 (dd, $^2J_{6a',6b'}$ = 13.5 Hz, $^3J_{5',6b'}$ =

5.16 Hz, 1H, H-6b'), 2.44 (t, $^{4}J_{OCH',C\equiv CH}$ = 2.4 Hz, $^{4}J_{OCH,C\equiv CH}$ = 2.4 Hz, 1H, C≡C*H*), 2.09 (s, 3H, NHAc) ppm; ^{13}C NMR (125 MHz, $CDCl_3$, 300 K): δ = 170.49 (NH<u>C</u>(O)CH_3), 165.71, 165.50, 165.45, 165.41, 165.06 (5 <u>C</u>(O)Ph), 133.66, 133.33, 133.31, 133.26, 133.17 (5 Bz-<u>C</u>H*$_{para}$*), 130.18, 130.10, 129.98, 129.77, 129.69 (10 Bz-<u>C</u>H*$_{ortho(a,b)}$*), 129.21, 129.04, 128.77, 128.76, 128.55 (5 Bz-<u>C</u>$_q$), 128.60, 128.37, 128.34, 128.29, 128.15 (10 Bz-<u>C</u>H*$_{ortho(a,b)}$*), 98.72 (C-1), 97.03 (C-1'), 78.54 (OCH_2<u>C</u>≡CH), 75.69 (OCH_2C≡<u>C</u>H), 74.99 (C-3), 74.79 (C-4), 73.44 (C-5), 71.97 (C-2), 70.94 (C-2'), 70.37 (C-5'), 69.85 (C-3'), 69.58 (C-4'), 56.63 (O<u>C</u>H_2C≡CH), 51.20 (C-6'), 40.58 (C-6), 23.54 (NHC(O)<u>C</u>H_3) ppm; ESI-HRMS: *m/z* = 967.3029 $[M+H]^+$ (calcd *m/z* = 967.3032 for $[M+H]^+$).

2-Propargyl 6-acetamido-2,3-di-O-benzoyl-6-deoxy-4-*O*-[2',3',4'-tri-*O*-benzoyl-6'-deoxy-6'-[3-(2,3,4,6-tetra-*O*-acetyl-α-D-mannopyranosyloxy)acetamido]]-*α*-D-glucopyranosyl)-*β*-D-glucopyranoside (24)

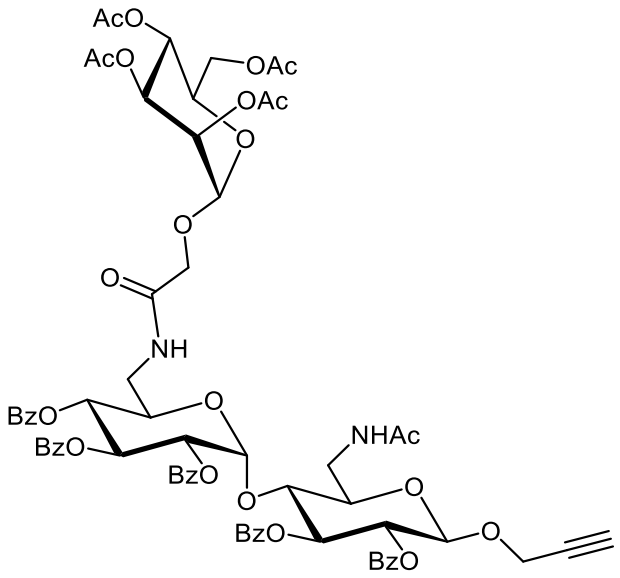

The azido-functionalized glycoside **23** (80 mg, 82.7 µmol) and the carboxymethylmannoside **4** (67.0 mg, 165 µmol) were reacted according to the general procedure A using NHS (28.5 mg, 248 µmol), EDC·HCl (47.5 mg, 248 µmol), PMe_3 (1 M in THF, 414 µL) in THF (5.00 mL). Flash chromatography with cyclohexane/ethyl acetate (1:9) yielded the protected target glycocluster **24** (55.0 mg, 50 %) as an amorphous solid; R_f 0.24 (cyclohexane/ethyl acetate, 1:9); $[\alpha]^{20}_D$ = +59.6 (*c* 0.01, CH_2Cl_2); IR (ATR): ν_{max}/cm^{-1} = 3324, 2929, 2850, 1733, 1625, 1573, 1451, 1369, 1244, 1088, 1069, 1026, 707; ^{1}H NMR (600 MHz, $CDCl_3$, 300 K): δ = 7.99-7.92 (m, 2H, Bz*$_{ortho}$*), 7.86-7.80 (m, 2H, Bz*$_{ortho}$*), 7.71-7.64 (m, 2H, Bz*$_{ortho}$*), 7.63-7.55 (m, 3H, Bz*$_{para}$*, Bz*$_{ortho}$*), 7.53-7.28 (m, 11H, Bz*$_{ortho}$*, Bz*$_{meta}$*, Bz*$_{para}$*, N*H*), 7.23-7.11 (m, 6H, Bz*$_{meta}$*), 6.34 (dd, $^3J_{NH,6a}$ = 5.8 Hz, $^3J_{NH,6b}$ = 5.1 Hz, 1H, N*H*), 6.00 (t, $^3J_{2',3'}$ = 10.1 Hz, $^3J_{3',4'}$ = 10.1 Hz, 1H, H-3'), 5.69 (t, $^3J_{2,3}$ = 9.2 Hz, $^3J_{3,4}$ = 9.2 Hz, 1H, H-3), 5.62 (d, $^3J_{1',2'}$ =

4.1 Hz, 1H, H-1'), 5.51 (dd, $^{3}J_{2,3}$ = 3.4 Hz, $^{3}J_{3,4}$ = 10.1 Hz, 1H, H-3$_{Man}$), 5.43-5.37 (m, 2H, H-4', H-2$_{Man}$), 5.37-5.27 (m, 3H, H-2, H-2', H-4$_{Man}$), 5.00 (d, $^{3}J_{1,2}$ = 7.7 Hz, 1H, H-1), 4.89 (d, $^{3}J_{1,2}$ = 0.9 Hz, 1H, H-1$_{Man}$), 4.49-4.38 (m, 2H, H-5', OC*H*$_2$), 4.38-4.30 (m, 2H, H-6a$_{Man}$, OC*H*$_2$), 4.26-4.06 (m, 5H, H-4, H-6a, H-5$_{Man}$, H-6b$_{Man}$, Man-OC*H*$_2$), 3.97-3.87 (m, 3H, H-5, H-6a', Man-OC*H*$_2$), 3.56-3.41 (m, 2H, H-6b, H-6b'), 2.46 (t, $^{4}J_{OCH',C\equiv CH}$ = 2.4 Hz, $^{4}J_{OCH,C\equiv CH}$ = 2.4 Hz, 1H, C≡C*H*), 2.17, 2.12, 2.09, 1.96, 1.96 (each s, each 3H, 4 OAc, NHAc) ppm; ^{13}C NMR (125 MHz, $CDCl_3$, 300 K): δ = 170.97, 170.83, 170.27, 170.16 (4 C(O)CH$_3$), 169.90, 168.17 (2 NHC(O)), 165.98, 165.77, 165.36, 165.36, 164.97 (5 C(O)Ph), 133.63, 133.23, 133.19, 133.18, 133.10 (5 Bz-CH$_{para}$), 130.23, 130.09, 129.97, 129.75, 129.69 (10 Bz-CH$_{ortho(a,b)}$), 129.31, 129.07, 128.85, 128.69, 128.44 (5 Bz-C$_q$), 128.54, 128.31, 128.22, 128.20, 128.02 (10 Bz-CH$_{ortho(a,b)}$), 98.61 (C-1), 98.23 (C-1'), 97.47 (C-1$_{Man}$), 78.60 (OCH$_2$C≡CH), 76.37 (OCH$_2$C≡CH), 75.65 (C-4), 75.03 (C-3), 73.45 (C-5), 72.09 (C-2'), 70.72 (C-2), 70.54 (C-3'), 69.95 (C-5'), 69.91 (C-4'), 69.61 (C-5$_{Man}$), 69.37 (C-2$_{Man}$), 68.90 (C-3$_{Man}$), 66.78 (C-6$_{Man}$), 65.97 (C-4$_{Man}$), 62.42 (Man-OCH$_2$), 56.42 (OCH$_2$C≡CH), 41.27 (C-6), 39.11 (C-6'), 23.36 (NHC(O)CH$_3$), 21.02, 20.93, 20.78, 20.78 (4 C(O)CH$_3$) ppm; ESI-HRMS: *m/z* = 1351.3948 $[M+Na]^+$ (calcd *m/z* = 1351.3952 for $[M+Na]^+$).

2-Propargyl 6-acetamido-6-deoxy-4-*O*-[6'-deoxy-6'-[3-(α-D-mannopyranosyloxy)acetamido]]-*α*-D-glucopyranosyl-*β*-D-glucopyranoside (25)

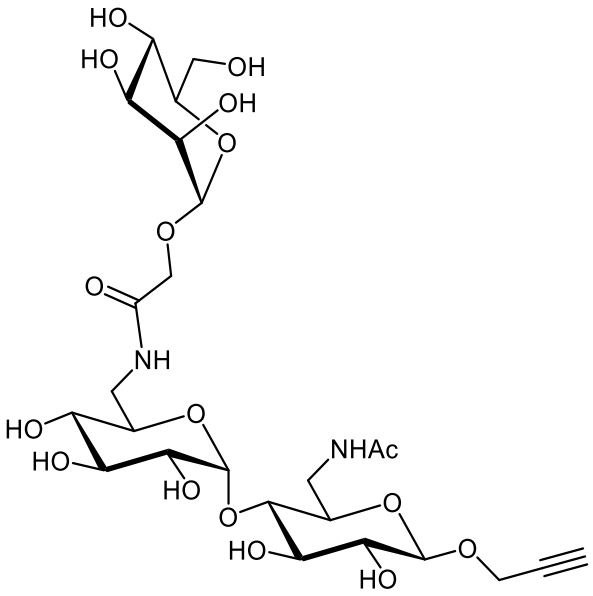

The protected glycocluster **24** (70.0 mg, 52.7 µmol) was deprotected according to general procedure B using NaOMe (5.4 M in MeOH) in MeOH (*c* = 0.03 M). The target glycocluster **25** (30.4 mg, 90 %) was obtained as a colorless foam after lyophilisation; R_f 0.05 (CH_2Cl_2/MeOH, 8:2); $[\alpha]^{20}_D$ = -42.1 (*c* 0.01, H_2O); IR (ATR): ν_{max}/cm^{-1} = 3286, 2004, 1648, 1541, 1364, 1044, 673; ^{1}H NMR (600 MHz, D_2O, 300 K): δ = 5.37 (d, $^{3}J_{1',2'}$ = 3.9 Hz, 1H, H-1'), 4.88 (d, $^{3}J_{1,2}$ = 1.1 Hz, 1H, H-1$_{Man}$), 4.62 (d, $^{3}J_{1,2}$ = 8.0 Hz, 1H, H-1), 4.49-4.40 (m, 2H, OC*H*$_2$), 4.24 (d, $^{2}J_{OCH,OCH'}$ = 15.4 Hz, 1H, Man-OC*H*$_2$), 4.07 (d, $^{2}J_{OCH,OCH'}$ = 15.4 Hz, 1H, Man-OC*H*$_2$), 4.04 (dd, $^{3}J_{2,3}$ = 3.3 Hz, $^{3}J_{1,2}$ = 1.7 Hz, 1H, H-

2_{Man}), 3.90-3.84 (m, 2H, H-6a$_{Man,}$ H-3$_{Man}$), 3.83-3.65 (m, 7H, H-3, H-6a, H-3', H-5', H-6a', H-4$_{Man}$, H-6b$_{Man}$), 3.63-3.58 (m, 3H, H-2', H-5, H-5$_{Man}$), 3.47 (t, $^{3}J_{3,4}$ = 9.2 Hz, $^{3}J_{4,5}$ = 9.2 Hz, 1H, H-4), 3.42 (dd, $^{2}J_{6a',6b'}$ = 14.1 Hz, $^{3}J_{5',6b'}$ = 7.4 Hz, H-6b'), 3.34 (dd, $^{3}J_{2,3}$ = 9.4, Hz, $^{3}J_{1,2}$ = 8.1 Hz, H-2), 3.28 (t, $^{3}J_{3',4'}$ = 9.6 Hz, $^{3}J_{4',5'}$ = 9.6 Hz, 1H, H-4'), 3.19 (dd, $^{2}J_{6a,6b}$ = 14.1 Hz, $^{3}J_{5,6b}$ = 8.6 Hz, H-6b), 2.93 (t, $^{4}J_{OCH',C\equiv CH}$ = 2.4 Hz, $^{4}J_{OCH,C\equiv CH}$ = 2.4 Hz, 1H, C≡C*H*), 2.03 (s, 3H, NHAc) ppm; ^{13}C NMR (125 MHz, D_2O, 300 K): δ = 174.06 (NH<u>C</u>(O)CH_3), 171.64 (NH<u>C</u>(O)-Man), 100.26 (C-1), 99.89 (C-1'), 99.86 (C-1$_{Man}$), 79.18 (C-4), 76.04 (C-3), 73.22 (C-2'), 72.83 (C-3'), 72.67 (C-2), 72.42 (C-5), 71.57 (C-5'), 71.31 (C-5$_{Man}$), 71.22 (C-4'), 70.35 (C-3$_{Man}$), 69.68 (C-2$_{Man}$), 66.52 (C-4$_{Man}$), 65.63 (Man-O<u>C</u>H_2), 60.80 (C-6$_{Man}$), 56.44 (O<u>C</u>H_2C≡CH), 40.52 (C-6), 39.72 (C-6'), 21.85 (NH<u>C</u>(O)CH_3) ppm; ESI-HRMS: *m/z* = 641.2396 $[M+H]^+$ (calcd *m/z* = 641.2399 for $[M+H]^+$).

3 Biological testing

Equipment

The equipment was sterilized in an autoclave before usage. To determine the optical density of the bacterial suspension a Jenway Spectrophotometer Model 7305 was used.

Buffer and bacteria

For the biological testing the following buffers and media were used. All solutions were prepared with bidestilled water and were autoclaved before usage. The solutions were prepared by following procedures:

LB medium: Trypton (10.0 g), sodium chloride (10.0 g) and yeast extract (5.00 g) were dissolved in 1 L bidest. water and then adjusted to pH = 7.0. The solution was autoclaved and afterwards antibiotic (ampicillin (100 mg), chloramphenicol (50.0 mg)) were added.

PBS buffer: Sodium chloride (8.00 g), potassium chloride (200 mg), sodium biphosphate (1.44 g) and potassium biphosphate (200 mg) were dissolved in 1 L bidest. water and the pH value was adjusted to 7.2.

PBST buffer: Tween®20 (0.05% v/v) was added to PBS buffer.

Carbonate buffer (pH 9.6): sodium carbonate (1.59 g) and sodium hydrogen carbonate (2.52 g) were dissolved in distilled deionized water (1.00 L).

Bacteria

For the binding assays the GFP-expressing *E. coli* bacteria strain PKL1162, produced in the laboratory of Per Klemm, was used.[3] This *E. coli* strain PKL1162 was constructed by insertion of the plasmid pPKL1174 into the strain SAR18. The pPKL1174 plasmid contains the *fim* gene cluster, which is responsible for the expression of type 1 fimbriae. SAR18 includes the *gfp* gene in its genome, controlled by a constitutive promoter. The final bacterial strain PKL1162 expresses type 1 fimbriae as the only fimbriae type in addition to green fluorescence protein (GFP) allowing fluorescence read-out.

Cultivation of bacteria

GFP-expressing *E. coli* bacteria (strain PKL1162) were cultured in 5 mL LB medium and incubated overnight at 37 °C and 100 rpm. Afterwards the mixture was centrifuged at 4 °C and 5000 rpm for 15 min. The bacteria pellet was washed twice with PBS buffer (2.00 mL) and then resuspended in PBS buffer. Finally the suspension was adjusted to OD_{600} = 0.4.

Mannan coating of microtiter plates

The published assay[4] was adapted and modified as follows: Black 96-well microtiter plates (Nunc™, Maxisorp®) were incubated with a solution of mannan from Saccharomyces cerevisiae (1.2 mg/mL in carbonate buffer, 120 µL/well) and desiccated overnight at 37 °C and 100 rpm. Then the plates were washed with PBST (3 x 150 µL/well) and blocked with polyvinyl alcohol (PVA) (1% in PBS, 120 µL/well) at 37 °C and 120 rpm for 2 h. Afterwards the microtiter plates were washed with PBST (3 x 150 µL/well).

Inhibition assay with GFP-PKL1162 *E. coli* bacteria

Inhibitor solutions of the respective glycosides **1**, **2**, **3**, and **25** (20 mM in PBS buffer) as well as methyl α-D-mannopyranoside (MeMan, 200 mM in PBS buffer) were prepared and serial dilutions (1:2, 10 steps) of each solution added to the mannan-coated microtiter plates (50 µL/well). Next, the prepared bacterial suspension (OD_{600} = 0.4, 50 µL/well) was added and the microtiter plates were incubated at 37 °C and 100 rpm for 45 min. The plates were washed with PBS buffer (3 x 150 µL/well) and then the wells were filled with PBS (100 µL/well) and the fluorescence intensity (485 nm/ 535 nm) was determined. On each individual plate the standard inhibitor MeMan was tested in parallel. Each compound was tested in duplicates or triplicates, respectively.

Inhibition curves of adhesion-inhibition assay with GFP expressing *E. coli* bacteria.

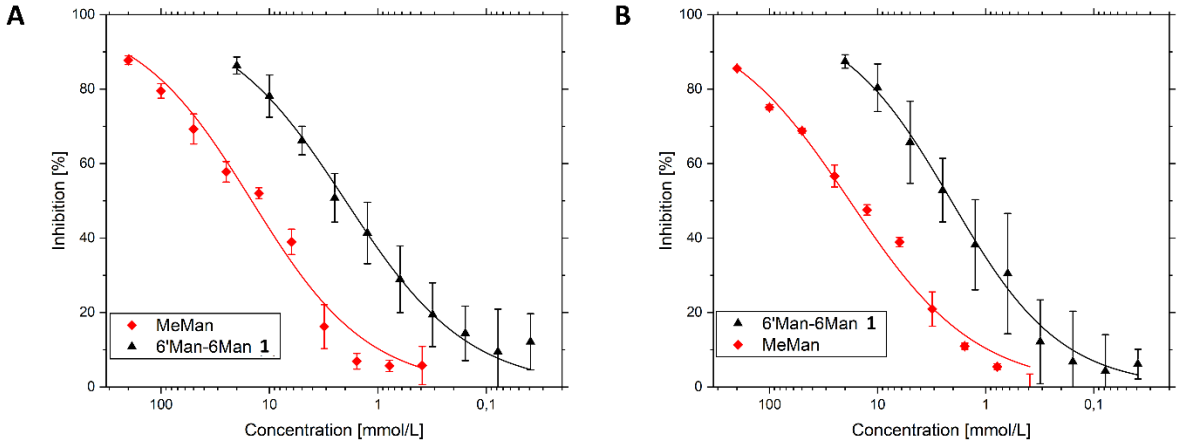

Figure S3.1 Inhibition curves obtained with maltoside **1** as inhibitor of type 1 fimbriae-mediated bacterial adhesion to mannan. MeMan was tested in parallel on the same plate. Sigmoidal dose-responsive inhibition curves were fitted by non-linear regression. Error bars are standard deviations from duplicate or triplicate results on one plate.

Table S3.1 IC_{50} values and corresponding RIP values as deduced from the inhibition curves obtained with MeMan and the glycocluster **6'Man-6Man** (**1**).

Plate	Entry	MeMan	6'Man-6Man (1)
A	IC_{50}[a] [mmol]	14.57 (±1.58)	1.98 (±0.13)
	RIP[b]	1.00	7.34 (±1.28)
B	IC_{50}[a] [mmol]	18.12 (±1.61)	2.08 (±0.15)
	RIP[b]	1.00	8.71 (±1.40)
	Mean RIP[c]	1.00	8.03 (±1.39)

[a] IC_{50} values are average values of duplicate or triplicate results on one plate; fitting errors are given in brackets.

[b] RIP values are based on the inhibitory potency of methyl α-D-mannopyranoside (MeMan) tested on the same microplate (IP (MeMan) ≡ 1); RIP(glycocluster) = IC_{50}(MeMan)/IC_{50}(glycocluster). Fitting errors in brackets are determined by error propagation according to the following formula:
Error = [1/IC_{50}(**1**) x error(IC_{50}(MeMan))]+[-(IC_{50}(MeMan)/IC_{50}(**1**)^2) x error(IC_{50}(**1**))].

[c] Mean RIP values of two independent experiments with error propargation in brackets.
Error = [error(IC_{50}(MeMan)) + error(IC_{50}(**1**))]/2.

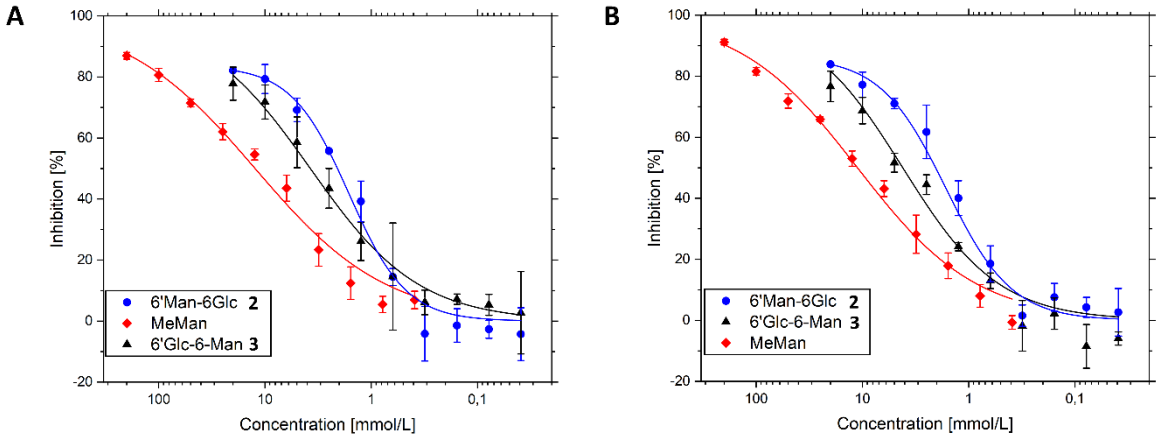

Figure S3.2 Inhibition curves obtained with maltose-based glycoclusters **2** and **3** as inhibitors of type 1 fimbriae-mediated bacterial adhesion to mannan. MeMan was tested simultaneously on each plate. Sigmoidal dose-responsive inhibition curves were fitted by non-linear regression. Error bars are standard deviations from duplicate or triplicate values on one plate.

Table S3.2 IC_{50} values and corresponding RIP values as deduced from the inhibition curves obtained with MeMan, **6'Man-6Glc** (**2**) and **6'Glc-6Man** (**3**).

Plate	Entry	MeMan	6'Man-6Glc (2)	6'Glc-6Man (3)
A	IC_{50}[a] [mmol]	12.39 (±1.19)	2.08 (±0.03)	3.74 (±0.31)
	RIP[b]	1.00	5.96 (±0.66)	3.31 (±0.59)
B	IC_{50}[a] [mmol]	11.14 (±0.97)	2.05 (±0.15)	4.17 (±0.48)
	RIP[b]	1.00	5.44 (±0.87)	2.67 (±0.54)
	Mean RIP[c]	1.00	5.70 (±0.77)	2.99 (±0.57)

[a] IC_{50} values are average values of duplicate or triplicate results on one plate; fitting errors are given in brackets.

[b] RIP values are based on the inhibitory potency of methyl α-D-mannopyranoside (MeMan) tested on the same microplate (IP (MeMan) ≡ 1); RIP(glycocluster) = IC_{50}(MeMan)/IC_{50}(glycocluster). Fitting errors in brackets are determined by error propagation as explained for Table S3.1.

[c] Mean RIP values of two independent experiments with error propagation as explained for Table S3.1.

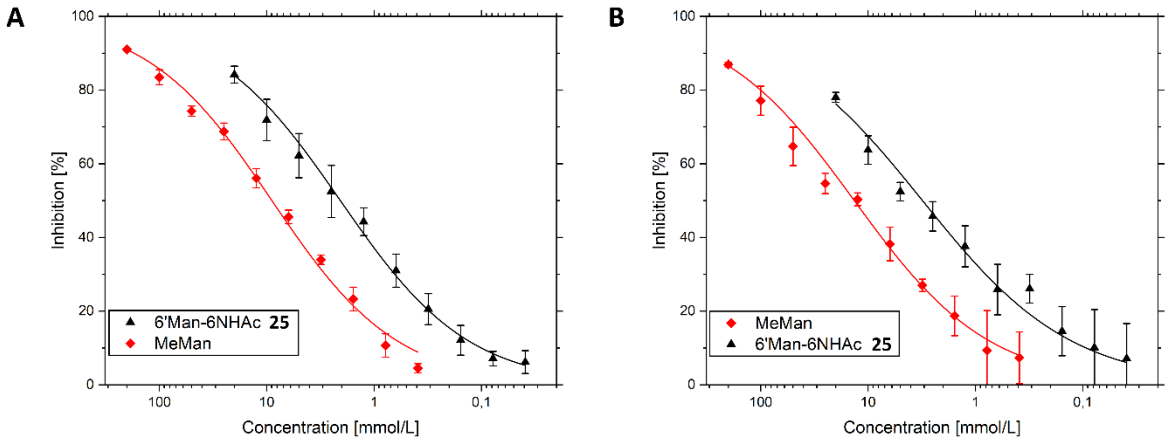

Figure S3.3 Inhibition curves obtained with maltoside **25** as inhibitor of type 1 fimbriae-mediated bacterial adhesion to mannan. MeMan was tested simultaneously on each plate. Sigmoidal dose response inhibition curves were fitted by non-linear regression. Error bars are standard deviations from duplicate or triplicate values on one plate.

Table S3.3 IC_{50} values and corresponding RIP values as deduced from the inhibition curves obtained with MeMan and **6'Man-6NHAc** (**25**).

Plate	Entry	MeMan	6'Man-6NHAc (25)
A	IC_{50} [a] [mmol]	13.43 (±0.77)	3.11 (±0.34)
	RIP [b]	1.00	4.32 (±0.72)
B	IC_{50} [a] [mmol]	8.94 (±0.67)	2.06 (±0.12)
	RIP [b]	1.00	4.34 (±0.58)
	Mean RIP[c]	1.00	4.33 (±0.65)

[a] IC_{50} values are average values of duplicate or triplicate results on one plate; fitting errors are given in brackets.

[b] RIP values are based on the inhibitory potency of methyl α-D-mannopyranoside (MeMan) tested on the same microplate (IP (MeMan) ≡ 1); RIP(glycocluster) = IC_{50}(MeMan)/IC_{50}(glycocluster). Fitting errors in brackets are determined by error propagation as explained for Table S3.1.

[c] Mean RIP values of two independent experiments with error propagation as explained for Table S3.1.

4 Molecular modelling

For molecular modelling the Schrödinger software package implementing the Maestro interface was used.[5] All ligands were built using Maestro and prepared for docking using LigPrep and the OPLS3e force field.[6] Crystal structures of FimH in its open gate form (pdb: 1KLF)[7] or closed gate conformation (pdb: 1UWF)[8] conformation were constructed using the protein preparation wizard implemented in Maestro.

Glide docking[9]

Receptor grids for docking were built using Glide,[9] by defining an outer box of 36 Å around the centroid of the ligand as complexed within the binding site of the respective FimH crystal structure. Hydroxy groups of Tyr48 and Tyr137 were set rotatable. Both receptor grids were built using the OPLS3e force field. Extra precision (XP) docking was carried out with Glide,[9] setting the ligand sampling to flexible. Ring conformations (energy window 2.5 kcal mol^{-1}) and nitrogen inversions were allowed during sampling. Epic state penalties were added to docking scores. At most, 20 poses were reported per ligand and a post-docking minimization was performed with a threshold for rejecting minimized poses of 0.50 kcal mol^{-1}. Additionally, poses with a RMSD less than 0.5 Å and a maximum atomic displacement less than 1.3 Å were treated as duplicates and discarded. Results are collected in Tables S4.1 and S4.2.

Calculation of binding energies was performed by subjecting the top scoring binding poses from Glide docking to a MM-GBSA[10] (molecular mechanics generalized born surface area) calculation, giving the free binding energy ΔG_{Bind} in kcal mol^{-1}. The MM-GBSA calculations were performed using the VGSB solvation model and the OPLS3e force field. Results are collected in Tables S4.3 and S4.4.

Induced fit docking[11]

Induced fit docking (IFD) was performed using the standard IFD protocol[11] with the OPLS3e force field. The receptor protein (FimH) was defined as an outer box of 36 Å around the centroid of the ligand as complexed within the binding site of FimH (pdb: 1UWF). Ligands were set flexible and sampled for ring conformations with an energy window of 2.5 kcal mol^{-1}. Non-planar amide bonds were penalized. Glide redocking was performed with extra precision (XP) for structures within 30 kcal mol^{-1} of the best structure, employing a maximum of 20 top-ranked structures. Docking poses found for glycoclusters **2** and **3** where the β-D-glucosyl residue was bound to the mannose binding pocket of FimH instead of the α-D-mannosyl moiety were discarded.[12] Results are collected in Table S4.5.

The top five binding poses according to the IFD score ranking were subjected to a binding pose metadynamics[13] simulation to determine the most stable protein-ligand complex. For each binding pose metadynamics simulations (10 trials of 10 ns) were

performed and averaged. Then, the binding pose with the lowest metadynamics composite score was selected as the most stable one. Results are collected in Table S4.6 and in Figure S4.4.

Calculation of binding energies was performed by subjecting the most stable binding poses from binding pose metadynamics simulations to a MM-GBSA[10] (molecular mechanics generalized born surface area) calculation, giving the free binding energy ΔG_{Bind} in kcal mol^{-1}. The MM-GBSA calculations were performed using the VGSB solvation model and the OPLS3e force field. Results are reported in Table S4.7. These computed binding energies are correlated with results from biological testing (RIP values, Figure S4.1).

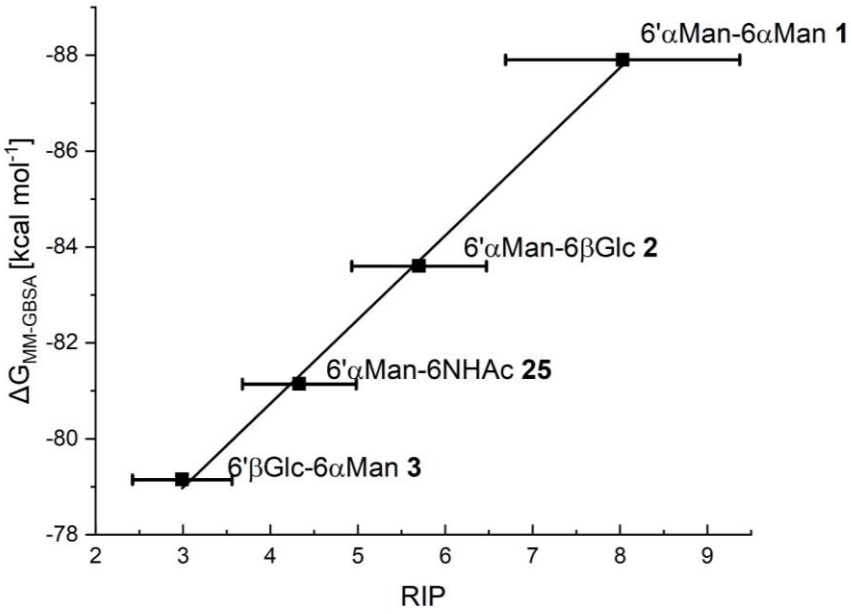

Figure S4.1 Comparison of computed binding energies from MM-GBSA[10] calculations with relative inhibitory potency (RIP) values from biological testing. Error bars are displayed for experimental RIP values (cf. Tables S3.1-3). Higher RIP values and lower binding energies correspond to stronger binding. The computed results are in excellent correlation with the experimental results.

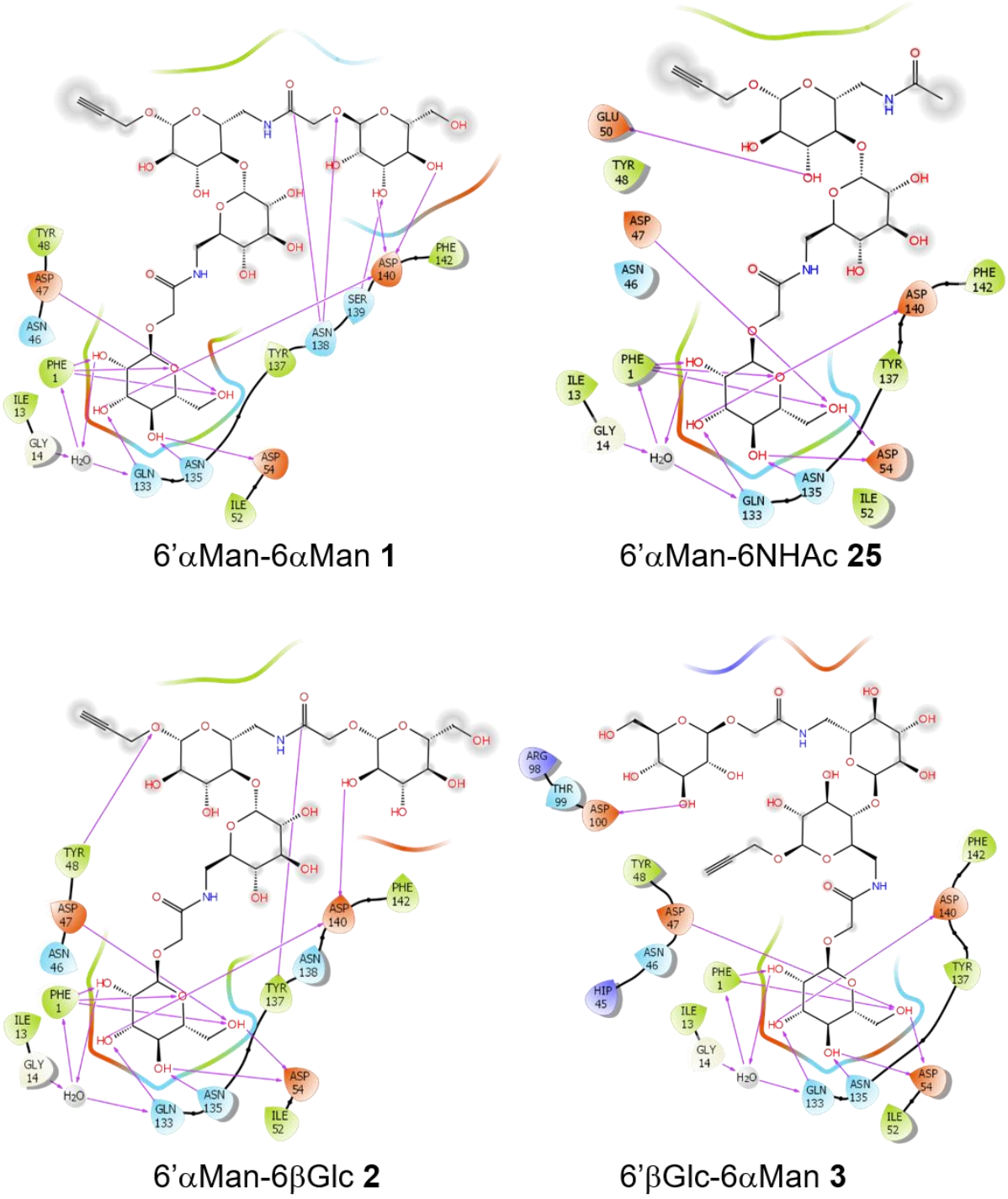

Figure S4.2 Two-dimensional representation of the most stable ligand-protein complexes from induced fit docking (IFD) for glycoclusters **1**, **2**, **3**, and **25**. The hydrogen bond network is shown in magenta. FimH amino acids are represented teardrop-shaped in feature-related colours: red: negatively charged; dark blue: positive; light blue: polar; green: hydrophobic. The polypeptide chain is indicated as black line and the mannose binding pocket as multi-coloured line (interruption indicates solvent exposure). Grey shades indicated solvent exposure.

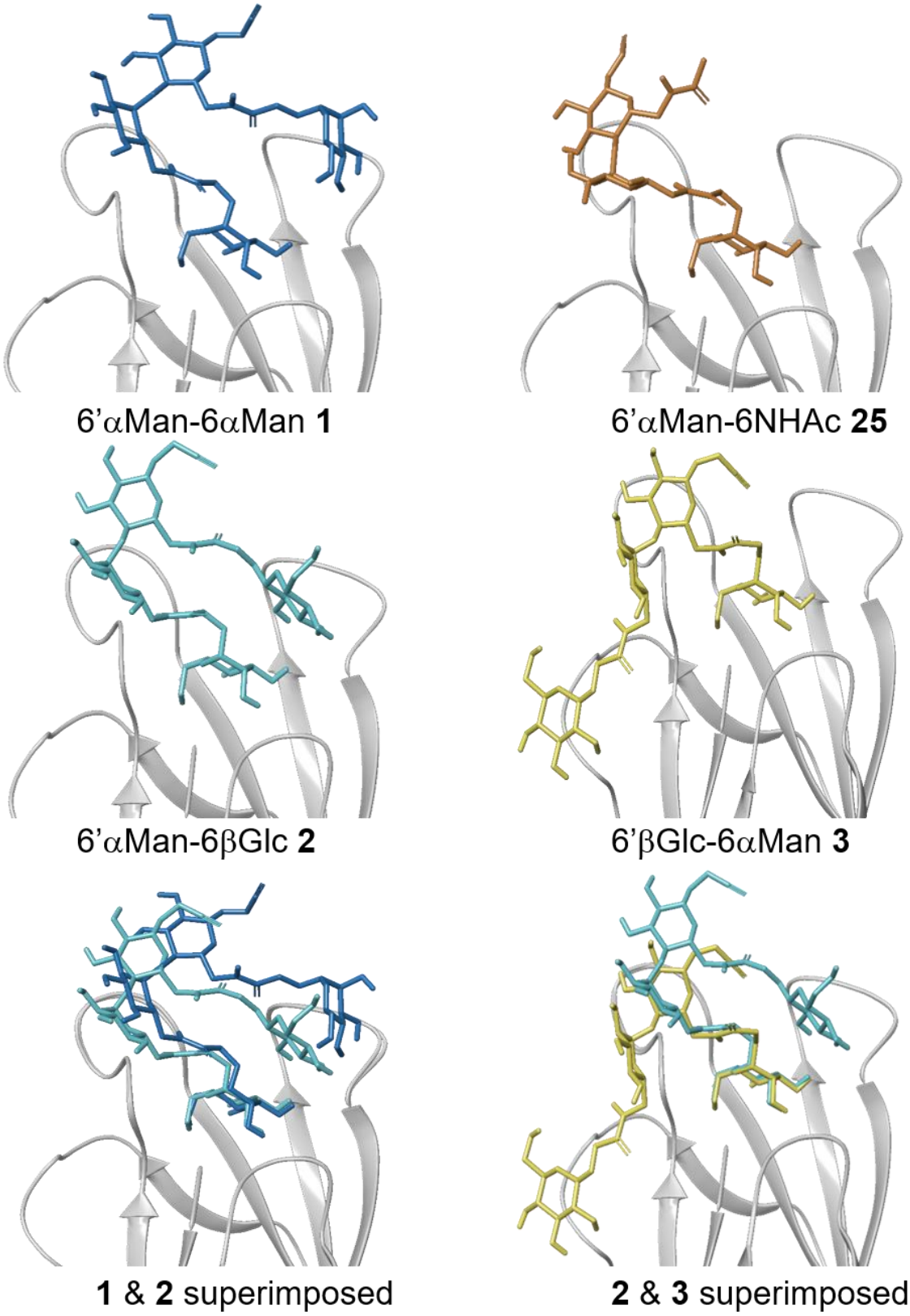

Figure S4.3 Three-dimensional representation of the most stable ligand-protein complexes from induced fit docking (IFD) for glycoclusters **1**, **2**, **3**, and **25**. FimH (pdb: 1UWF)[8] is displayed as ribbon diagram, ligands are shown as stick models. The superimposed ligand poses of **1** and **2** illustrate their similar binding to FimH. Likewise, the difference between the regioisomeric glycoclusters **2** and **3** becomes clear.

Table S4.1 Scoring values for docking of glycoclusters 6'αMan-6αMan **1**, 6'αMan-6βGlc **2**, 6'βGlc-6αMan **3** and 6'αMan-6NHAc **25** into the closed gate (pdb: 1UWF) conformation of FimH using Glide.

Glycocluster	Docking Score	XP HBond	Glide evdw	Glide ecoul	Glide energy	Glide emodel
6'αMan-6αMan **1**	-12.391	-6.458	-27.004	-50.063	-77.066	-113.279
6'αMan-6αMan **1**	-11.785	-6.458	-28.964	-46.747	-75.711	-111.842
6'αMan-6αMan **1**	-11.554	-6.458	-28.663	-46.880	-75.543	-113.082
6'αMan-6αMan **1**	-11.552	-6.458	-28.302	-44.127	-72.429	-114.025
6'αMan-6αMan **1**	-11.250	-6.458	-26.955	-51.557	-78.512	-112.508
6'αMan-6αMan **1**	-11.081	-6.458	-26.089	-47.811	-73.899	-113.391
6'αMan-6αMan **1**	-10.931	-6.458	-28.750	-45.887	-74.637	-113.466
6'αMan-6αMan **1**	-10.914	-6.458	-27.441	-46.682	-74.122	-112.277
6'αMan-6αMan **1**	-10.890	-6.458	-29.625	-46.438	-76.063	-114.140
6'αMan-6αMan **1**	-10.637	-6.458	-27.046	-48.367	-75.413	-117.779
6'αMan-6αMan **1**	-9.664	-6.458	-30.189	-38.854	-69.043	-111.749
6'αMan-6αMan **1**	-9.661	-6.458	-28.128	-39.479	-67.607	-111.930
6'αMan-6αMan **1**	-9.082	-6.458	-26.462	-43.887	-70.349	-110.580
6'αMan-6αMan **1**	-9.034	-6.458	-27.831	-42.417	-70.248	-111.839
6'αMan-6αMan **1**	-9.017	-6.458	-33.306	-37.469	-70.775	-117.690
6'αMan-6αMan **1**	-8.881	-6.458	-32.107	-34.883	-66.989	-115.183
6'αMan-6αMan **1**	-8.522	-6.458	-36.632	-38.242	-74.874	-116.003
6'αMan-6αMan **1**	-8.345	-6.458	-33.582	-38.371	-71.952	-115.900
6'αMan-6αMan **1**	-8.228	-6.458	-26.421	-43.839	-70.261	-113.085
6'αMan-6βGlc **2**	-12.481	-7.867	-29.028	-48.609	-77.636	-121.029
6'αMan-6βGlc **2**	-12.014	-7.867	-33.632	-45.456	-79.089	-116.810
6'αMan-6βGlc **2**	-10.891	-7.867	-32.727	-40.528	-73.255	-111.260
6'αMan-6βGlc **2**	-10.733	-7.867	-28.907	-44.455	-73.362	-114.585
6'αMan-6βGlc **2**	-10.713	-7.867	-26.867	-45.934	-72.801	-113.227
6'αMan-6βGlc **2**	-9.877	-7.867	-26.320	-43.237	-69.556	-114.406
6'βGlc-6αMan **3**	-10.675	-7.422	-32.779	-39.133	-71.913	-111.380
6'βGlc-6αMan **3**	-9.641	-7.422	-26.606	-45.154	-71.760	-110.042
6'αMan-6NHAc **25**	-11.218	-7.801	-21.025	-43.138	-64.163	-107.721
6'αMan-6NHAc **25**	-10.946	-7.801	-21.604	-42.610	-64.214	-104.320
6'αMan-6NHAc **25**	-10.817	-7.801	-19.475	-44.778	-64.253	-106.675
6'αMan-6NHAc **25**	-10.691	-7.801	-22.280	-42.730	-65.010	-104.422
6'αMan-6NHAc **25**	-10.309	-7.801	-21.431	-42.733	-64.164	-105.137
6'αMan-6NHAc **25**	-10.303	-7.801	-21.254	-44.941	-66.195	-105.242
6'αMan-6NHAc **25**	-10.167	-7.801	-21.139	-43.601	-64.740	-105.014
6'αMan-6NHAc **25**	-9.984	-7.801	-23.177	-45.033	-68.211	-103.485
6'αMan-6NHAc **25**	-9.869	-7.801	-21.837	-45.630	-67.467	-108.994
6'αMan-6NHAc **25**	-9.762	-7.801	-21.709	-44.701	-66.410	-105.180
6'αMan-6NHAc **25**	-9.761	-7.801	-22.070	-43.970	-66.040	-106.508

Table S4.2 Scoring values for docking of glycoclusters 6'αMan-6αMan **1**, 6'αMan-6βGlc **2**, 6'βGlc-6αMan **3** and 6'αMan-6NHAc **25** into the open gate (pdb: 1KLF) conformation of FimH using Glide.

Glycocluster	Docking Score	XP HBond	Glide evdw	Glide ecoul	Glide energy	Glide emodel
6'αMan-6αMan **1**	-9.930	-6.427	-28.548	-51.733	-80.281	-131.458
6'αMan-6αMan **1**	-9.859	-6.427	-30.392	-49.566	-79.959	-133.423
6'αMan-6αMan **1**	-9.338	-6.427	-27.654	-51.888	-79.542	-129.403
6'αMan-6αMan **1**	-9.033	-6.427	-30.858	-48.771	-79.630	-127.578
6'αMan-6αMan **1**	-8.984	-6.427	-27.785	-50.473	-78.258	-133.109
6'αMan-6αMan **1**	-8.938	-6.427	-28.472	-51.166	-79.638	-129.113
6'αMan-6αMan **1**	-8.839	-6.427	-27.540	-51.692	-79.232	-132.646
6'αMan-6αMan **1**	-8.806	-6.427	-29.008	-50.835	-79.842	-124.462
6'αMan-6αMan **1**	-8.752	-6.427	-29.995	-49.863	-79.858	-129.361
6'αMan-6αMan **1**	-8.321	-6.427	-31.654	-48.377	-80.031	-132.619
6'αMan-6βGlc **2**	-10.044	-6.179	-20.384	-50.597	-70.981	-123.578
6'αMan-6βGlc **2**	-8.929	-6.179	-19.970	-50.948	-70.918	-107.713
6'αMan-6βGlc **2**	-8.872	-6.179	-21.647	-44.166	-65.812	-99.776
6'αMan-6βGlc **2**	-8.825	-6.179	-20.880	-44.494	-65.374	-107.530
6'αMan-6βGlc **2**	-8.224	-6.179	-16.324	-52.862	-69.185	-102.914
6'αMan-6βGlc **2**	-8.167	-6.179	-15.503	-53.970	-69.473	-99.937
6'αMan-6βGlc **2**	-7.696	-6.179	-16.047	-53.802	-69.848	-110.911
6'βGlc-6αMan **3**	-9.839	-5.725	-32.397	-45.126	-77.523	-108.187
6'βGlc-6αMan **3**	-9.651	-5.725	-32.145	-40.078	-72.223	-109.383
6'βGlc-6αMan **3**	-9.446	-5.725	-31.025	-41.997	-73.022	-107.291
6'βGlc-6αMan **3**	-9.314	-5.725	-22.722	-46.147	-68.869	-104.596
6'βGlc-6αMan **3**	-9.116	-5.725	-36.656	-34.635	-71.291	-108.396
6'βGlc-6αMan **3**	-9.109	-5.725	-33.121	-39.994	-73.114	-102.877
6'βGlc-6αMan **3**	-8.841	-5.725	-30.686	-40.009	-70.695	-101.917
6'βGlc-6αMan **3**	-8.637	-5.725	-24.079	-48.837	-72.915	-106.073
6'βGlc-6αMan **3**	-8.056	-5.725	-19.035	-41.602	-60.637	-105.192
6'βGlc-6αMan **3**	-6.775	-5.725	-21.096	-43.335	-64.431	-105.960
6'αMan-6NHAc **25**	-8.928	-5.853	-29.582	-36.492	-66.074	-106.302
6'αMan-6NHAc **25**	-8.905	-5.853	-28.077	-37.630	-65.707	-102.288
6'αMan-6NHAc **25**	-8.493	-5.853	-21.707	-43.659	-65.366	-105.600
6'αMan-6NHAc **25**	-8.419	-5.853	-21.587	-42.353	-63.940	-107.451
6'αMan-6NHAc **25**	-8.366	-5.853	-21.552	-43.474	-65.026	-105.312
6'αMan-6NHAc **25**	-8.366	-5.853	-28.581	-37.346	-65.926	-104.486
6'αMan-6NHAc **25**	-8.258	-5.853	-28.683	-37.802	-66.486	-103.388
6'αMan-6NHAc **25**	-8.241	-5.853	-27.785	-37.155	-64.940	-105.992
6'αMan-6NHAc **25**	-8.153	-5.853	-22.350	-43.021	-65.371	-105.611
6'αMan-6NHAc **25**	-8.096	-5.853	-23.864	-42.482	-66.346	-100.631

Table S4.3 Values of computed binding energies ΔG_{Bind} (in kcal mol^{-1}) obtained from MM-GBSA calculations for 6'αMan-6αMan **1**, 6'αMan-6βGlc **2**, 6'βGlc-6αMan **3** and 6'αMan-6NHAc **25** into the closed gate (pdb: 1UWF) conformation of FimH. Top scoring binding poses were selected.

Glycocluster	Docking Score	ΔG_{Bind}	$\Delta G_{Bind\_Coulomb}$	$\Delta G_{Bind\_Covalent}$	ΔG_{Bind_Hbond}	ΔG_{Bind_Lipo}	$\Delta G_{Bind\_Solv\_GB}$	ΔG_{Bind_vdW}	Lig Strain Energy
6'αMan-6αMan **1**	-12.391	-59.82	-62.27	13.17	-9.48	-12.30	46.42	-35.36	40.189195
6'αMan-6βGlc **2**	-12.481	-89.52	-75.63	4.71	-8.94	-15.02	50.63	-45.26	10.085274
6'βGlc-6αMan **3**	-10.675	-60.47	-34.45	-0.46	-8.54	-10.57	37.48	-43.94	35.824435
6'αMan-6NHAc **25**	-11.218	-53.34	-63.17	11.12	-10.04	-10.00	46.43	-27.68	34.475577

Table S4.4 Values of computed binding energies ΔG_{Bind} (in kcal mol^{-1}) obtained from MM-GBSA calculations for 6'αMan-6αMan **1**, 6'αMan-6βGlc **2**, 6'βGlc-6αMan **3** and 6'αMan-6NHAc **25** into the open gate (pdb: 1KLF) conformation of FimH. Top scoring binding poses were selected.

Glycocluster	Docking Score	ΔG_{Bind}	$\Delta G_{Bind\_Coulomb}$	$\Delta G_{Bind\_Covalent}$	ΔG_{Bind_Hbond}	ΔG_{Bind_Lipo}	$\Delta G_{Bind\_Solv\_GB}$	ΔG_{Bind_vdW}	Lig Strain Energy
6'αMan-6αMan **1**	-9.930	-70.29	-49.83	8.09	-9.58	-15.16	41.94	-45.76	34.976729
6'αMan-6βGlc **2**	-10.044	-57.71	-52.39	8.96	-10.28	-11.35	31.97	-24.62	39.387004
6'βGlc-6αMan **3**	-9.839	-72.09	-66.46	14.27	-8.62	-17.77	46.60	-40.11	29.624071
6'αMan-6NHAc **25**	-8.928	-65.95	-47.62	2.92	-8.06	-12.20	33.61	-34.59	19.689377

Table S4.5 Scoring values from IFD docking of glycoclusters 6'αMan-6αMan **1**, 6'αMan-6βGlc **2,** 6'βGlc-6αMan **3** and 6'αMan-6NHAc **25**. Entries shaded in grey are poses where the β-D-glucopyranosyl moiety of the glycocluster is bound to the FimH binding pocket; these were discarded for further analysis.

Glycocluster	IFD Score	Docking Score	XP HBond	Glide evdw	Glide lipo	Glide ecoul	Glide energy	Glide emodel
6'αMan-6αMan **1**	-313.16	-12.624	-9.486	-27.603	-0.070	-43.086	-70.690	-112.108
6'αMan-6αMan **1**	-312.68	-11.814	-8.503	-30.477	-0.115	-48.036	-78.513	-121.311
6'αMan-6αMan **1**	-312.50	-11.636	-7.764	-33.919	-0.099	-40.994	-74.913	-109.589
6'αMan-6αMan **1**	-312.26	-11.909	-8.321	-28.710	-0.085	-46.734	-75.445	-129.564
6'αMan-6αMan **1**	-311.91	-11.344	-8.308	-26.628	-0.172	-45.702	-72.330	-114.502
6'αMan-6αMan **1**	-311.70	-11.388	-8.416	-21.348	-0.728	-40.792	-62.140	-100.750
6'αMan-6αMan **1**	-311.42	-11.265	-6.117	-39.117	-0.228	-33.293	-72.410	-111.730
6'αMan-6αMan **1**	-310.66	-11.081	-5.683	-27.631	-0.221	-41.372	-69.003	-101.666
6'αMan-6αMan **1**	-310.59	-10.850	-6.973	-21.622	-0.347	-42.561	-64.184	-106.878
6'αMan-6αMan **1**	-310.40	-9.660	-6.389	-29.439	-0.154	-40.706	-70.145	-112.010
6'αMan-6αMan **1**	-310.02	-9.621	-5.738	-34.885	-0.410	-27.075	-61.960	-90.341
6'αMan-6αMan **1**	-309.80	-10.046	-7.703	-27.646	-0.611	-40.039	-67.685	-92.367
6'αMan-6αMan **1**	-309.77	-10.111	-5.526	-38.361	-0.461	-23.180	-61.541	-85.286
6'αMan-6αMan **1**	-309.70	-9.342	-5.086	-26.600	-0.570	-27.652	-54.252	-78.670
6'αMan-6αMan **1**	-309.56	-10.164	-5.579	-32.254	-0.566	-28.290	-60.544	-77.161
6'αMan-6αMan **1**	-309.38	-9.236	-4.631	-28.524	-0.511	-30.279	-58.803	-87.986
6'αMan-6αMan **1**	-308.91	-9.181	-5.361	-26.967	-0.309	-32.290	-59.257	-86.520
6'αMan-6αMan **1**	-308.58	-8.908	-4.385	-33.187	-0.547	-30.020	-63.207	-98.723
6'αMan-6αMan **1**	-308.02	-8.344	-5.330	-26.954	-0.372	-27.849	-54.803	-88.499
6'αMan-6βGlc **2**	-313.01	-12.656	-8.637	-31.910	-0.090	-49.622	-81.532	-137.631
6'αMan-6βGlc **2**	-312.32	-11.481	-7.838	-23.413	-0.099	-45.208	-68.621	-113.799
6'αMan-6βGlc **2**	-311.80	-11.822	-7.934	-24.142	-0.079	-52.595	-76.737	-114.230

6'αMan-6βGlc **2**	-311.79	-10.921	-6.025	-27.401	-0.455	-38.908	-66.310	-108.125
6'αMan-6βGlc **2**	-311.73	-10.517	-7.789	-27.636	-0.242	-41.889	-69.525	-94.045
6'αMan-6βGlc **2**	-311.53	-11.649	-7.819	-23.986	-0.145	-43.884	-67.871	-113.358
6'αMan-6βGlc **2**	-311.45	-11.493	-7.046	-29.006	-0.129	-43.999	-73.004	-124.843
6'αMan-6βGlc **2**	-311.38	-11.529	-5.750	-42.742	0.000	-37.986	-80.728	-120.592
6'αMan-6βGlc **2**	-311.24	-11.032	-7.424	-33.249	-0.183	-41.228	-74.477	-121.522
6'αMan-6βGlc **2**	-311.16	-11.055	-6.155	-17.078	-0.015	-43.331	-60.408	-101.479
6'αMan-6βGlc **2**	-311.13	-10.793	-8.070	-30.120	-0.151	-35.183	-65.303	-101.899
6'αMan-6βGlc **2**	-310.90	-10.373	-7.690	-25.152	-0.042	-45.859	-71.012	-106.192
6'αMan-6βGlc **2**	-310.57	-10.625	-7.070	-18.957	-0.019	-43.764	-62.721	-94.879
6'αMan-6βGlc **2**	-310.43	-10.462	-6.127	-35.936	-0.264	-35.747	-71.682	-106.764
6'αMan-6βGlc **2**	-309.18	-9.274	-6.393	-28.632	-0.264	-30.449	-59.081	-95.155
6'βGlc-6αMan **3**	-313.49	-12.666	-9.215	-23.357	-0.112	-50.757	-74.114	-109.202
6'βGlc-6αMan **3**	-312.70	-12.121	-7.211	-29.011	-0.123	-51.747	-80.758	-120.143
6'βGlc-6αMan **3**	-312.62	-12.385	-8.849	-30.440	-0.133	-46.143	-76.583	-120.885
6'βGlc-6αMan **3**	-312.31	-12.383	-8.329	-36.055	-0.060	-44.660	-80.716	-118.326
6'βGlc-6αMan **3**	-311.73	-11.547	-7.231	-26.036	-0.175	-43.772	-69.808	-113.514
6'βGlc-6αMan **3**	-310.67	-10.322	-6.742	-26.087	-0.284	-38.979	-65.066	-110.337
6'βGlc-6αMan **3**	-310.64	-10.200	-6.392	-35.745	-0.522	-41.724	-77.469	-120.034
6'βGlc-6αMan **3**	-310.53	-10.318	-7.220	-30.242	-0.247	-38.624	-68.866	-113.064
6'βGlc-6αMan **3**	-310.34	-9.954	-6.289	-31.084	-0.283	-37.785	-68.868	-103.792
6'βGlc-6αMan **3**	-310.25	-10.122	-6.554	-33.447	-0.549	-33.937	-67.385	-123.230
6'βGlc-6αMan **3**	-310.19	-10.272	-6.823	-29.451	-0.262	-37.575	-67.026	-106.880
6'βGlc-6αMan **3**	-310.06	-10.258	-6.598	-26.957	-0.239	-39.475	-66.432	-96.589
6'βGlc-6αMan **3**	-309.87	-10.085	-5.063	-33.615	-0.227	-31.700	-65.316	-98.691
6'βGlc-6αMan **3**	-309.86	-9.771	-6.927	-34.598	-0.381	-31.002	-65.600	-95.803
6'βGlc-6αMan **3**	-309.66	-9.752	-6.273	-27.057	-0.130	-38.678	-65.736	-98.181
6'βGlc-6αMan **3**	-309.44	-9.013	-5.788	-33.096	-0.255	-29.586	-62.681	-93.326
6'βGlc-6αMan **3**	-308.99	-9.465	-6.161	-27.055	-0.178	-33.430	-60.485	-83.383
6'αMan-6NHAc **25**	-314.78	-10.781	-7.888	-26.871	-0.221	-40.014	-66.885	-109.900
6'αMan-6NHAc **25**	-314.20	-10.245	-6.141	-23.706	-0.273	-36.521	-60.226	-100.011
6'αMan-6NHAc **25**	-314.14	-10.480	-6.929	-29.346	-0.233	-40.261	-69.608	-103.994
6'αMan-6NHAc **25**	-313.93	-9.704	-6.383	-25.700	-0.286	-36.995	-62.696	-100.706
6'αMan-6NHAc **25**	-313.83	-9.944	-6.157	-28.234	-0.342	-39.344	-67.578	-102.849
6'αMan-6NHAc **25**	-313.62	-9.715	-6.690	-30.221	-0.294	-43.164	-73.385	-118.220
6'αMan-6NHAc **25**	-313.53	-9.823	-7.134	-24.823	-0.164	-38.047	-62.870	-95.917
6'αMan-6NHAc **25**	-313.49	-10.493	-7.341	-26.007	-0.197	-39.439	-65.446	-101.594
6'αMan-6NHAc **25**	-313.41	-10.306	-6.528	-24.870	-0.252	-36.581	-61.451	-100.495
6'αMan-6NHAc **25**	-310.14	-7.163	-4.161	-17.246	-0.197	-28.559	-45.806	-56.209

Table S4.6 Scoring values of binding pose metadynamics calculation for the top five scoring binding poses from IFD. Lower composite (comp.) score correlates to more stable protein-ligand complexes.

Glycocluster	IFD Score	Comp. Score	Pose Score	Persis-tence	Persis-tence Length	Persis-tence Sum	HBond Persis-tence	HBond Persis-tence Length	HBond Persis-tence Sum
6'αMan-6αMan **1**	-312.26	0.454	3.872	0.684	10.000	6.836	0.684	10.000	6.836
6'αMan-6αMan **1**	-312.50	1.540	4.709	0.634	11.000	6.973	0.634	11.000	6.973
6'αMan-6αMan **1**	-313.16	1.724	4.851	0.625	10.000	6.255	0.625	10.000	6.255
6'αMan-6αMan **1**	-311.91	2.195	4.967	0.555	10.000	5.545	0.555	10.000	5.545
6'αMan-6αMan **1**	-312.68	2.487	5.570	0.617	12.000	7.400	0.617	12.000	7.400
6'αMan-6βGlc **2**	-312.32	-0.853	3.147	0.800	10.000	8.000	0.800	10.000	8.000
6'αMan-6βGlc **2**	-313.01	-0.018	3.694	0.742	12.000	8.909	0.742	12.000	8.909
6'αMan-6βGlc **2**	-311.80	0.528	4.013	0.697	12.000	8.364	0.697	12.000	8.364
6'αMan-6βGlc **2**	-311.53	2.848	5.930	0.616	10.000	6.164	0.616	10.000	6.164
6'αMan-6βGlc **2**	-311.73	5.052	8.824	0.755	10.000	7.545	0.755	10.000	7.545
6'βGlc-6αMan **3**	-310.64	-1.943	2.123	0.813	9.000	7.318	0.813	9.000	7.318
6'βGlc-6αMan **3**	-310.67	-0.309	3.414	0.745	11.000	8.191	0.745	11.000	8.191
6'βGlc-6αMan **3**	-312.70	-0.284	3.472	0.751	11.000	8.264	0.751	11.000	8.264
6'βGlc-6αMan **3**	-313.49	0.054	2.947	0.579	14.000	8.100	0.579	14.000	8.100
6'βGlc-6αMan **3**	-312.31	2.088	5.402	0.663	10.000	6.627	0.663	10.000	6.627
6'αMan-6NHAc **25**	-313.93	1.014	5.120	0.821	9.000	7.391	0.821	9.000	7.391
6'αMan-6NHAc **25**	-314.78	1.333	4.865	0.706	10.000	7.064	0.706	10.000	7.064
6'αMan-6NHAc **25**	-314.14	1.807	5.553	0.749	10.000	7.491	0.749	10.000	7.491
6'αMan-6NHAc **25**	-313.83	2.023	5.486	0.693	10.000	6.927	0.693	10.000	6.927
6'αMan-6NHAc **25**	-314.20	2.395	6.031	0.727	10.000	7.273	0.727	10.000	7.273

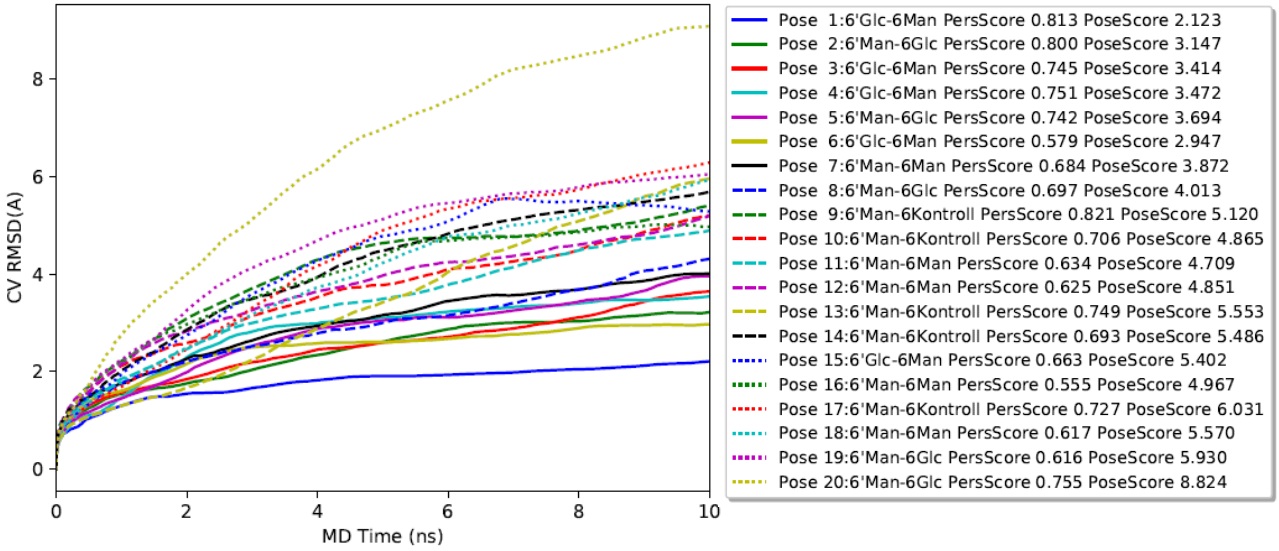

Figure S4.4 Plot of the averaged RMSD as collective variables (CV) in Å over the duration of the binding pose metadynamics[13] simulation. 6'αMan-6αMan **1** (poses 7, 11, 12, 16, 18); 6'αMan-6βGlc **2** (poses 2, 5, 8, 19, 20); 6'βGlc-6αMan **3** (poses 1, 3, 4, 6, 15); 6'αMan-6NHAc **25** (poses 9, 10, 13, 14, 17).

Table S4.7 Values of computed binding energies ΔG_{Bind} (in kcal mol^{-1}) obtained from MM-GBSA calculations for 6'αMan-6αMan **1**, 6'αMan-6βGlc **2**, 6'βGlc-6αMan **3** and 6'αMan-6NHAc **25** into the closed gate (pdb: 1UWF) conformation of FimH. Most stable binding poses from IFD ranked by binding pose metadynamics simulations were selected.

Glycocluster	IFD Score	ΔG_{Bind}	$\Delta G_{Bind\_Coulomb}$	$\Delta G_{Bind\_Covalent}$	ΔG_{Bind_Hbond}	ΔG_{Bind_Lipo}	$\Delta G_{Bind\_Solv\_GB}$	ΔG_{Bind_vdW}	Lig Strain Energy
6'αMan-6αMan **1**	-312.26	-87.90	-70.43	8.70	-9.67	-17.29	39.84	-39.03	19.861299
6'αMan-6βGlc **2**	-312.32	-83.60	-59.55	10.45	-8.83	-19.51	37.61	-43.77	22.633489
6'βGlc-6αMan **3**	-310.64	-79.15	-47.26	6.85	-9.51	-18.65	39.57	-50.15	27.265820
6'αMan-6NHAc **25**	-313.93	-81.14	-66.46	8.28	-8.07	-15.13	34.57	-34.32	14.480677

5 NMR spectra of the synthesized compounds

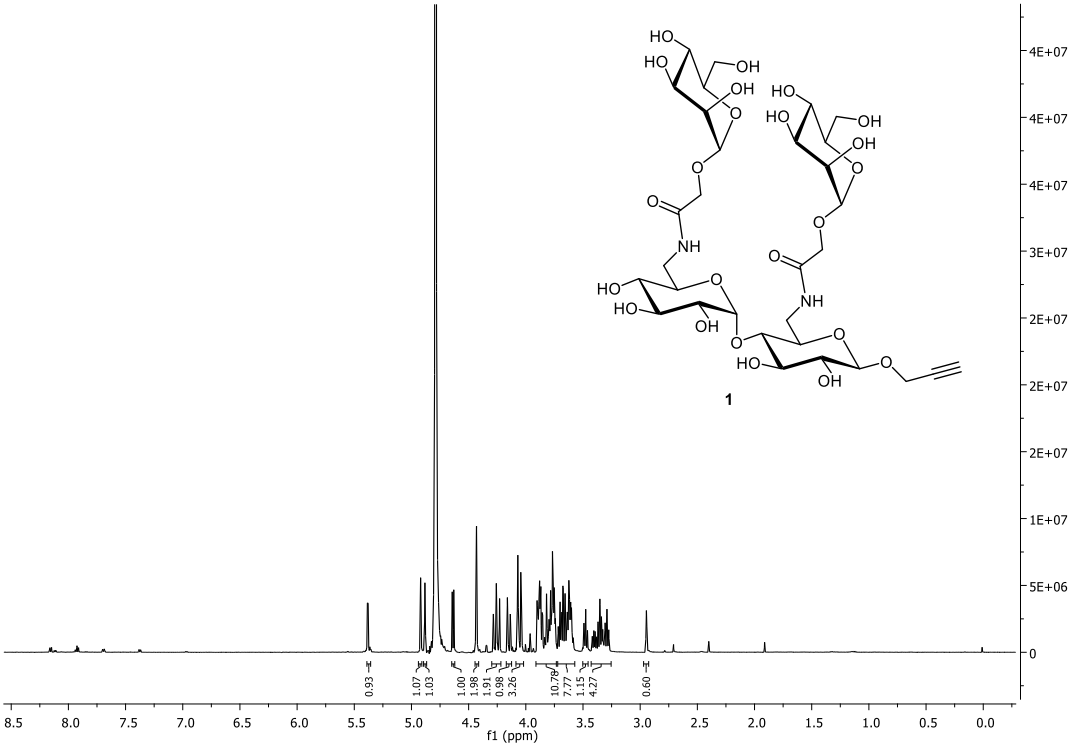

Figure S5.1 ^{1}H NMR spectrum of **1** (600 MHz, D_2O_3, 300 K).

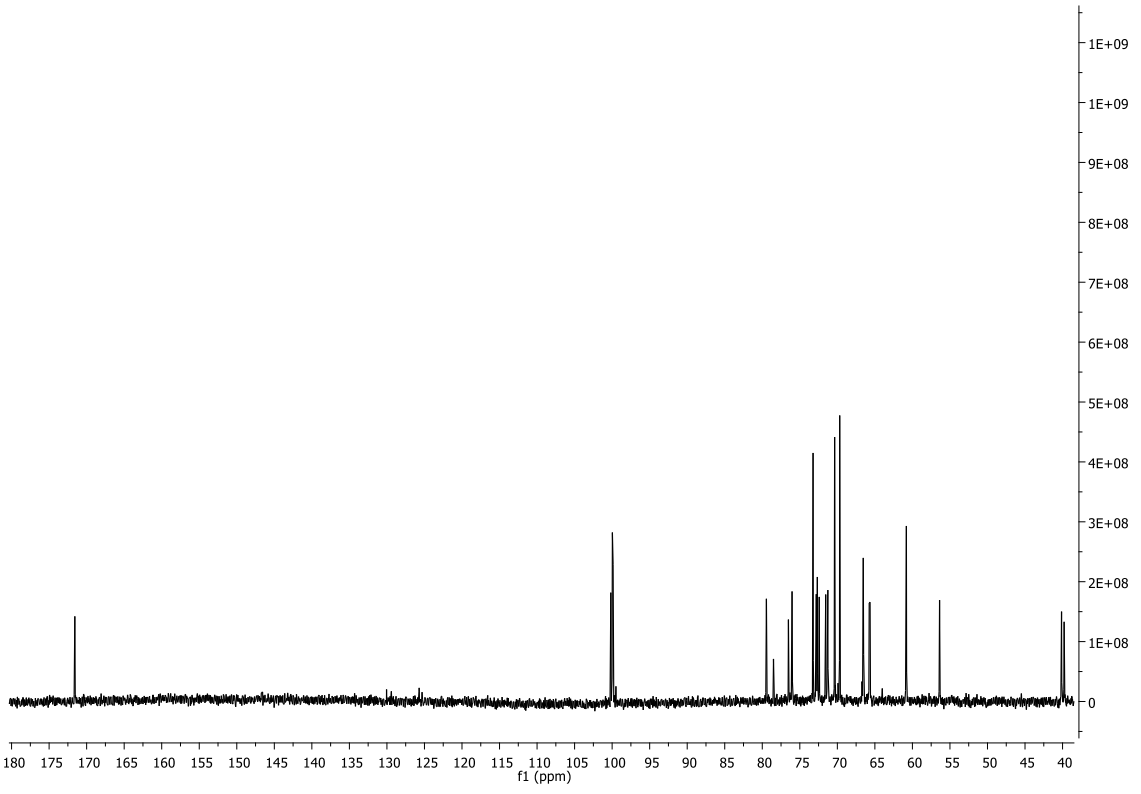

Figure S5.2 ^{13}C NMR spectrum of **1** (125 MHz, D_2O, 300 K).

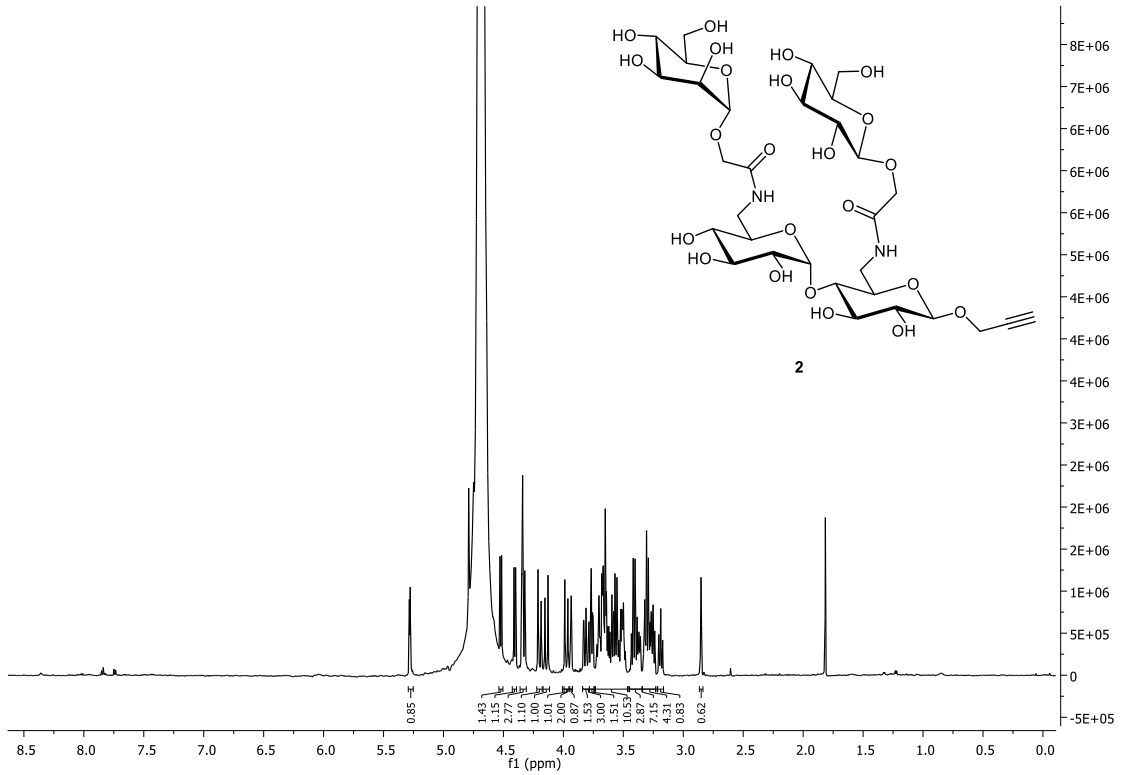

Figure S5.3 ^{1}H NMR spectrum of **2** (600 MHz, D_2O, 300 K).

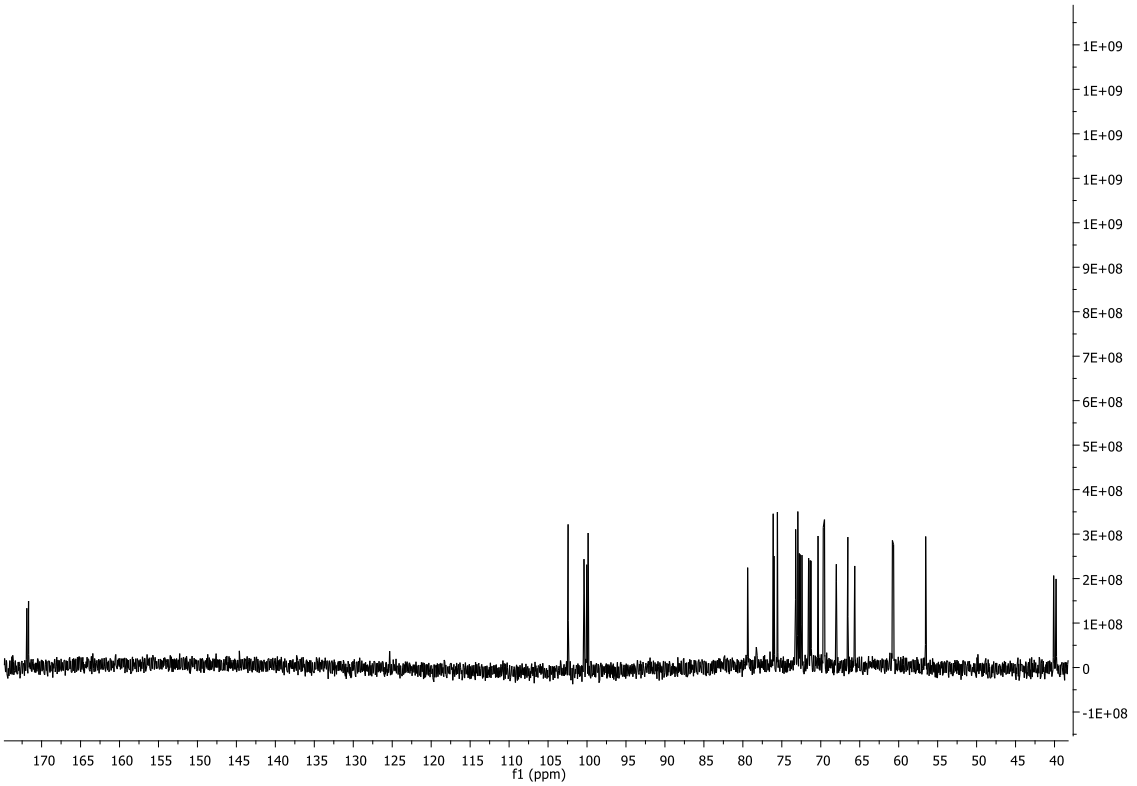

Figure S5.4 ^{13}C NMR spectrum of **2** (125 MHz, D_2O, 300 K).

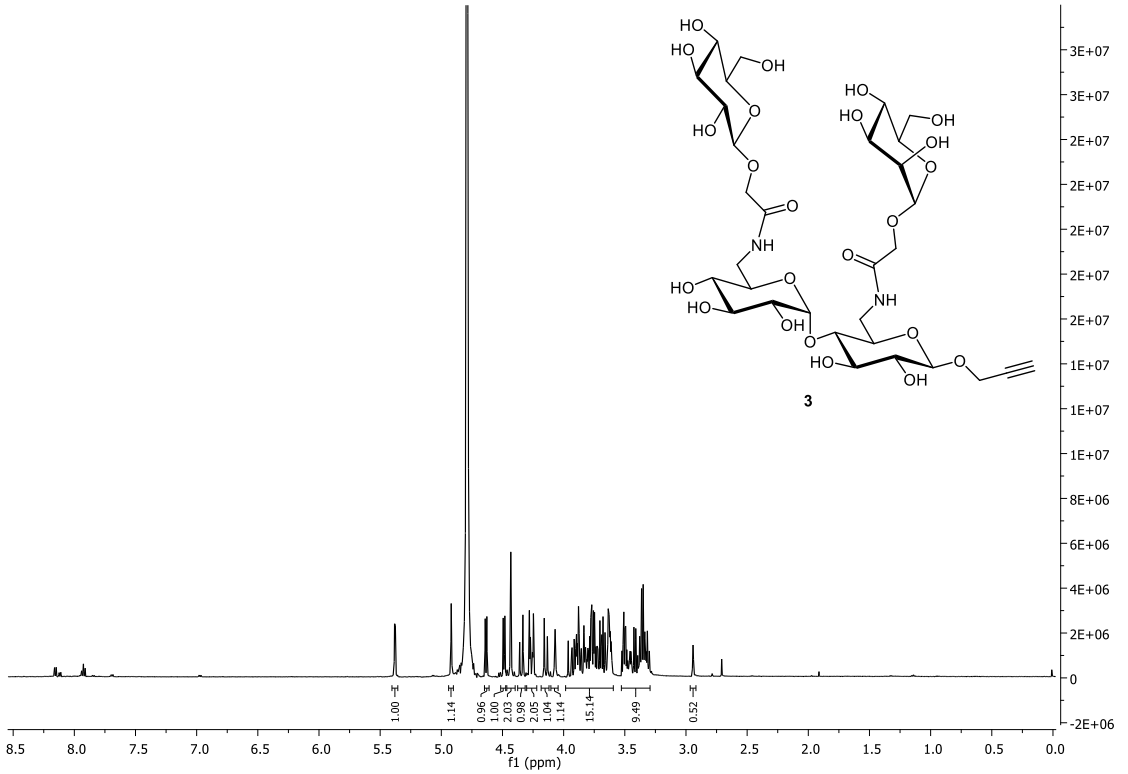

Figure S5.5 ^{1}H NMR spectrum of **3** (600 MHz, D_2O, 300 K).

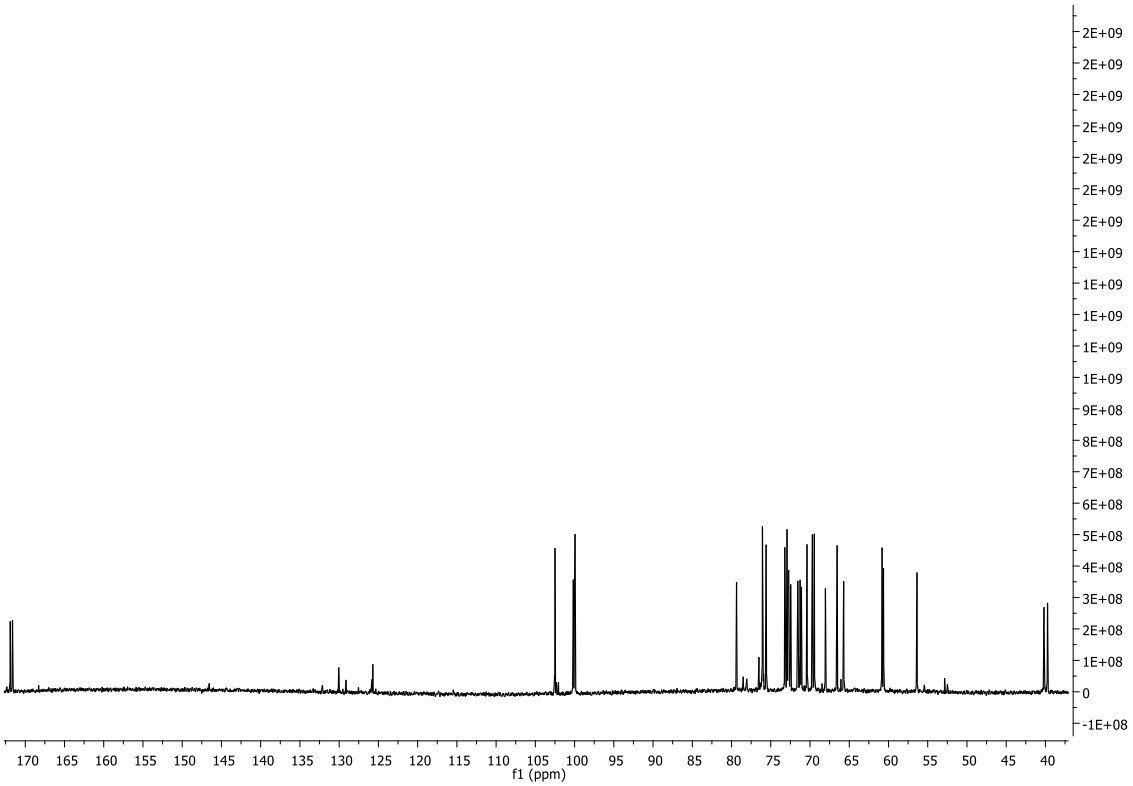

Figure S5.6 ^{13}C NMR spectrum of **3** (125 MHz, D_2O, 300 K).

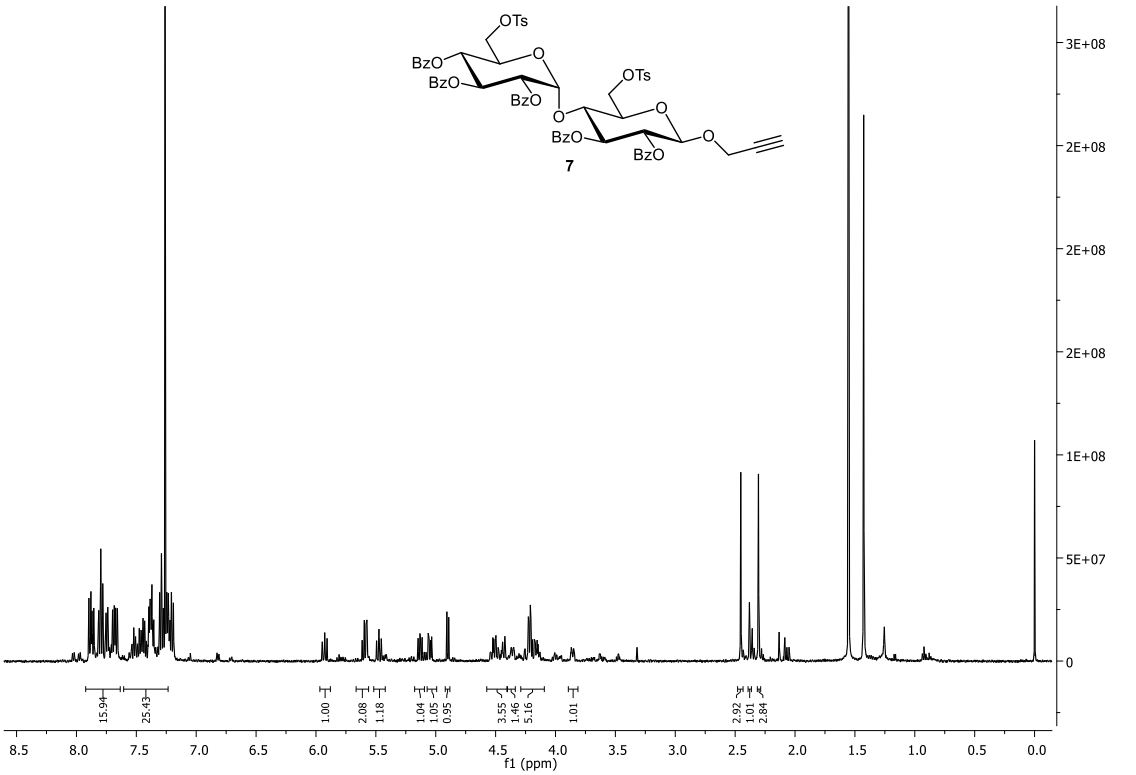

Figure S5.7 ^{1}H NMR spectrum of **7** (500 MHz, $CDCl_3$, 300 K).

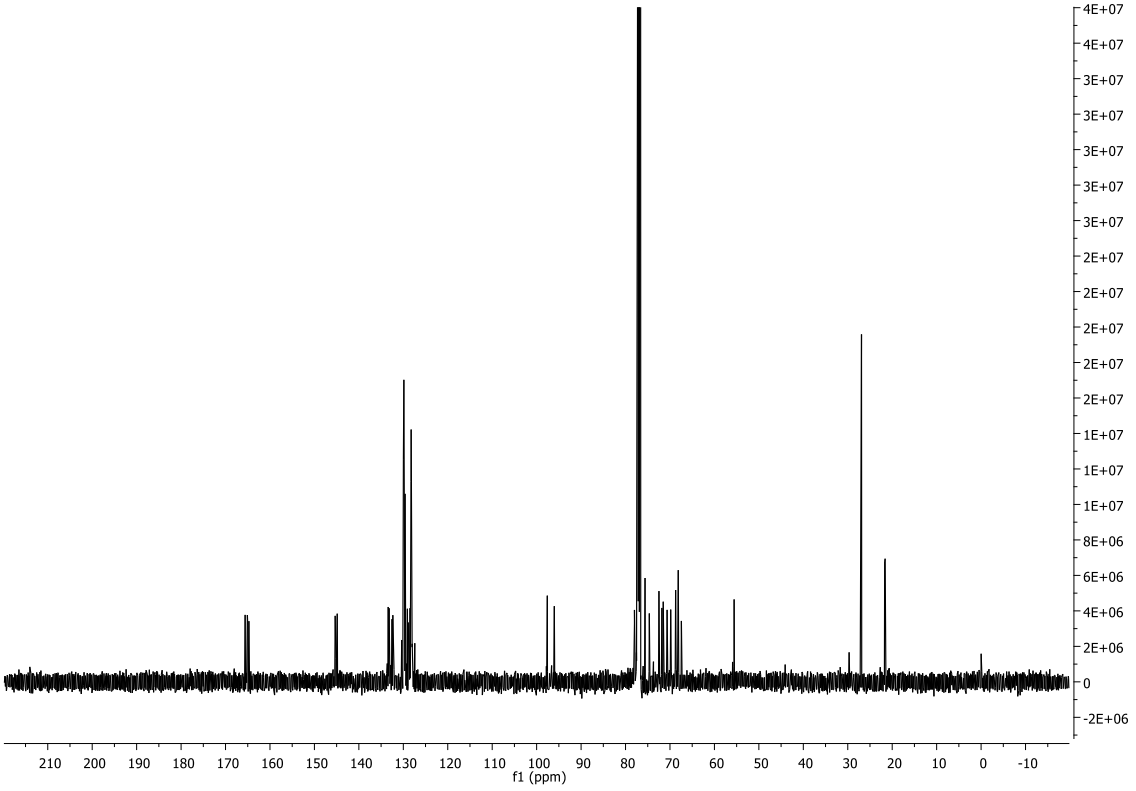

Figure S5.8 ^{13}C NMR spectrum of **7** (125 MHz, $CDCl_3$, 300 K).

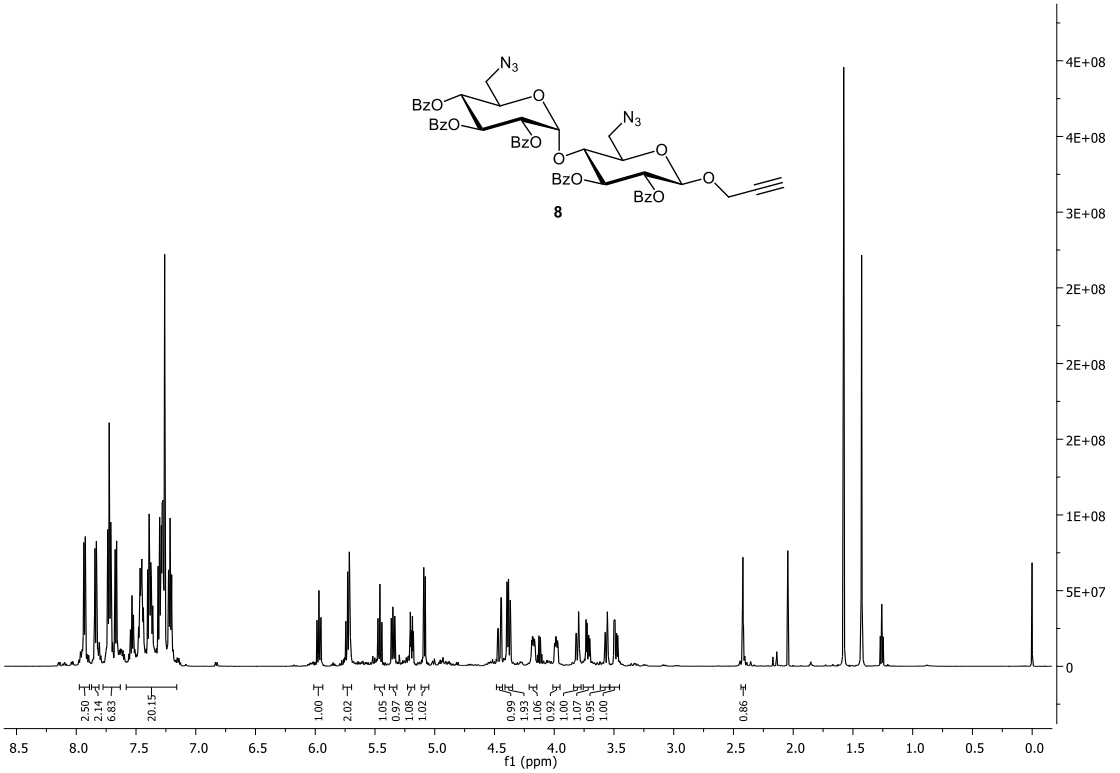

Figure S5.9 ^{1}H NMR spectrum of **8** (500 MHz, $CDCl_3$, 300 K).

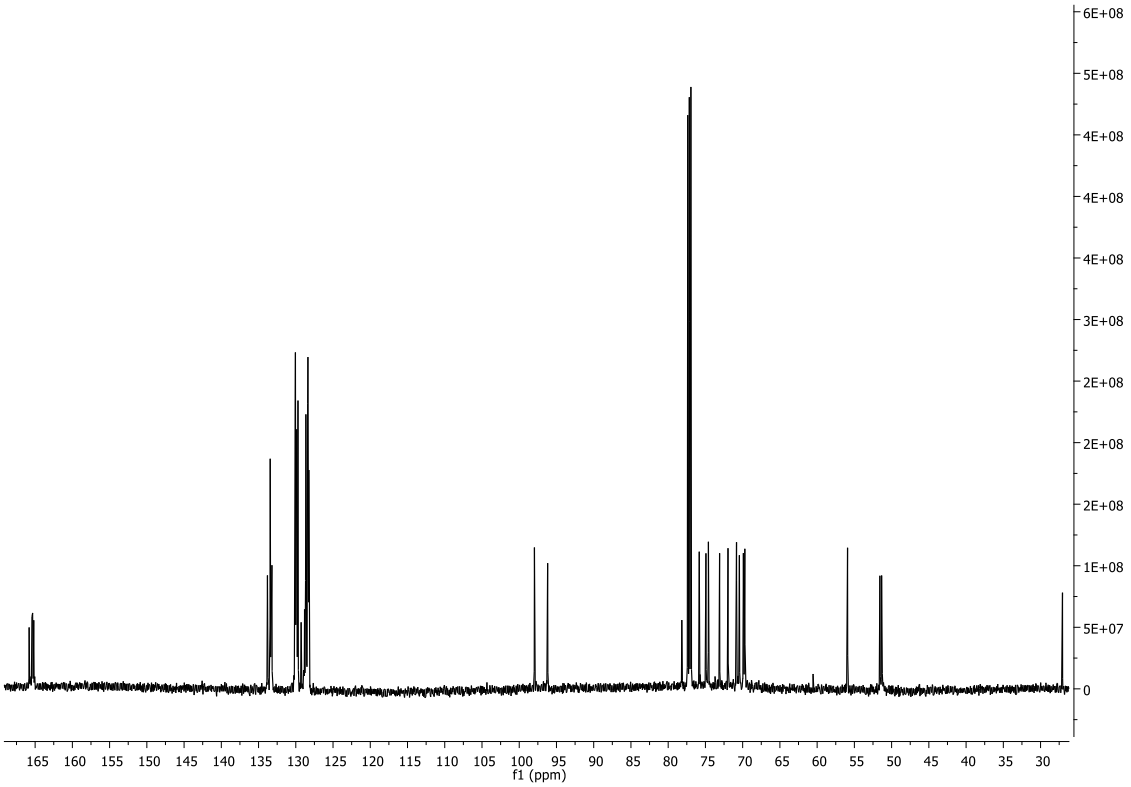

Figure S5.10 ^{13}C NMR spectrum of **8** (125 MHz, $CDCl_3$, 300 K).

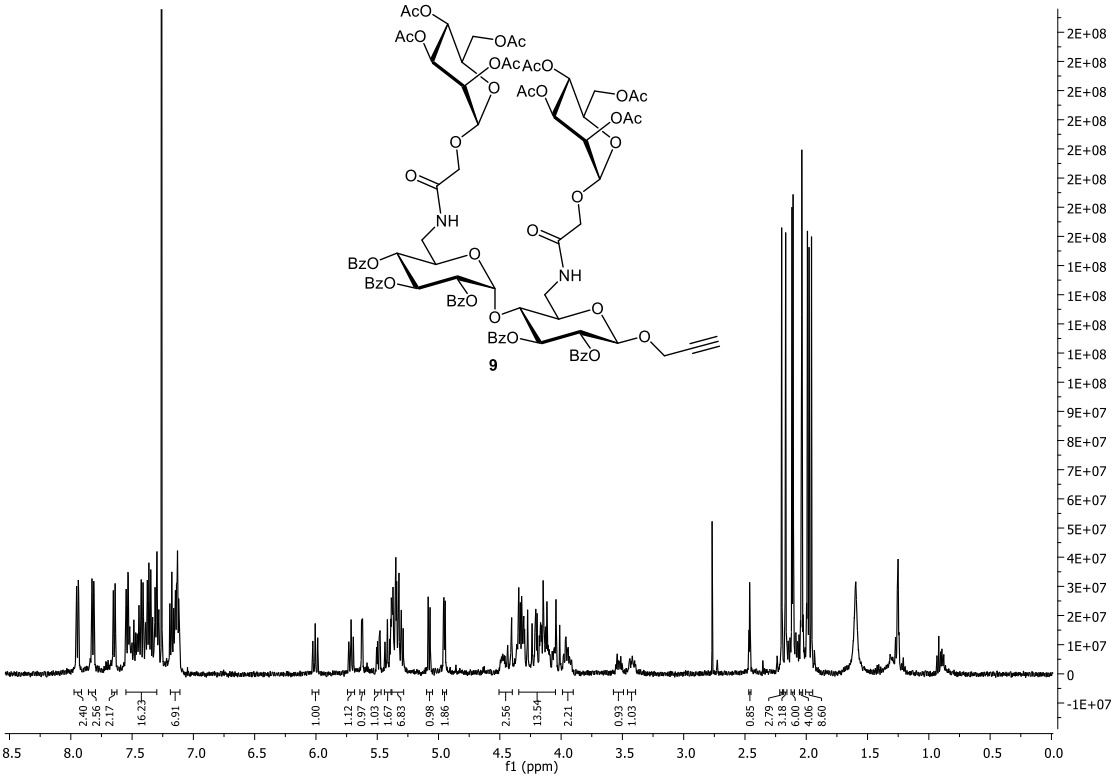

Figure S5.11 ^{1}H NMR spectrum of **9** (500 MHz, $CDCl_3$, 300 K).

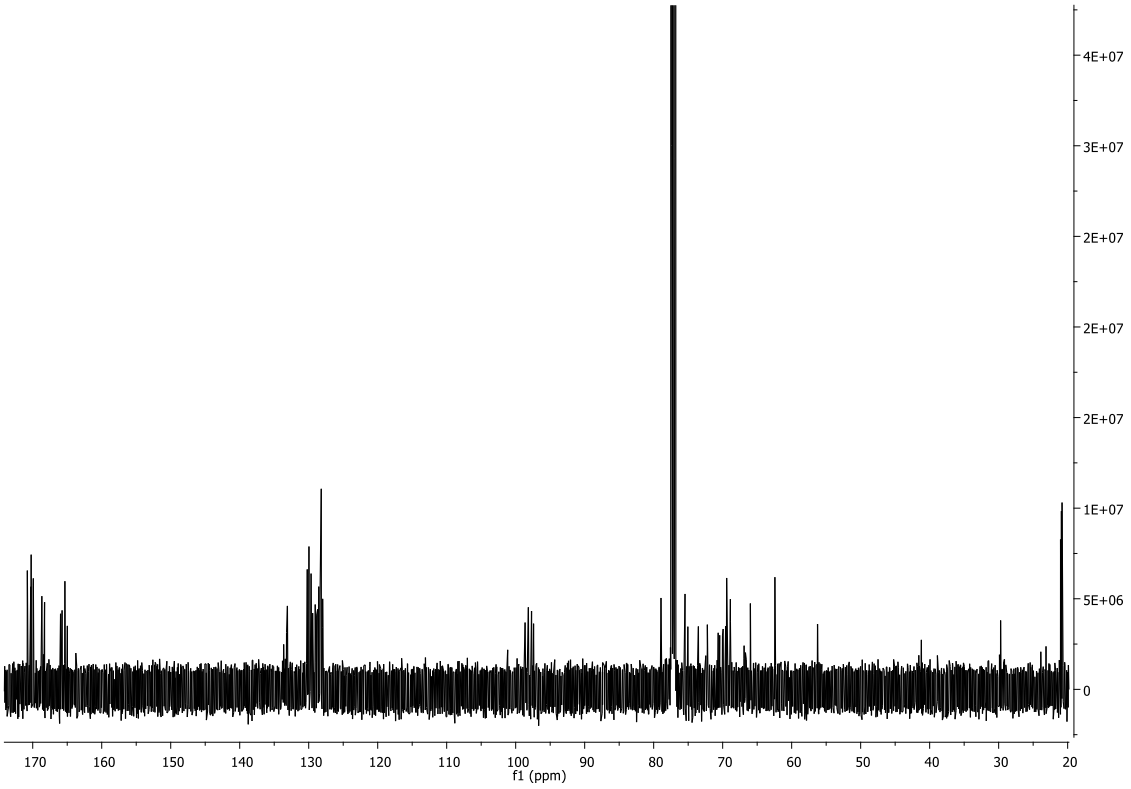

Figure S5.12 ^{13}C NMR spectrum of **9** (125 MHz, $CDCl_3$, 300 K).

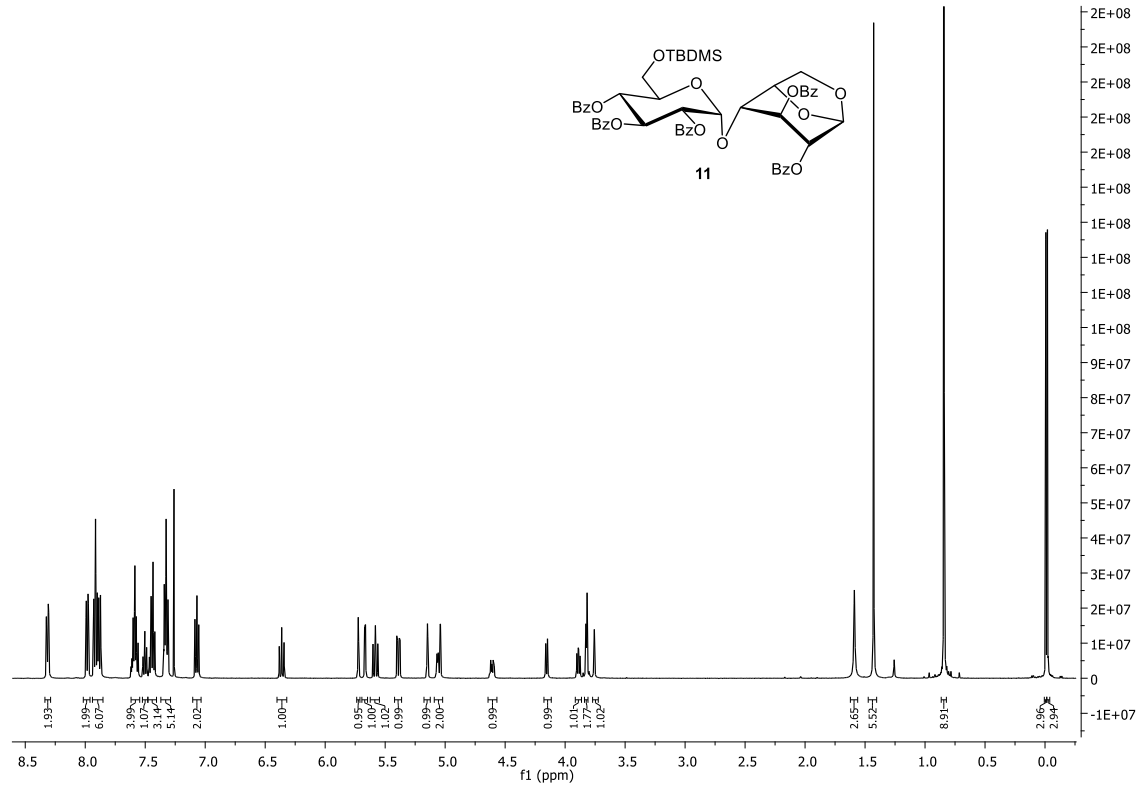

Figure S5.13 ^{1}H NMR spectrum of **11** (500 MHz, $CDCl_3$, 300 K).

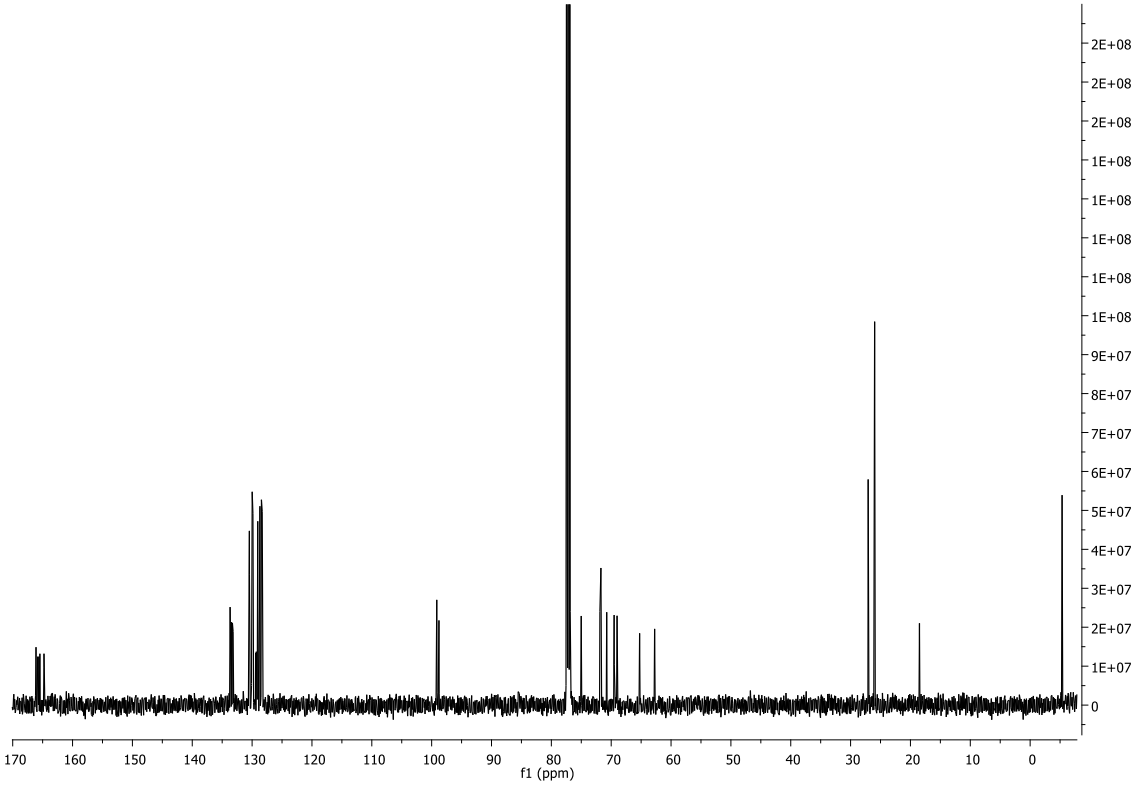

Figure S5.14 ^{13}C NMR spectrum of **11** (125 MHz, $CDCl_3$, 300 K).

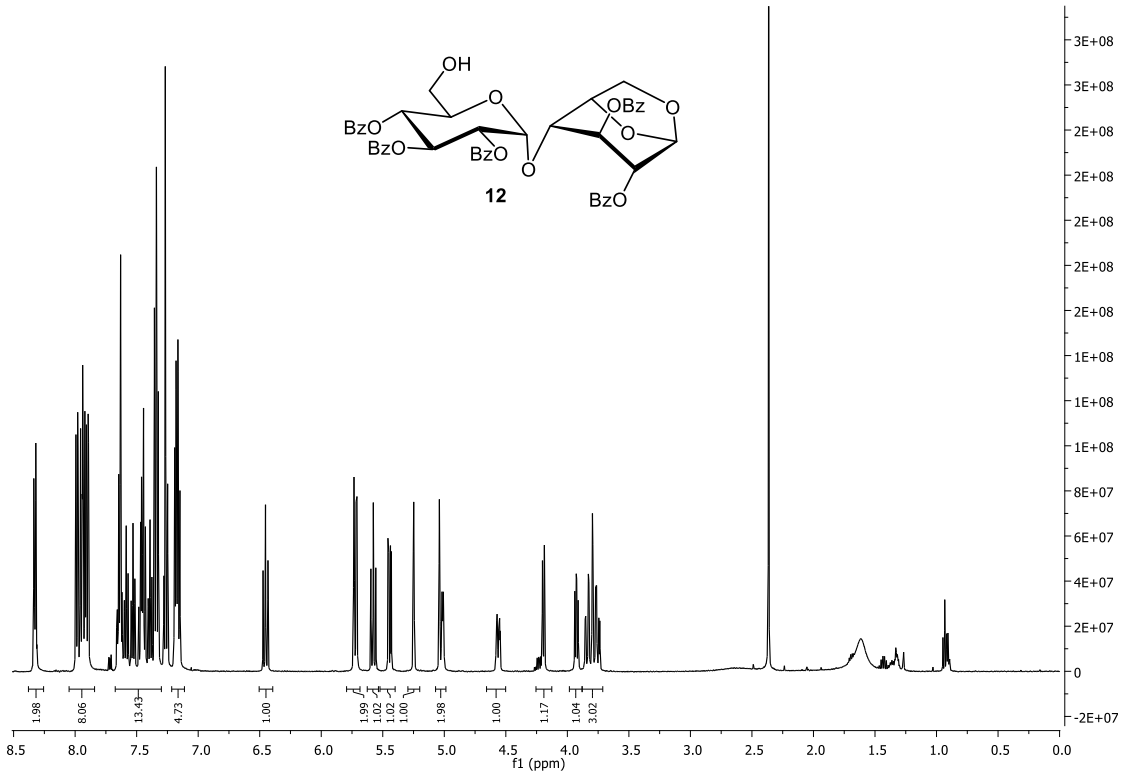

Figure S5.15 ^{1}H NMR spectrum of **12** (500 MHz, $CDCl_3$, 300 K).

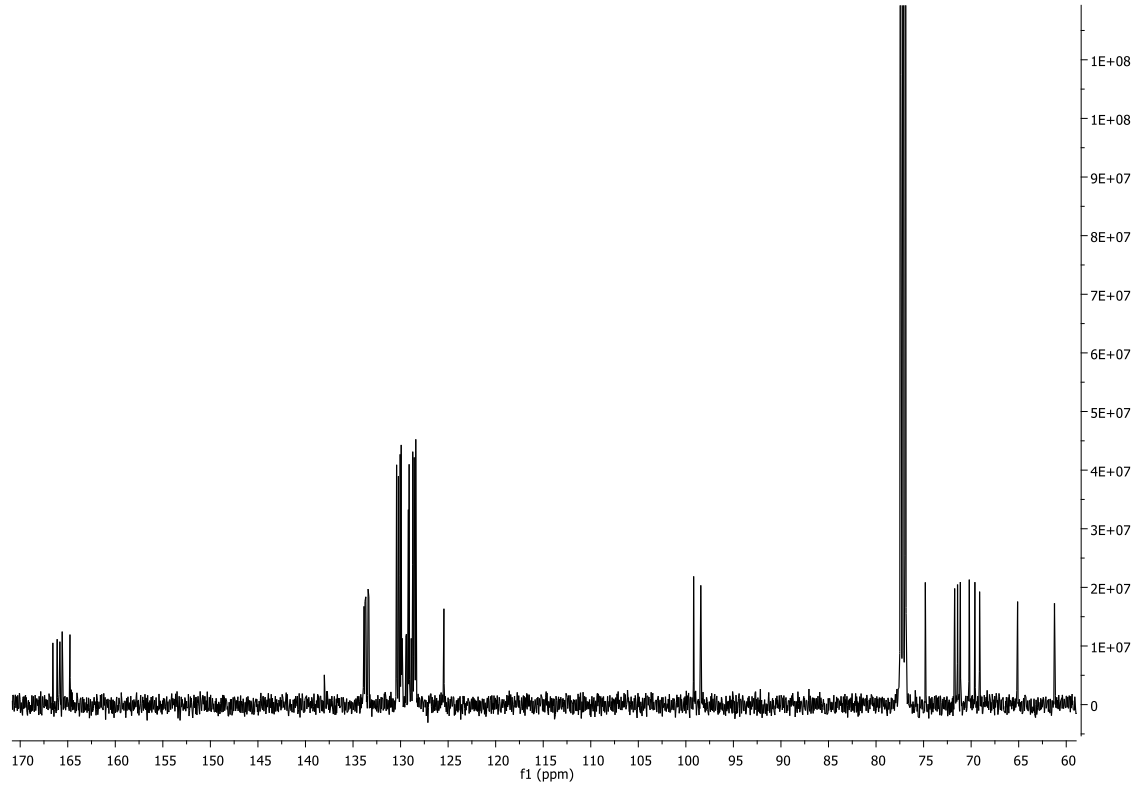

Figure S5.16 ^{13}C NMR spectrum of **12** (125 MHz, $CDCl_3$, 300 K).

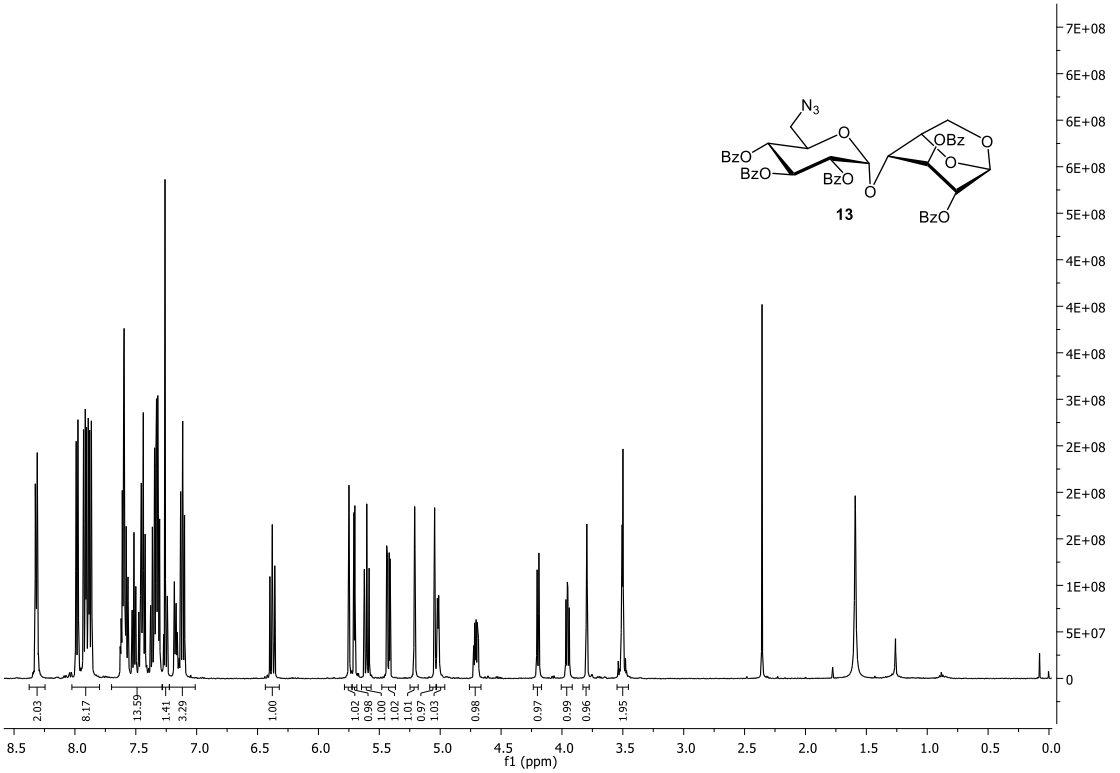

Figure S5.17 ^{1}H NMR spectrum of **13** (500 MHz, $CDCl_3$, 300 K).

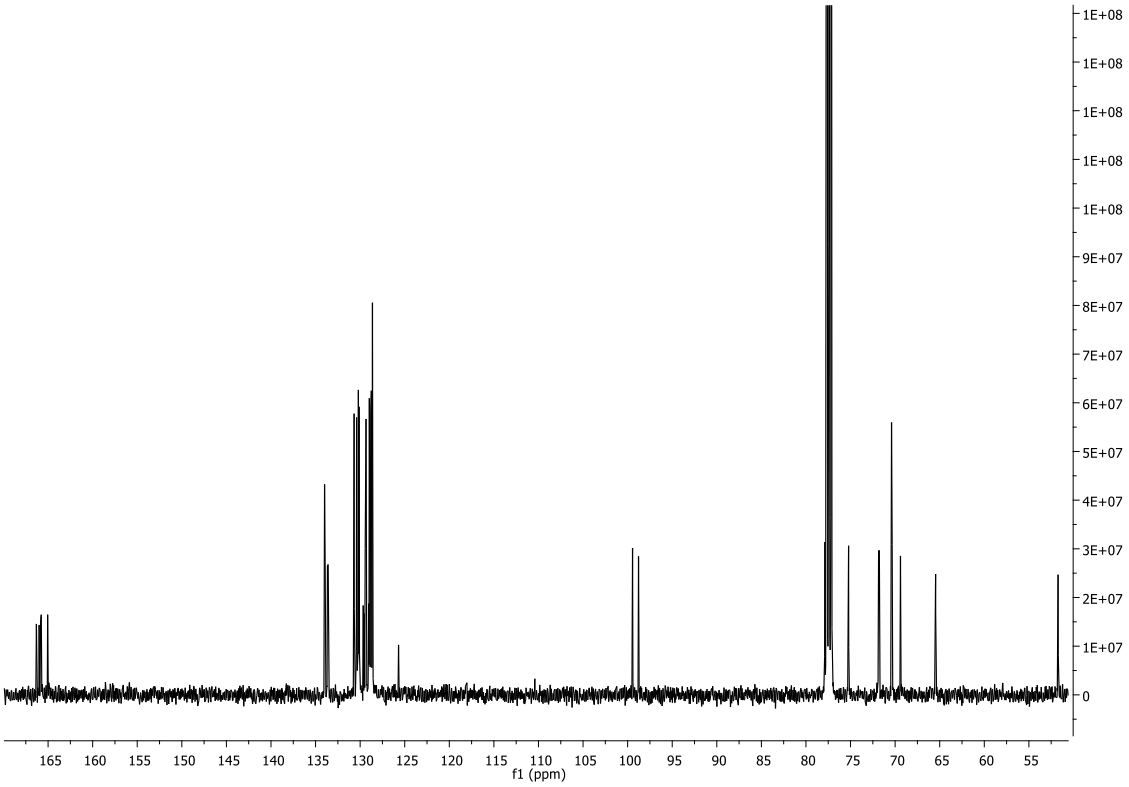

Figure S5.18 ^{13}C NMR spectrum of **13** (125 MHz, $CDCl_3$, 300 K).

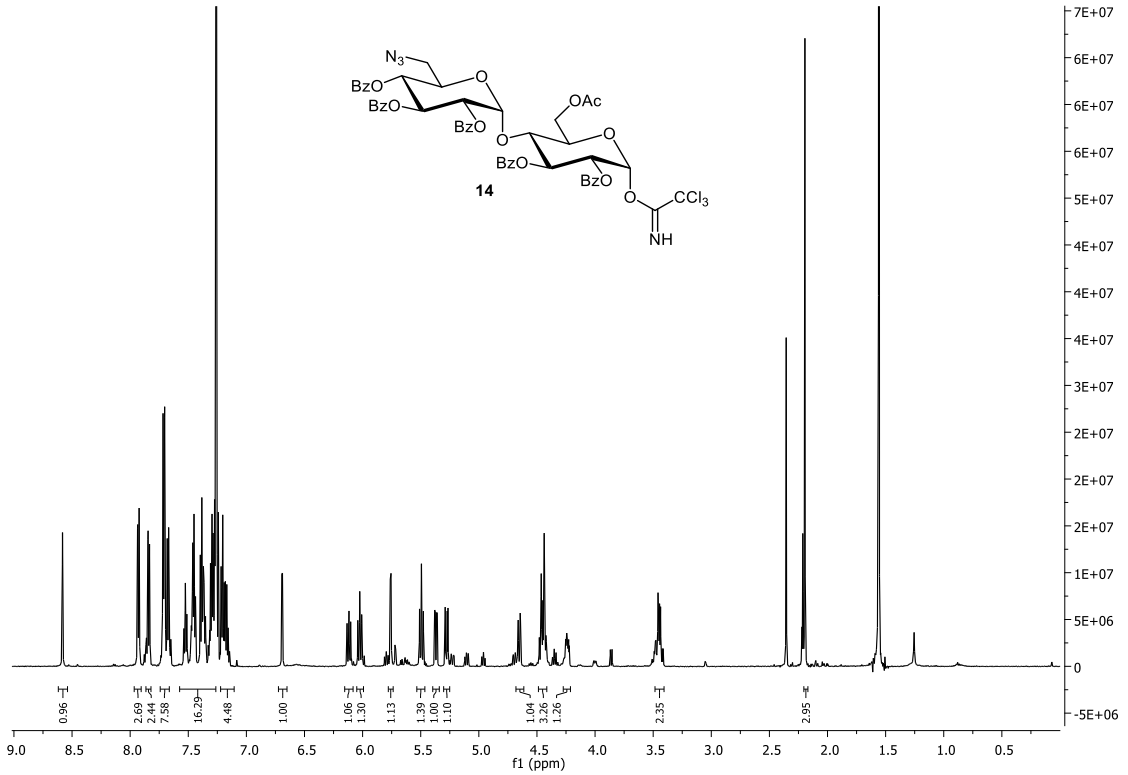

Figure S5.19 ^{1}H NMR spectrum of **14** (600 MHz, $CDCl_3$, 300 K).

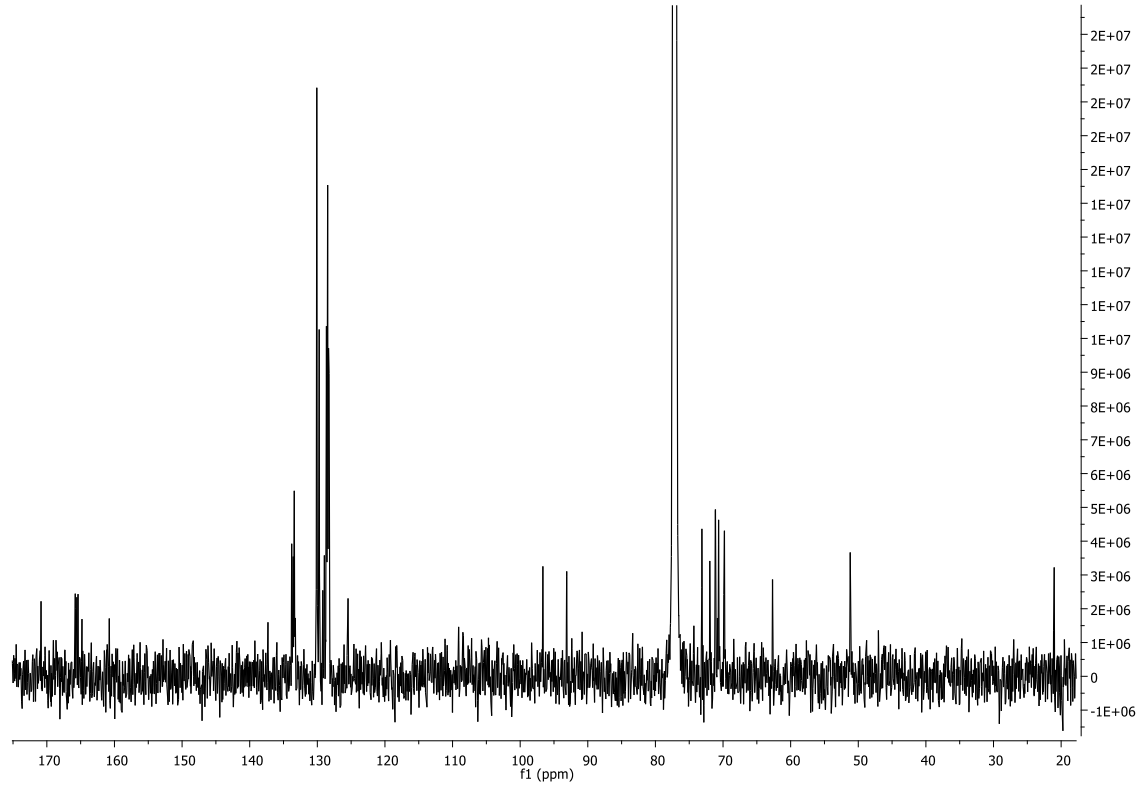

Figure S5.20 ^{13}C NMR spectrum of **14** (125 MHz, $CDCl_3$, 300 K).

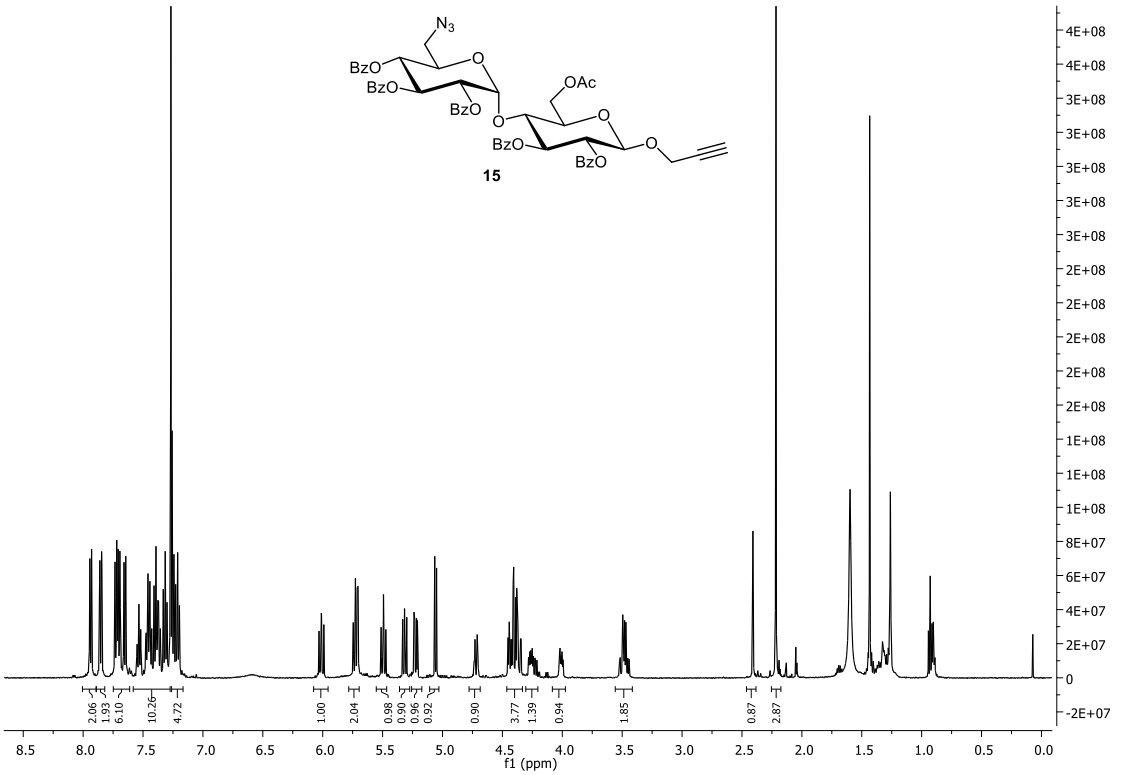

Figure S5.21 ^{1}H NMR spectrum of **15** (500 MHz, $CDCl_3$, 300 K).

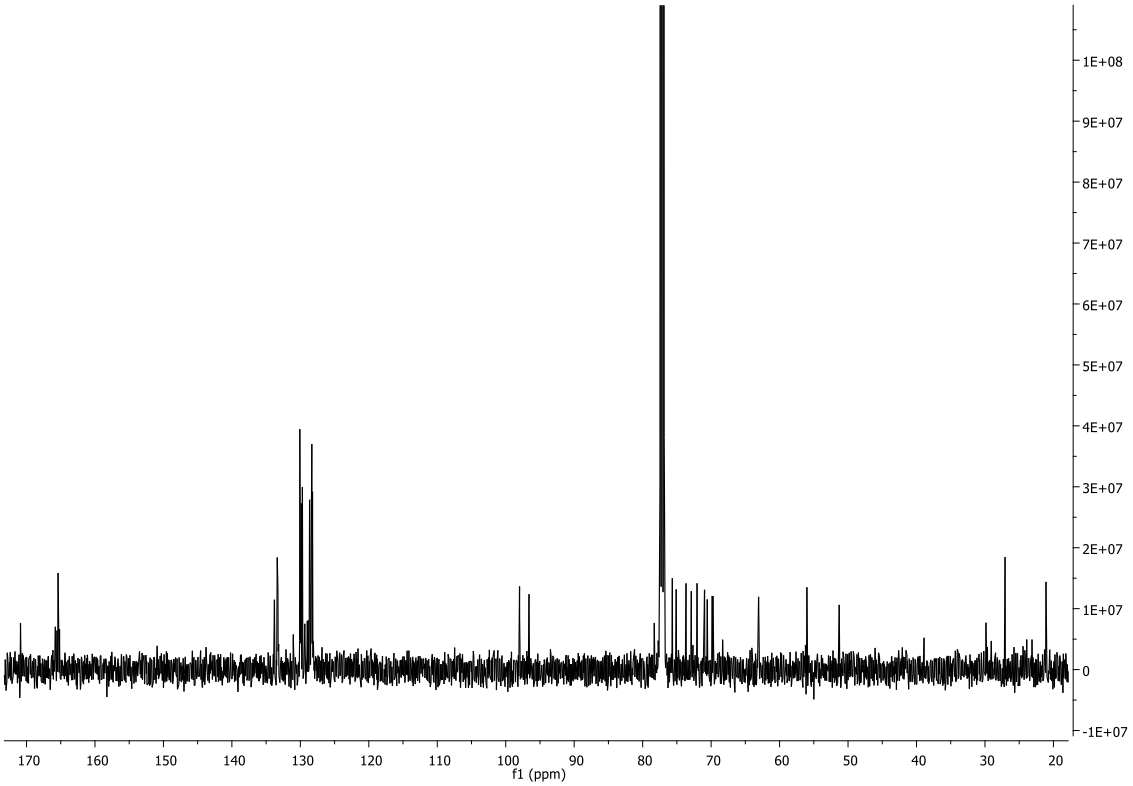

Figure S5.22 ^{13}C NMR spectrum of **15** (125 MHz, $CDCl_3$, 300 K).

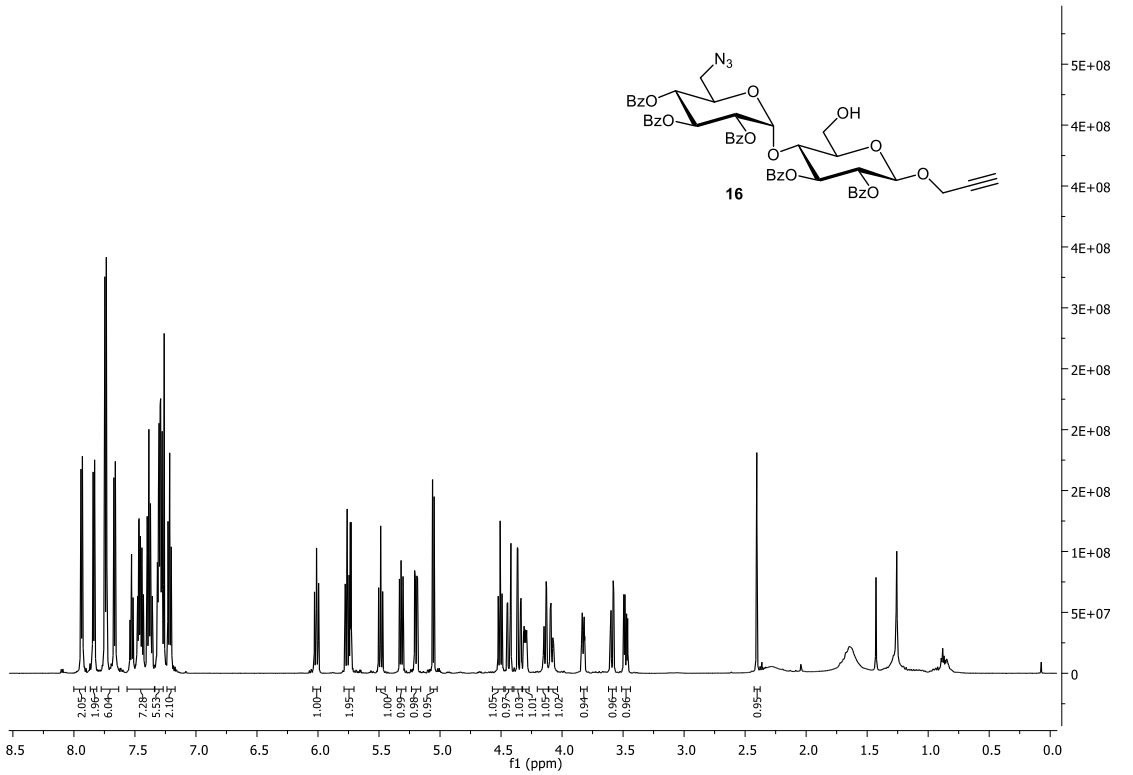

Figure S.5.23 ^{1}H NMR spectrum of **16** (600 MHz, $CDCl_3$, 300 K).

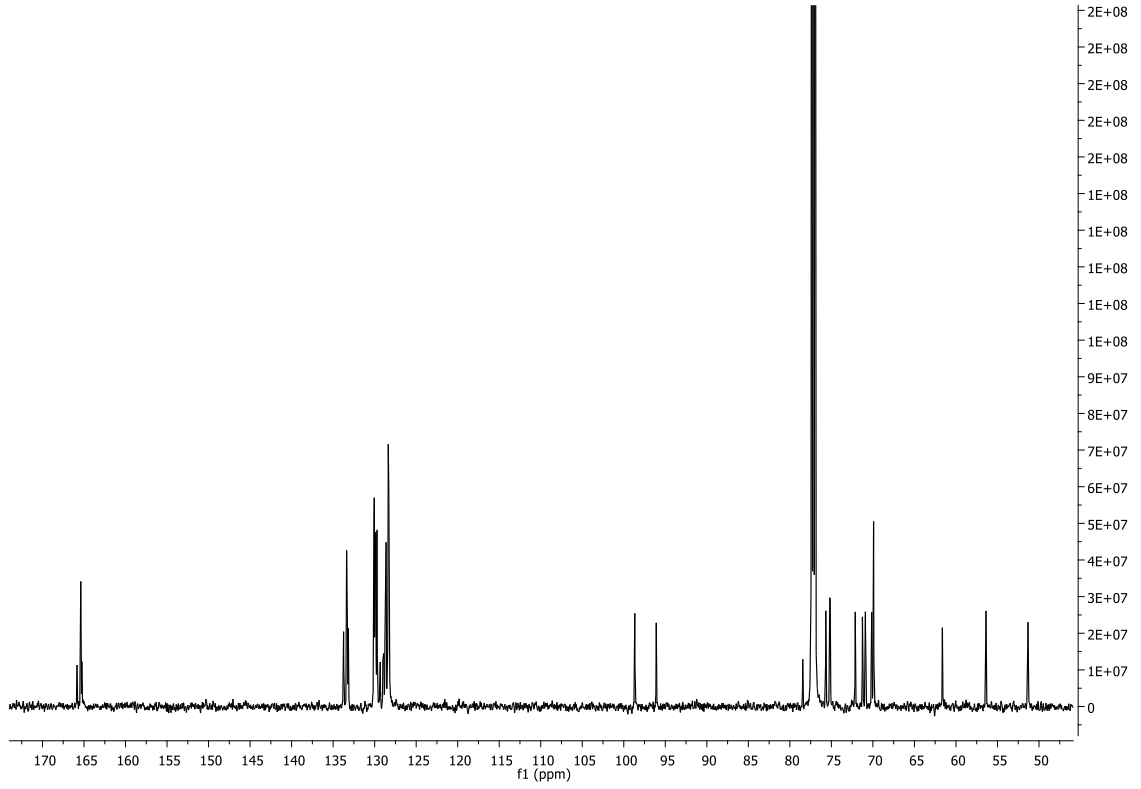

Figure S5.24 ^{13}C NMR spectrum of **16** (125 MHz, $CDCl_3$, 300 K).

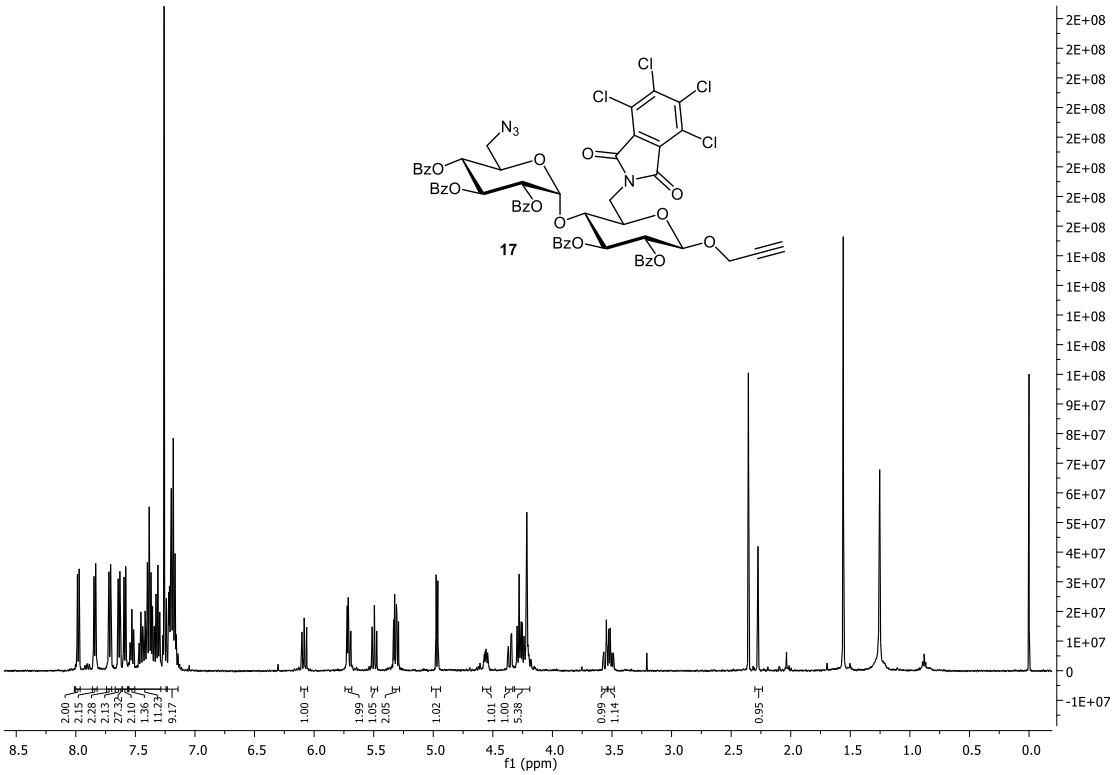

Figure S5.25 ^{1}H NMR spectrum of **17** (600 MHz, $CDCl_3$, 300 K).

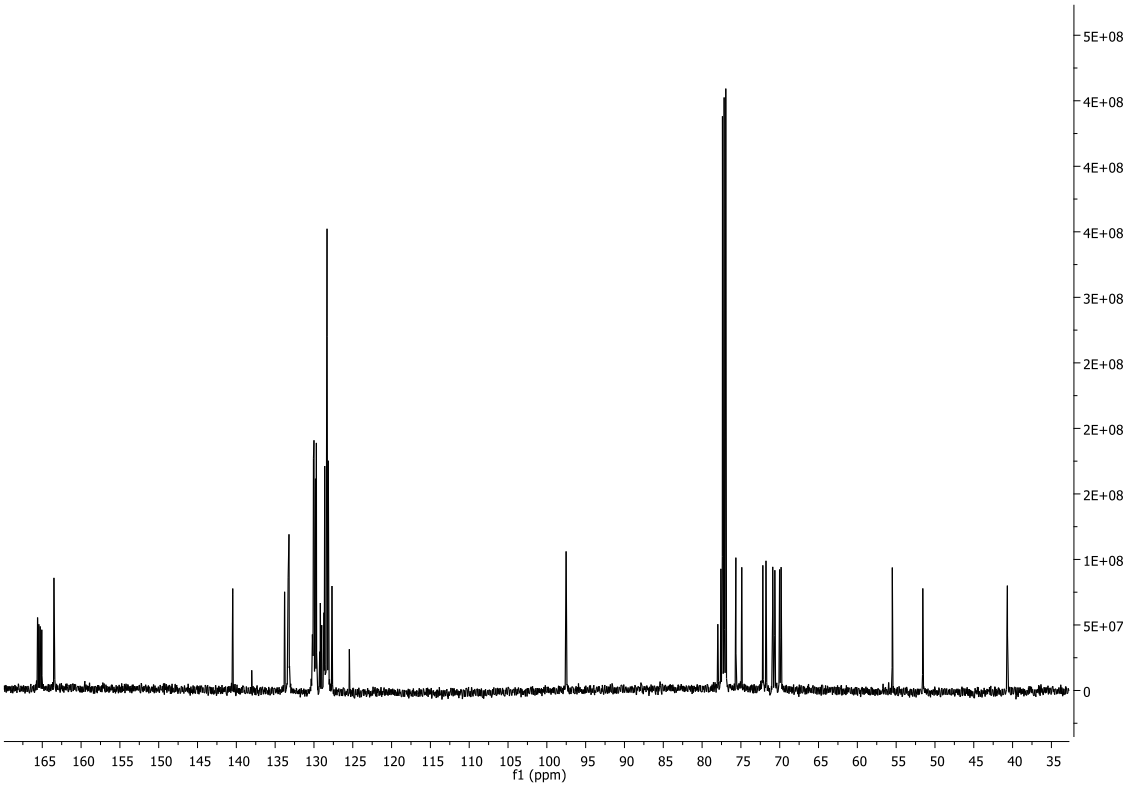

Figure S5.26 ^{13}C NMR spectrum of **17** (125 MHz, $CDCl_3$, 300 K).

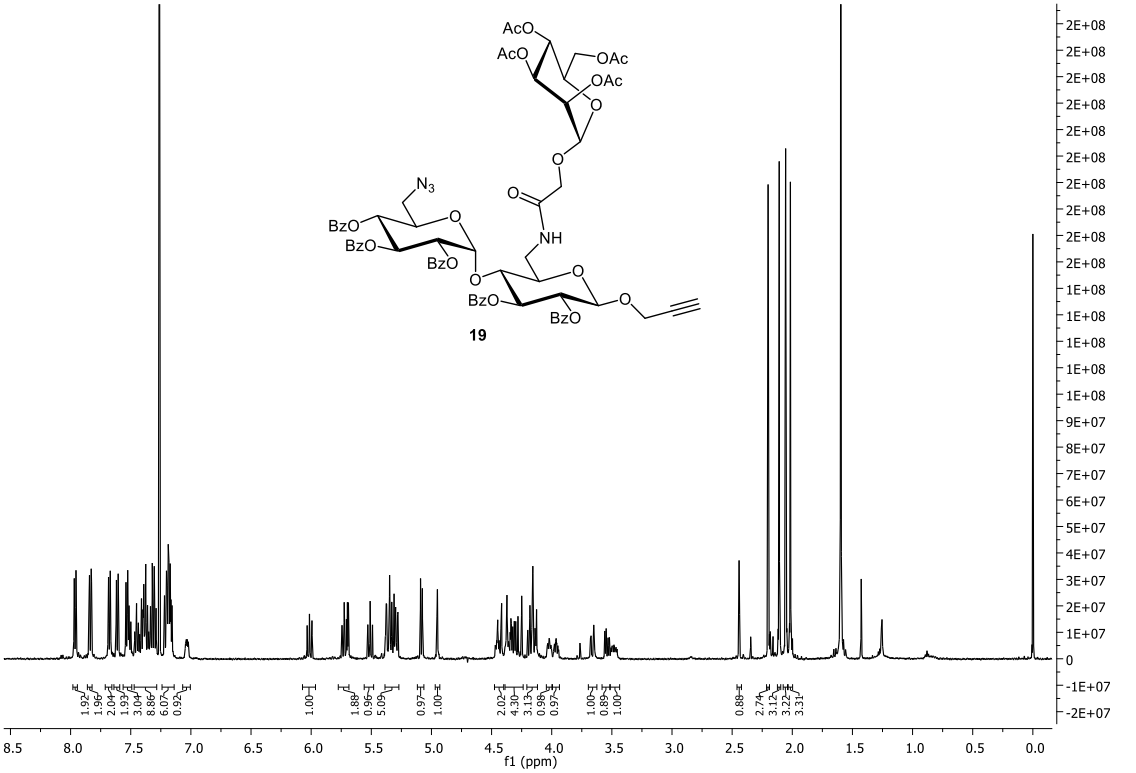

Figure S5.27 ^{1}H NMR spectrum of **19** (500 MHz, $CDCl_3$, 300 K).

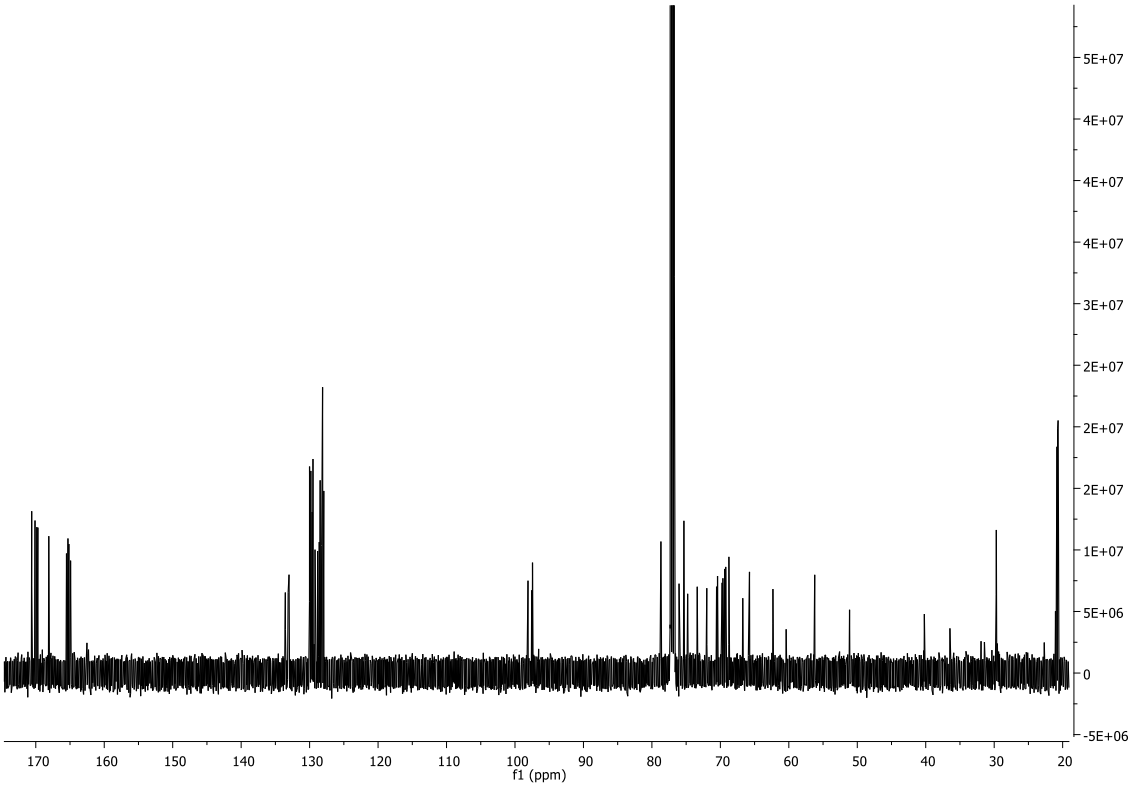

Figure S5.28 ^{13}C NMR spectrum of **19** (125 MHz, $CDCl_3$, 300 K).

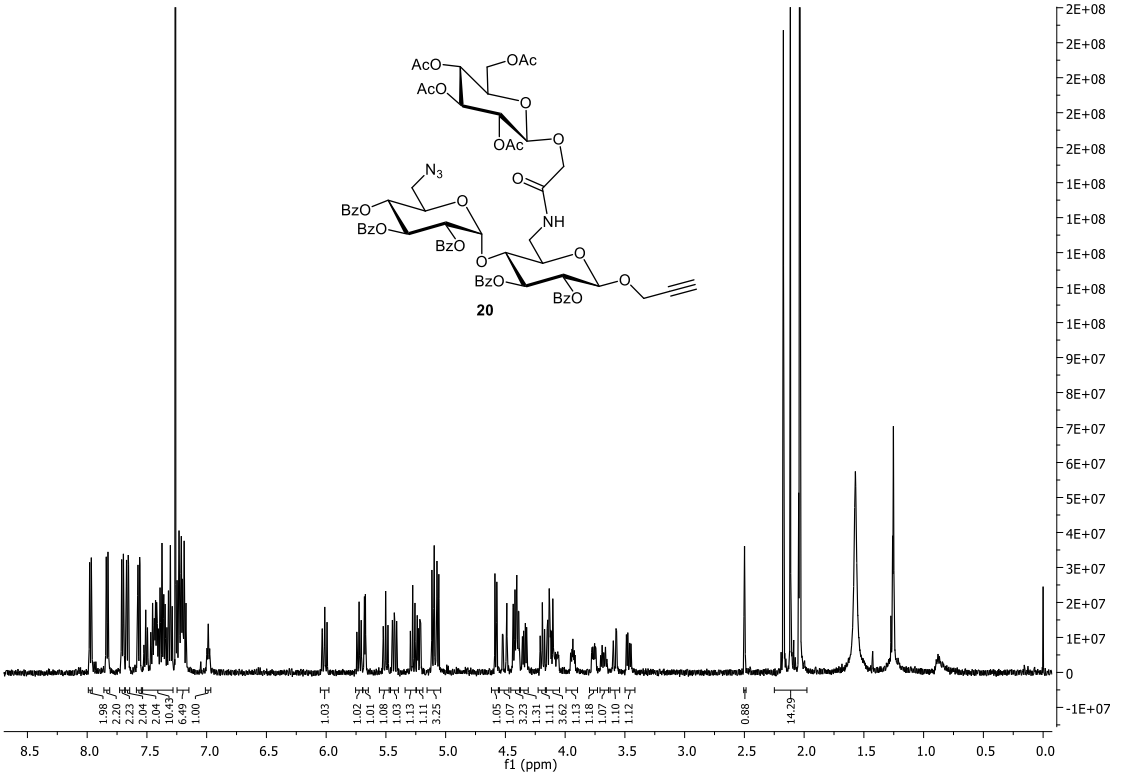

Figure S5.29 ^{1}H NMR spectrum of **20** (500 MHz, $CDCl_3$, 300 K).

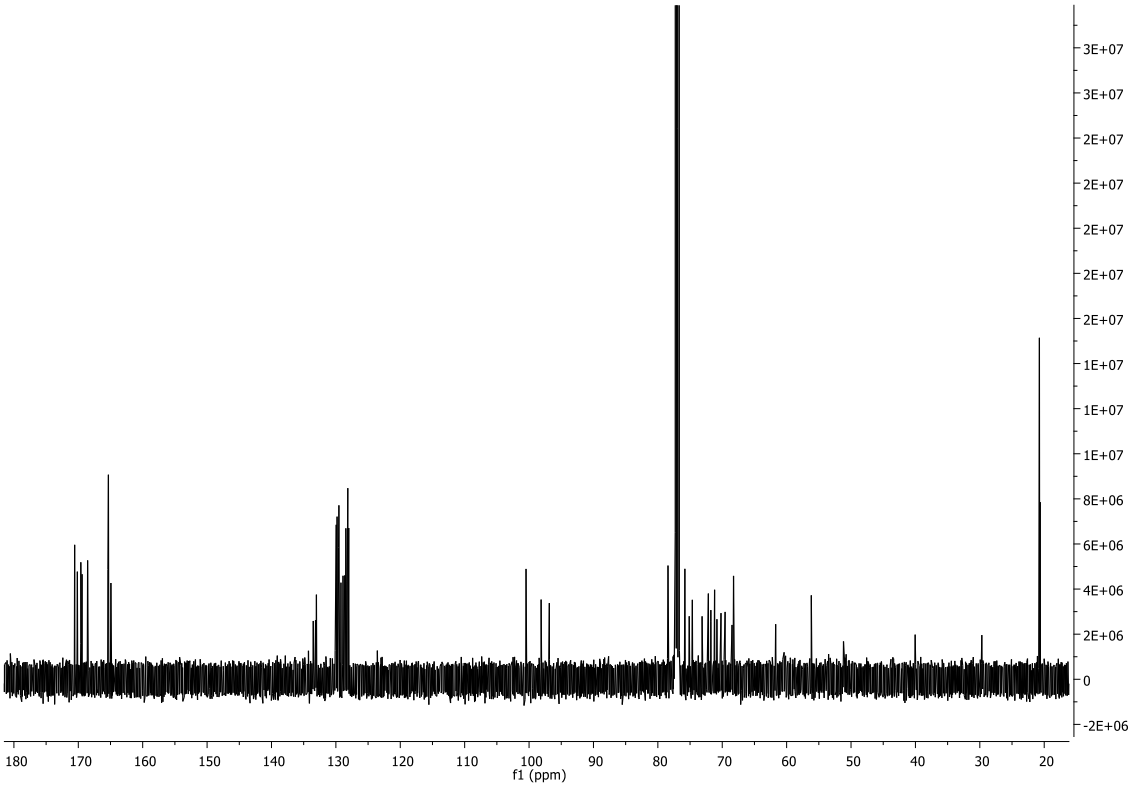

Figure S5.30 ^{13}C NMR spectrum of **20** (125 MHz, $CDCl_3$, 300 K).

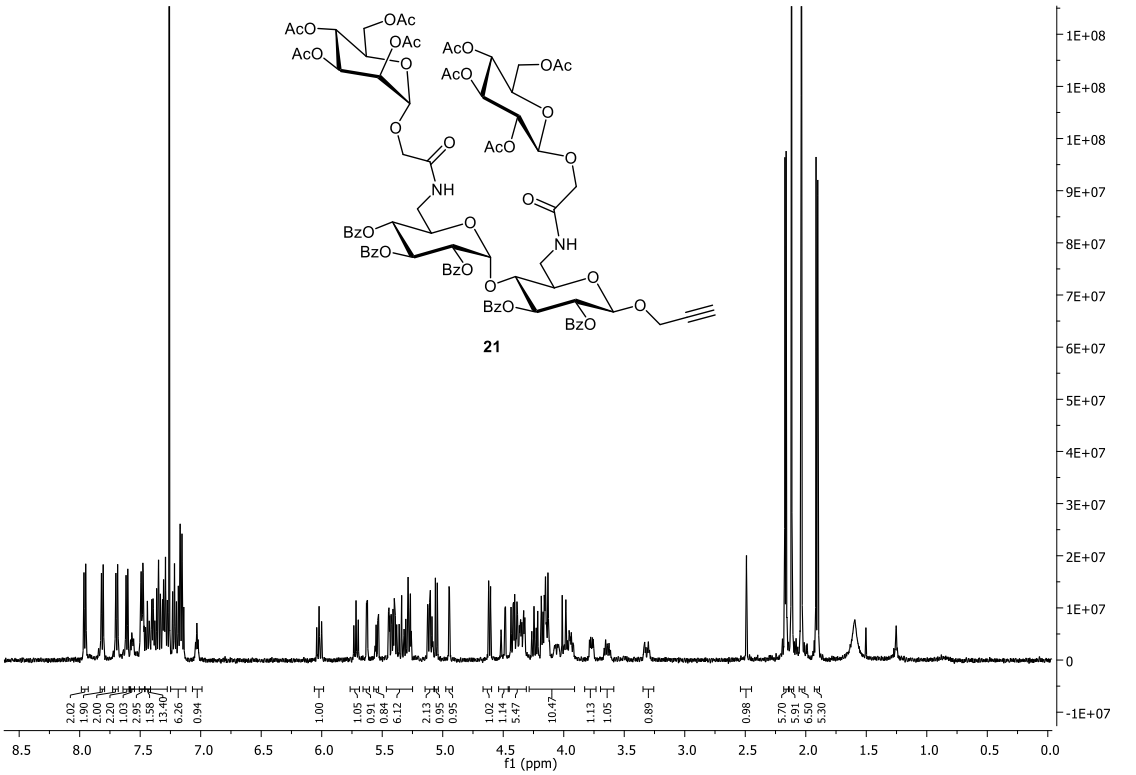

Figure S5.31 ^{1}H NMR spectrum of **21** (600 MHz, $CDCl_3$, 300 K).

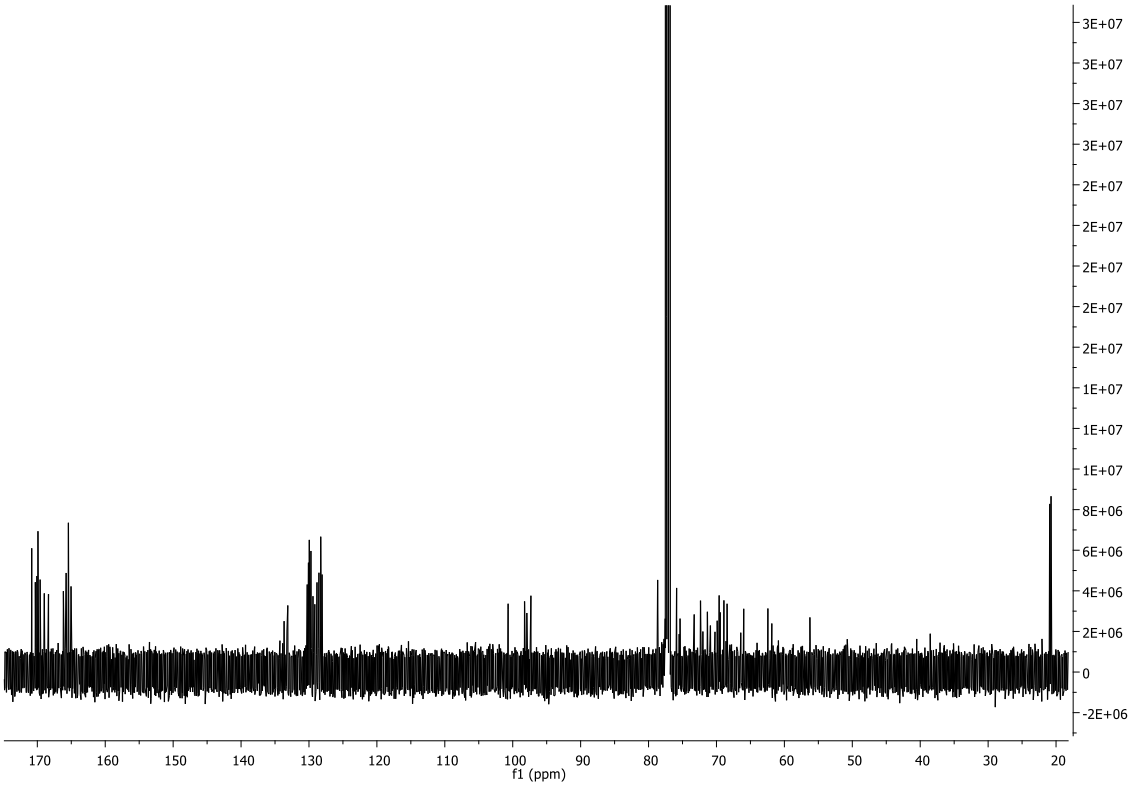

Figure S5.32 ^{13}C NMR spectrum of **21** (125 MHz, $CDCl_3$, 300 K).

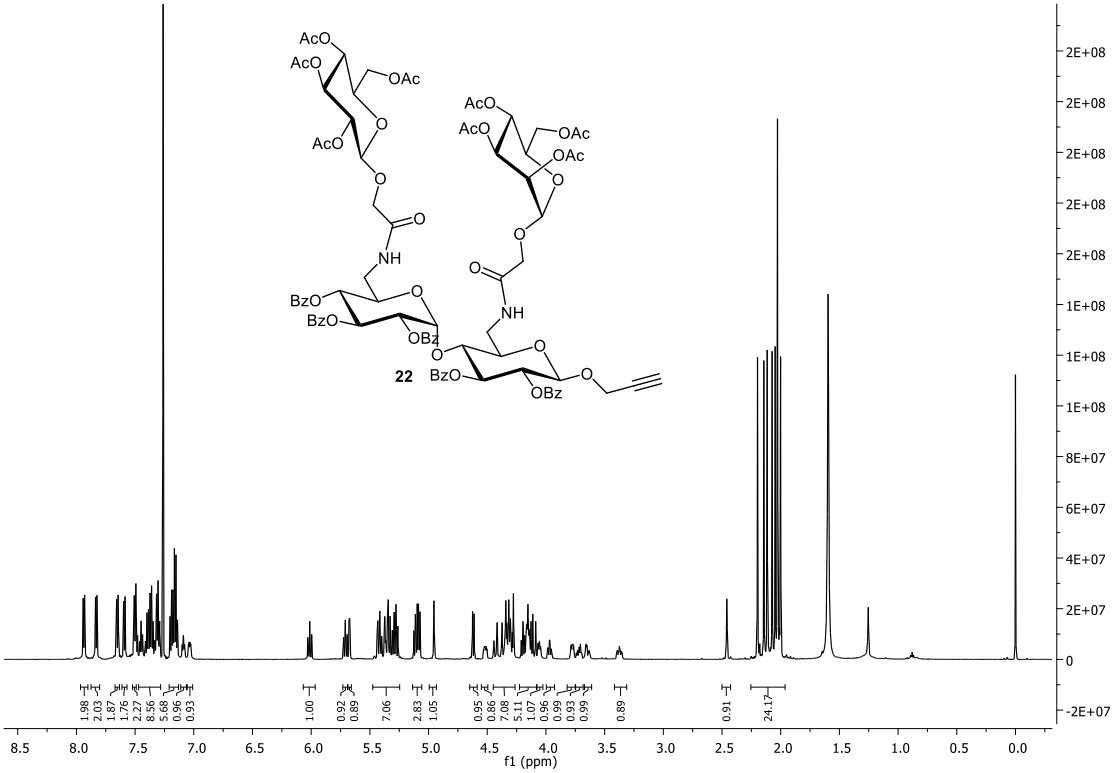

Figure S5.33 ^{1}H NMR spectrum of **22** (600 MHz, $CDCl_3$, 300 K).

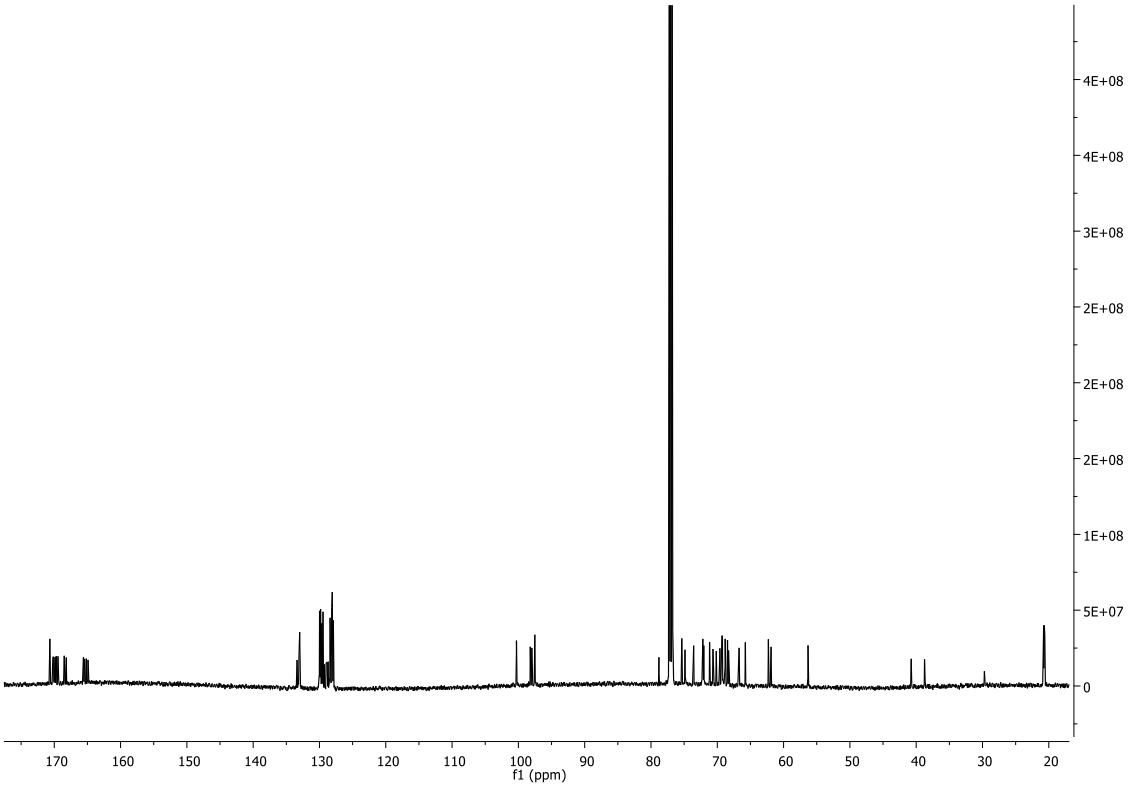

Figure S5.34 ^{13}C NMR spectrum of **22** (125 MHz, $CDCl_3$, 300 K).

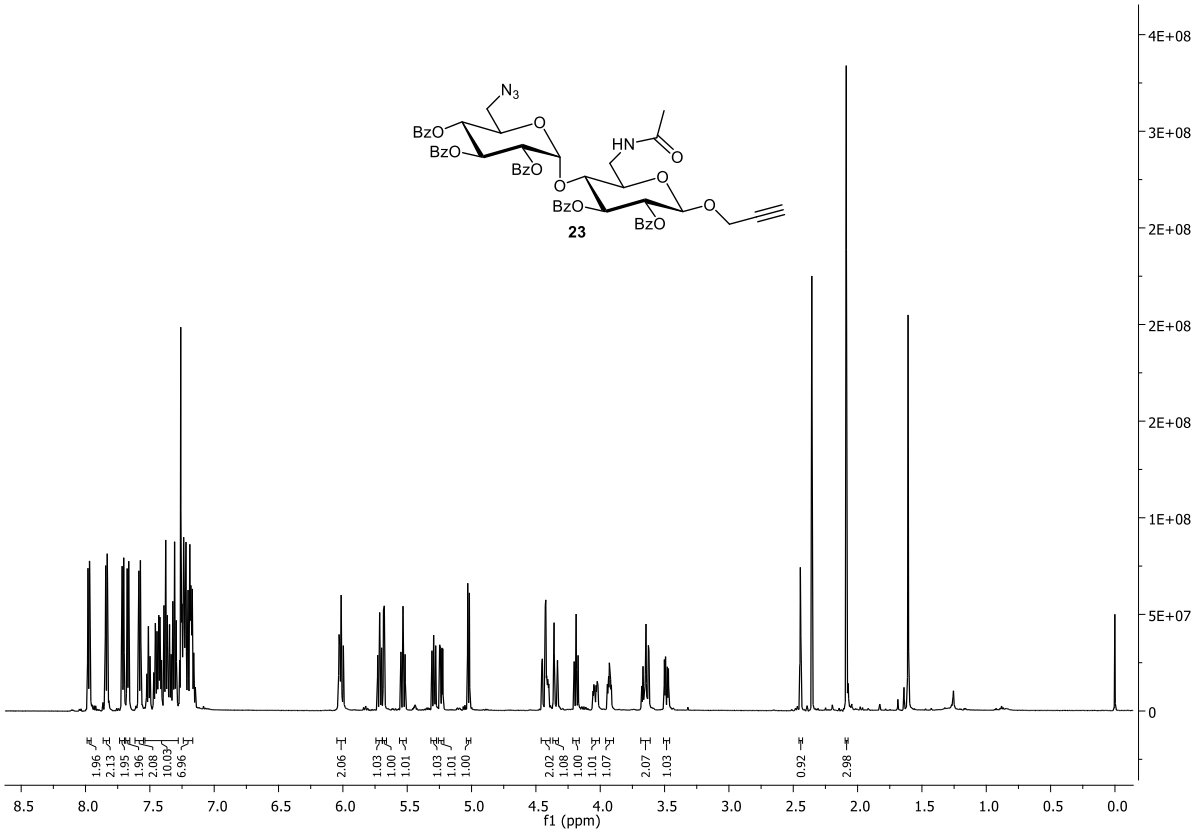

Figure S5.35 ^{1}H NMR spectrum of **23** (600 MHz, $CDCl_3$, 300 K).

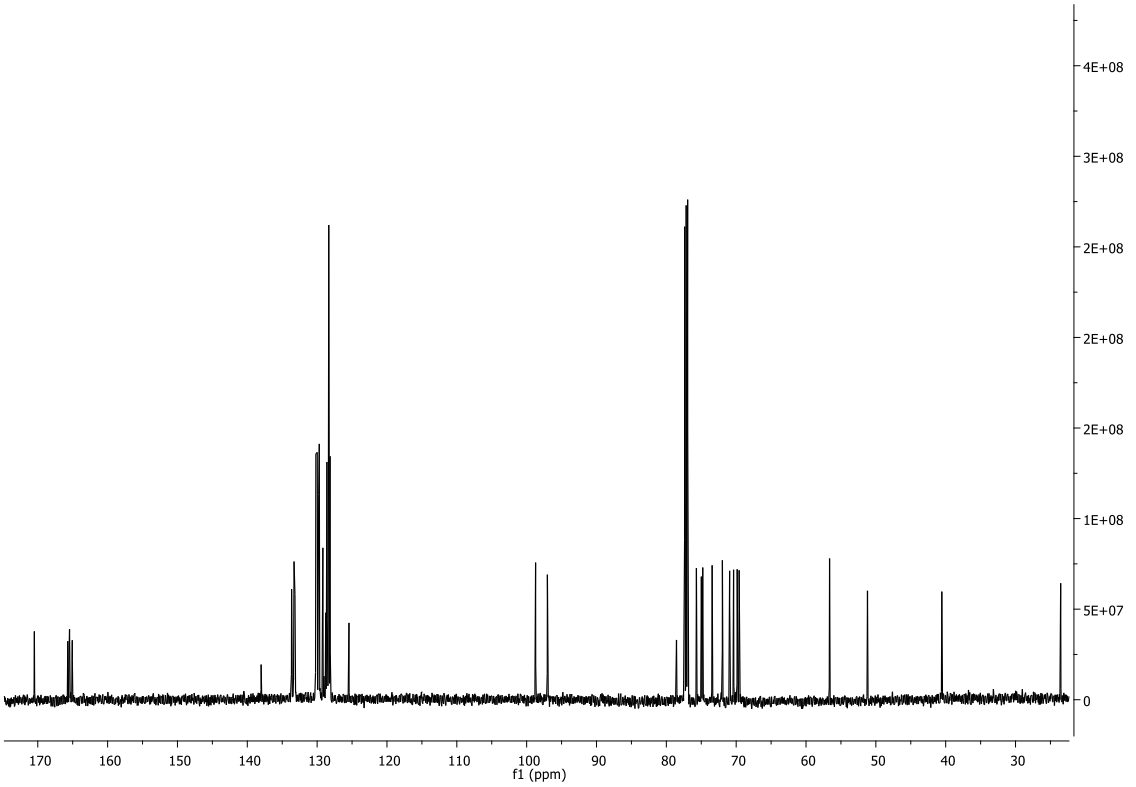

Figure S5.36 ^{13}C NMR spectrum of **23** (125 MHz, $CDCl_3$, 300 K).

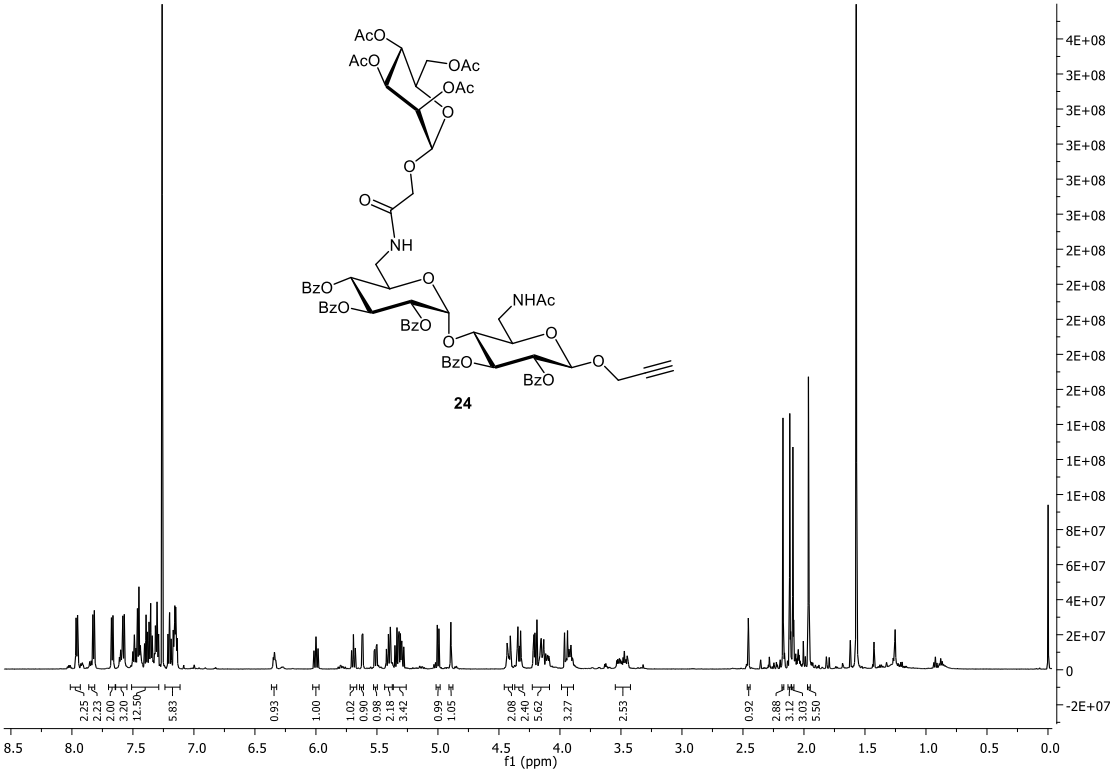

Figure S5.37 ^{1}H NMR spectrum of **24** (600 MHz, $CDCl_3$, 300 K).

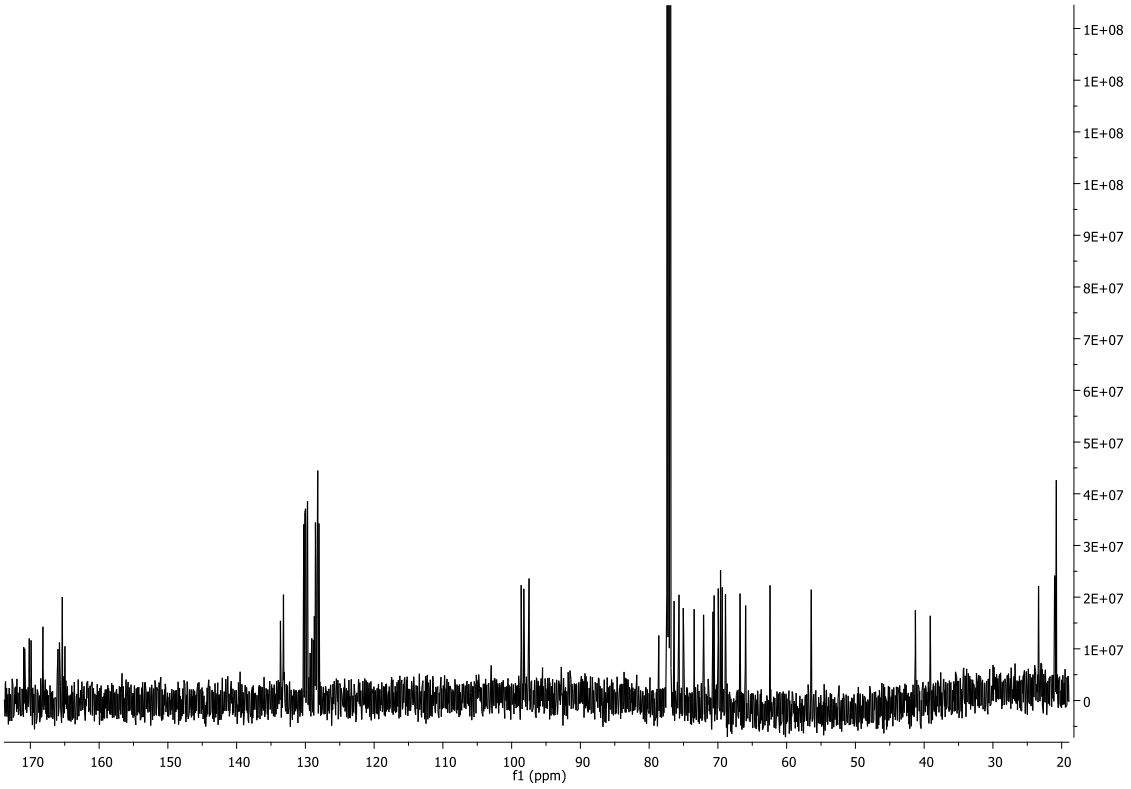

Figure S5.38 ^{13}C NMR spectrum of **24** (125 MHz, $CDCl_3$, 300 K).

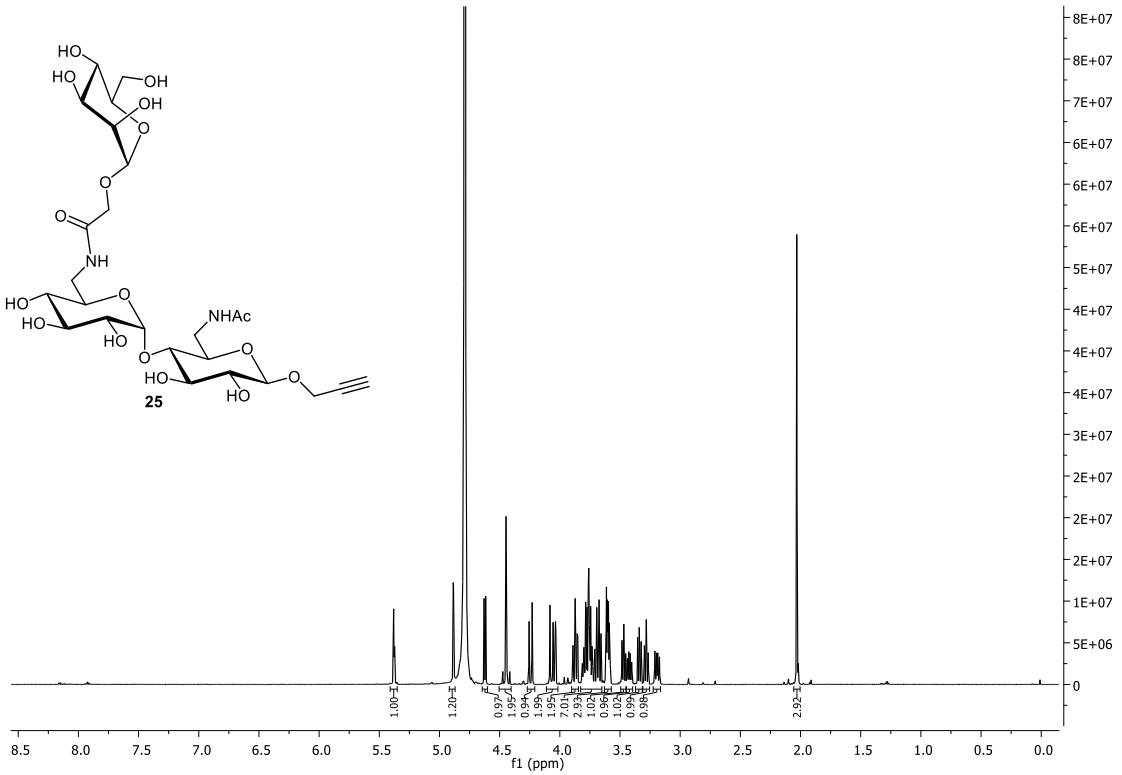

Figure S5.39 ^{1}H NMR spectrum of **25** (600 MHz, D_2O, 300 K).

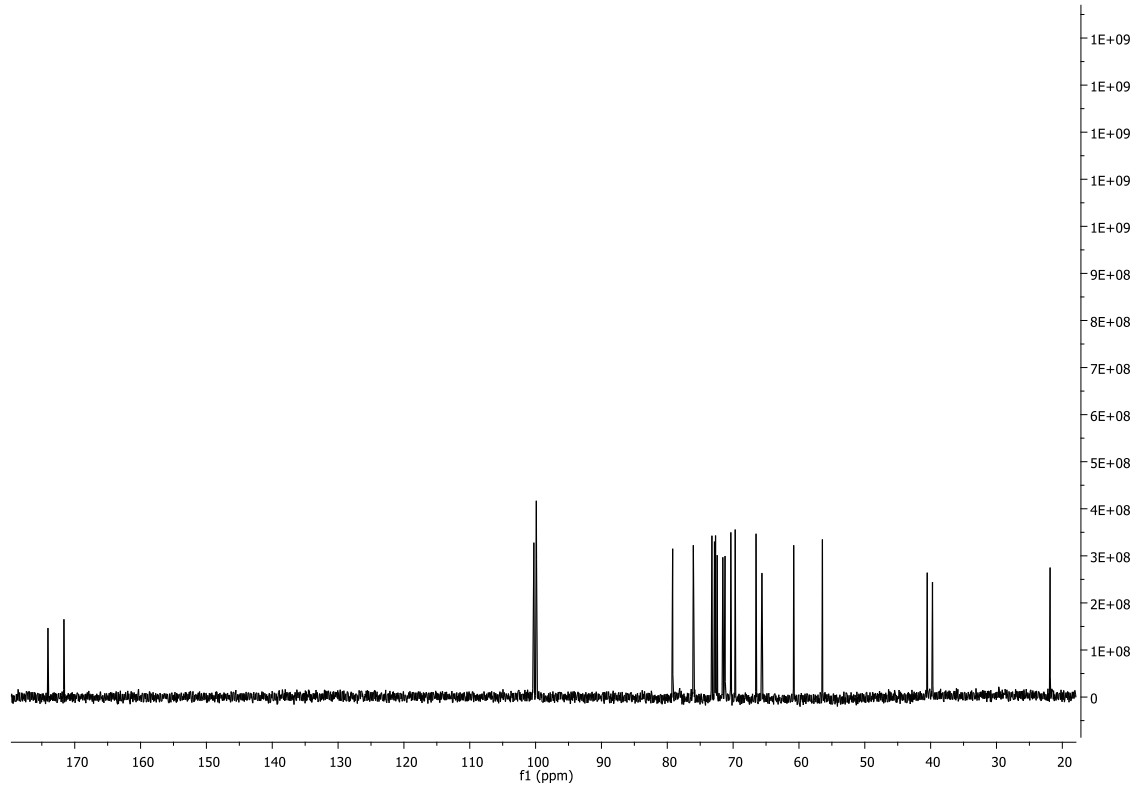

Figure S5.40 ^{13}C NMR spectrum of **25** (125 MHz, D_2O, 300 K).

6 References

[1] E. A. J. Post and S. P. Fletcher, *J. Org. Chem.,* 2019, **84**, 2741-2755.

[2] T. Tanaka, W. C. Huang, M. Noguchi, A. Kobayashi and S.-i. Shoda, *Tetrahedron Lett.,* 2009, **50**, 2154-2157.

[3] A. Reisner, J. A. J. Haagensen, M. A. Schembri, E. L. Zechner and S. Molin, *Mol. Microbiol.,* 2003, **48**, 933-946.

[4] M. Hartmann, A. Horst, P. Klemm and T. K. Lindhorst, *Chem. Commun.*, 2010, **46**, 330-332.

[5] Schrödinger Release 2020-4: Maestro, Schrödinger, LLC, New York, NY, **2020**.

[6] a) Schrödinger Release 2020-4: LigPrep, Schrödinger, LLC, New York, NY, **2020**; b) E. Harder, W. Damm, J. Maple, C. Wu, M. Reboul, J. Y. Xiang, L. Wang, D. Lupyan, M. K. Dahlgren, J. L. Knight, J. W. Kaus, D. S. Cerutti, G. Krilov, W. L. Jorgensen, R. Abel and R. A. Friesner, *J. Chem. Theory Comput.,* 2016, **12**, 1, 281-296.

[7] C.-S. Hung, J. Bouckaert, D. Hung, J. Pinkner, C. Widberg, A. DeFusco, C. G. Auguste, R. Strouse, S. Langermann and G. Waksman, *Mol. Microbiol.*, 2002, **44**, 903-915.

[8] J. Bouckaert, J. Berglund, M. Schembri, E. D. Genst, L. Cools, M. Wuhrer, C.-S. Hung, J. Pinkner, R. Slättegård, A. Zavialov, D. Choudhury, S. Langermann, S. J. Hultgren, L. Wyns, P. Klemm, S. Oscarson, S. D. Knight and H. D. Greve, *Mol. Microbiol.*, 2005, **55**, 441-455.

[9] Schrödinger Release 2020-4: Glide, Schrödinger, LLC, New York, NY, **2020**.

[10] Schrödinger Release 2020-4: Prime, Schrödinger, LLC, New York, NY, **2020**.

[11] Schrödinger Release 2020-4: Induced Fit Docking protocol; Glide, Schrödinger, LLC, New York, NY, **2020**; Prime, Schrödinger, LLC, New York, NY, **2020**.

[12] a) S. G. Gouin , G. Roos and J. Bouckaert , *Top. Med. Chem.*, 2014, **12**, 123-168S; b) G. Zhou, W. J. Mo, P. Sebbel, G. Min, T. A. Neubert, R. Glockshuber, X. R. Wu, T. T. Sun and X. P. Kong, *J. Cell. Sci.,* 2001, **114**, 22, 4095-4103.

[13] Schrödinger Release 2020-4: Binding Pose Metadynamics protocol; Desmond Molecular Dynamics System, D. E. Shaw Research, New York, NY, **2020**. Maestro-Desmond Interoperability Tools, Schrödinger, New York, NY, **2020**.